

**University of Alberta**

**The subglacial geomorphology of southeast Alberta: evidence for subglacial  
meltwater erosion**

by

**Claire Louise Beaney**



A thesis submitted to the Faculty of Graduate Studies and Research in partial fulfillment  
of the requirements for the degree of Master of Science.

Department of Earth and Atmospheric Sciences

Edmonton, Alberta

Fall, 1998



National Library  
of Canada

Acquisitions and  
Bibliographic Services

395 Wellington Street  
Ottawa ON K1A 0N4  
Canada

Bibliothèque nationale  
du Canada

Acquisitions et  
services bibliographiques

395, rue Wellington  
Ottawa ON K1A 0N4  
Canada

*Your file Votre référence*

*Our file Notre référence*

The author has granted a non-exclusive licence allowing the National Library of Canada to reproduce, loan, distribute or sell copies of this thesis in microform, paper or electronic formats.

The author retains ownership of the copyright in this thesis. Neither the thesis nor substantial extracts from it may be printed or otherwise reproduced without the author's permission.

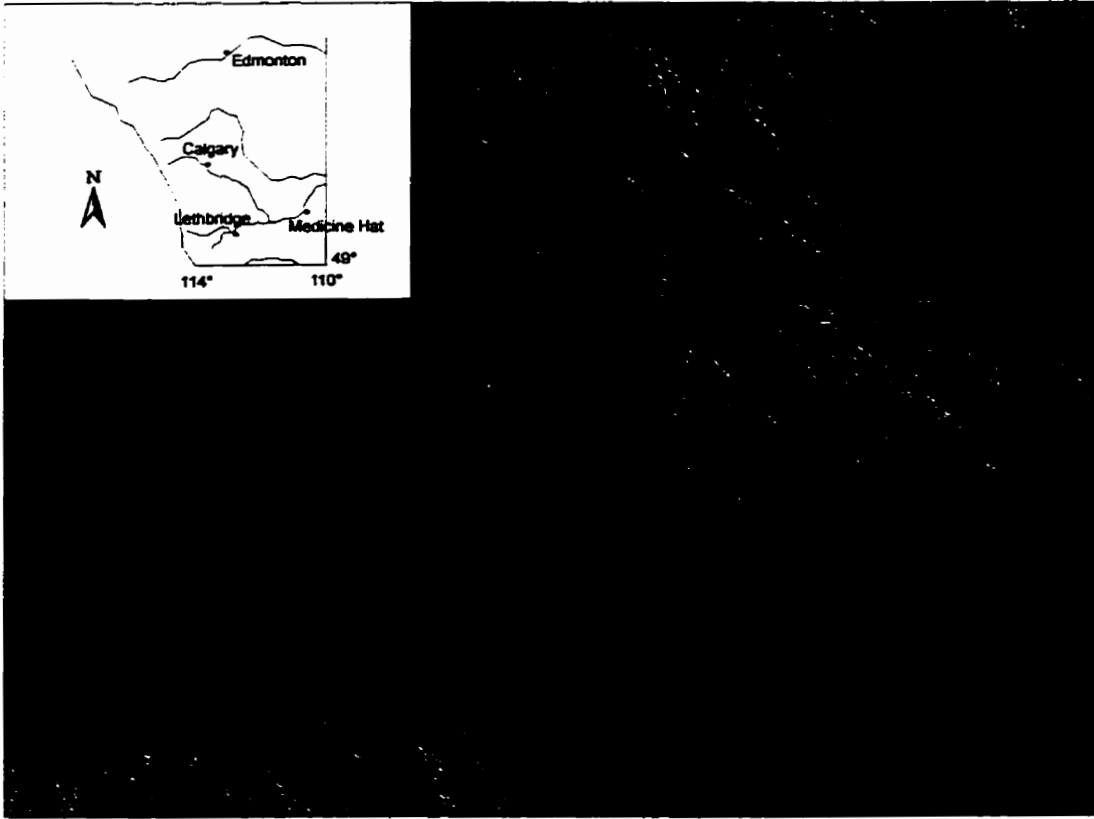
L'auteur a accordé une licence non exclusive permettant à la Bibliothèque nationale du Canada de reproduire, prêter, distribuer ou vendre des copies de cette thèse sous la forme de microfiche/film, de reproduction sur papier ou sur format électronique.

L'auteur conserve la propriété du droit d'auteur qui protège cette thèse. Ni la thèse ni des extraits substantiels de celle-ci ne doivent être imprimés ou autrement reproduits sans son autorisation.

0-612-34336-7

## ABSTRACT

A coherent pattern of subglacial landforms in southeast Alberta form an erosional landform continuum. Scoured bedrock tracts, flutes and transverse bedforms may have been produced by turbulent, subglacial sheet flows during the Livingstone Lake flood event. Tunnel channels are interpreted as products of erosion by catastrophic, channelised drainage beneath the Laurentide Ice Sheet. Transverse bedforms are interpreted as bedrock ridges modified by erosion beneath stationary waves in subglacial meltwater flows and are identical to antidunes produced by rivers. A one-dimensional hydraulic model of subglacial flow through the tunnel channel network calculates the discharge, velocity and Reynolds Numbers required for flow through channels with convex-up long profiles. Flow will occur when hydraulic head exceeds 910 m to 950 m, for the Lost River and Sage Creek channels, respectively. Maximum discharge that can be carried by the network is  $10^7 \text{ m}^3\text{s}^{-1}$ . The conclusions of this study provide further evidence for a meltwater origin for many subglacial landforms observed in Alberta and elsewhere.



DEM of the Cypress Hills-Foremost region of southeast Alberta.

## ACKNOWLEDGEMENTS

Now that my thesis has reached completion, I would like to thank my supervisor, John Shaw, for his support and encouragement over the past 2 years and without whom this thesis would never have reached this stage. You helped me find my way through the puzzle and helped me find the light at the end of the “subglacial” tunnel. Thank you, John.

Bruce Rains has also been a source of support during my time at the University of Alberta, and who has the uncanny knack of pointing out what is really important in academic life. I would also like to thank Faye Hicks from the Department of Civil Engineering for her enthusiasm in a project far removed from hydraulic engineering, but which turned out to be more closely related than either of us would have thought. I thank all my colleagues in the Department of Earth and Atmospheric Sciences, especially Mandy, Darren, Elizabeth, Rob and Jerome for encouragement, support and beer drinking. I also appreciate the able field assistance of Krista Walker, who I hope caught my enthusiasm for field work and the physical environment, and Mandy Munro-Stasiuk, who became my sounding board for ideas both in the field and the office.

This project would not have been possible without financial support from my University of Alberta PhD Scholarship, various Geological Society of America Research Grants for field work and a NSERC Operating Grant to John Shaw.

Finally, I would like to thank Mum, Dad and Sarah for your support, enthusiasm and love over the past 2 years, who made me realise that there is more to life than academics, and believed in me unconditionally, even when I couldn't believe in myself. Thank you.

## TABLE OF CONTENTS

<b>Chapter 1: Introduction</b>	<b>1 - 16</b>
Aims	1
Rationale of study	2
Study area	2
Bedrock Geology	5
Surficial Geology	5
References	13
<b>Chapter 2: The origin of subglacial landforms in southeast Alberta</b>	<b>17 - 65</b>
Introduction	17
Geomorphology	29
<i>Description</i>	29
<i>Interpretation</i>	44
Conclusions	52
References	55
<b>Chapter 3: Transverse bedforms: glaciotectonic deformation or fluvial erosion?</b>	<b>66 - 96</b>
Introduction	66
Methods	68
GPR investigation of transverse bedforms	72
Glaciotectonic deformation or fluvial erosion?	78
<i>Hypothesis 1: Fluvially modified thrust ridges</i>	80
<i>Hypothesis 2: Erosional antidune formation</i>	84
Conclusions	88
References	92

**Chapter 4: One-dimensional hydraulic modelling of subglacial tunnel channels**

**97 - 129**

Introduction	97
Fluid flow in a pressurised system	100
Model configuration	103
Model application	109
Results	110
Comparison of model results with flow parameters determined from independent evidence	120
Discussion and Conclusions	123
References	126

**Chapter 5: General discussion and conclusions**

**130 - 136**

References	134
------------	-----

## LIST OF TABLES

Table 1-1	Bedrock exposed at the surface in southeast Alberta (modified from Westgate, 1968, p. 10).	6
Table 3-1	Dielectric properties of selected materials (from pulseEKKO IV software version 4.2).	69
Table 4-1	Geometry of pipes used to configure the model as obtained from 1:50,000 topographic maps.	105
Table 4-2	Equations for conservation of mass to determine the hydraulic head at nodes 1 to 4.	107
Table 4-3	Equations for conservation of energy to determine flow parameters in each channel.	107
Table 4-4	Average channel discharge and velocity for Lost River and Sage Creek channels.	116
Table 4-5	Wavelength, velocity and densiometric Froude Numbers calculated for the transverse bedforms on the preglacial divide.	121
Table 4-6	Mean velocities required to transport surface boulders.	122
Table 4-7	Reynolds Numbers with changing discharge.	123



## LIST OF FIGURES

Figure 1-1	Map of Alberta, Canada, showing the location of the study area in southeast Alberta in relation to major cities and rivers in the province.	3
Figure 1-2	Detailed map of the study area in southeast Alberta showing major locations referred to in the study.	4
Figure 1-3	Bedrock geology map of southeast Alberta showing major formations exposed at the surface. Units are Cretaceous and Tertiary in age (modified from Westgate, 1968, Fig. 4).	7
Figure 1-4	Surficial geology map of southeast Alberta showing major landforms and drift sheets associated with early studies of the area (modified from Shetsen, 1987). Scale 1:500,000.	8
Figure 1-5	Reconstructed ice margins for the multiple Wisconsinan glacial events in southeast Alberta and northern Montana based on end moraine sequences and drift sheet identification (modified from Westgate, 1968, p. 74). Legend - 1. Elkwater event; 2. Wild Horse event; 3. Pakowki event; 4. Etzikom event; 5. Oldman event.	10
Figure 1-6	Reconstructed ice margins for multiple Late Wisconsinan glacial advances in southeast Alberta (modified from Kulig, 1996, Fig. 3). Legend - 1. Underahl advance; 2. Middle Creek advance; 3. Altawan advance; 4. Pakowki advance; 5. Etzikom advance.	11
Figure 2-1	Drumlin formation showing internal structures and distribution patterns according to the bed deformation hypothesis (from Boulton, 1987, Fig. 27).	19
Figure 2-2	Three theoretical types of drumlins produced by bed deformation - a) depositional, b) erosional, and c) deformational (modified from Hart, 1997, Fig. 2). Ice flow from right to left.	21
Figure 2-3	Observations and interpretations for the formation of selected subglacial landforms describing erosional and depositional landforms (from Shaw <i>et al.</i> , 1996, Fig. 1).	23

Figure 2-4	Map showing main components of subglacial landform assemblages associated with sheet flow erosion by the Livingstone Lake flood event, central and southern Alberta (modified from Rains <i>et al.</i> , 1993, Fig. 2).	24
Figure 2-5	Depositional and erosional drumlin types formed by subglacial meltwater processes: a) parabolic and spindle drumlins at Livingstone Lake, north Saskatchewan produced by deposition in subglacial cavities (from Shaw, 1996, Fig. 7.30a); b) Classical drumlin types eroded by subglacial meltwater and left as remnants (from Shaw, 1996, Fig. 7.29).	25
Figure 2-6	Hill-shaded digital elevation model (DEM) of southeast Alberta showing assemblage of subglacial landforms (sun angle at 45°N, elevation 25°).	30
Figure 2-7	Hill-shaded DEM of southeast Alberta showing assemblage of subglacial landforms (sun angle at 315°N, elevation 25°).	31
Figure 2-8	Glaciotectonically deformed bedrock in transverse ridge on preglacial divide showing a truncated surface.	33
Figure 2-9	a) Channel scour and infill in glaciofluvial sediments, b) Glaciofluvial sands with climbing ripples and cross-bedding, exposed at Pinhorn Grazing Reserve (south of Milk River) and preserved within scoured bedrock tract. Flow from left to right.	34
Figure 2-10	Photo mosaic showing undulating erosion surface at Sage Creek. Erosion surface truncates Late Cretaceous sandstone and shale, and glacial deposits producing hummocky terrain. Erosion also produces a flat topography where flow velocities were increased.	35
Figure 2-11	Boulder lags comprising mainly Shield clasts resting directly on bedrock surface indicate deposition and subsequent removal of glacial sediment by erosion capable of moving all but the largest boulders.	36
Figure 2-12	Bullet-shaped boulders with faceted faces were observed on the bedrock surface, indicating active basal transport and possible lodgement below the Laurentide Ice Sheet during ice advance.	38

Figure 2-13	Photographs showing remnant ridges within the main scoured tract showing characteristic proximal scours at upstream end of ridges. Ridges are composed of Late Cretaceous bedrock in these examples. Flow was from right to left.	39
Figure 2-14	Glaciofluvial sands with Type A climbing ripples and plane bedded sands preserved in remnant ridge at Onefour within main scoured zone. Sands unconformably overlie massive gravels (not seen in photo) which rest directly on bedrock.	40
Figure 2-15	Eroded depressions (s-forms), oriented NW-SE, superimposed on scoured bedrock tract at Onefour.	41
Figure 2-16	Lost River channel showing characteristic tunnel channel morphology and Late Cretaceous bedrock exposed along valley walls.	42
Figure 2-17	Long profiles for Lost River and Sage Creek showing convex-up profiles, indicative of subglacial meltwater erosion across the preglacial divide.	43
Figure 2-18	Transverse ridges observed on the preglacial divide showing Type 1, 3D wave forms; Type 2, nested wave forms; and Type 3, rhomboidal, interfering forms.	45
Figure 3-1	Hill-shaded DEM of southeast Alberta showing complex suite of transverse ridges on the preglacial divide (sun angle 315°N, elevation 25°).	66
Figure 3-2	Principle of ground penetrating radar (GPR) based on the propagation and reflection of electromagnetic energy from reflectors located beneath the surface. Depth of reflectors is a function of the two-way travel time of the signal and the near-surface velocity of the substrate material (modified from Jol and Smith, 1991, Fig. 3).	68
Figure 3-3	GPR unit in operation. 25 MHz antenna, showing transmitter/receiver units connected to two 6V batteries, seen in foreground. A fibre optic cable carries signals from the transmitter/receiver units to the GPR console carried in a backpack. Console is powered by a 12V battery. Traces are collected at 1 m intervals and displayed and recorded on a laptop computer operated by field assistant.	70

Figure 3-4	Late Cretaceous bedrock is exposed across the transverse ridge being profiled, although structure cannot be discerned from these limited exposures. Exposure is 75 cm high.	72
Figure 3-5	Topographic profile of transverse ridge profiled by GPR. VE=8X.	73
Figure 3-6	a) GPR profile obtained from reflection survey of transverse ridge. b) Interpreted profile.	74
Figure 3-7	Folded bedrock in transverse ridge, possibly resulting from glaciotectonic thrusting from the northwest by the advancing Laurentide Ice Sheet. The ridge form is erosional with the syncline being truncated at the surface.	76
Figure 3-8	Stereopair showing transverse ridges at study site with flutes superimposed on ridge surface. Scale 1:60 000. L refers to elongate lakes between ridges.	78
Figure 3-9	Hill-shaded DEM showing Type 1, Type 2, and Type 3 wave forms across the preglacial divide. These patterns may be controlled by flow characteristics associated with stationary waves within subglacial meltwater flows.	80
Figure 3-10	Formation of antidunes beneath stationary waves generated by a discontinuity to flow (from Yalin, 1972, Fig. 7.10). (For key to notation, see List of Symbols).	84
Figure 3-11	Generation of stationary waves in subglacial meltwater flows along a density interface. Perturbations on the bed may fix stationary waves along this density interface although this is not a requirement to wave formation.	85
Figure 3-12	Rhomboidal ripples produced in fine sand (from Allen, 1982, Fig. 10.13) are similar to Type 3, rhomboidal interfering forms identified in the study area.	87
Figure 3-13	Examples of transverse ridges and flutes produced by various fluid flows: a) Ridges and flutes produced by wind in sand. Flow away from reader; b) Transverse ribs and streamlined forms on the Peyto Glacier outwash plain, Alberta, Canada. Flow from right to left (Allen, 1982, Fig. 10.4).	88

Figure 4-1	Hill-shaded DEM showing tunnel channel network in southeast Alberta chosen for one-dimensional hydraulic model, with the locations of sites in Table 4-5 also marked.	103
Figure 4-2	Simplified network of channels and nodes used in model configuration for one-dimensional hydraulic flow model showing flow directions. Not to scale.	104
Figure 4-3	Generalised cross-sections of channels 1 to 6 used in model configuration.	106
Figure 4-4	Effect of channel roughness on discharge, velocity and Reynolds Number.	110
Figure 4-5	Effect of channel roughness on hydraulic head and head losses.	112
Figure 4-6	Hydraulic head required to drive flow the across the topographic divide in Lost River channel. VE=40X.	113
Figure 4-7	Hydraulic head required to drive the flow across the topographic divide in Sage Creek channel. VE=100X.	114 115
Figure 4-8	Effect of discharge on head losses in channels 1 to 6.	118
Figure 4-9	Effect of discharge on hydraulic head at nodes 2 to 4.	119

## LIST OF SYMBOLS

A	channel cross-sectional area perpendicular to flow
C	Chezy roughness coefficient
d	flow depth
D	sediment diameter
E	energy per unit mass
Fr	Froude Number
Fr <sub>d</sub>	densimetric Froude Number
g	acceleration due to gravity
G	mass flux per unit time
h	flow depth (Fig. 3-10 only)
h <sub>i</sub>	ice thickness
h <sub>t</sub>	head loss
H	hydraulic head
L	length of domain
n	Manning's roughness coefficient
p	water pressure
p <sub>i</sub>	ice overburden pressure
ρ	density of fluid
ρ <sub>i</sub>	density of ice
q <sub>s</sub>	sediment discharge
Q	discharge
S	channel gradient
S <sub>r</sub>	slope of the energy grade line
t	time coordinate
R	hydraulic radius
Re	Reynolds Number
V	velocity

$x$	longitudinal coordinate
$z$	vertical coordinate
$\gamma$	specific weight of fluid
$\lambda$	wavelength of surface waves (Fig. 3-10)
$\lambda$	wavelength
$\Lambda$	wavelength of bedforms (Fig. 3-10 only)

## CHAPTER 1: INTRODUCTION

### Aims

The study of subglacial geomorphology is a major focus of glacial and glaciological research. However, there is no consensus as to the processes responsible for producing the observed diversity of subglacial landforms (c.f., Menzies and Rose, 1989; Dardis and McCabe, 1994; Piotrowski, 1997). Generally, subglacial landforms have been interpreted as products of glaciotectonic deformation of the substrate (e.g., Boulton, 1979, 1987; Boyce and Eyles, 1991; Benn, 1994a; Hart, 1995a, 1997; Eklund and Hart, 1996) or produced by subglacial meltwater processes (e.g., Shaw, 1983, 1996; Shaw *et al.*, 1989; Kor *et al.*, 1991; Rains *et al.*, 1993; Brennand, 1994; Brennand and Shaw, 1994; Sjogren and Rains, 1995; Shaw *et al.*, 1996; Munro and Shaw, 1997). These hypotheses invoke very different processes to explain common morphological features. The processes have broad implications for ice sheet dynamics and are fundamental to our understanding of ice response to climate change.

The principal aim of this research is to investigate the subglacial landscape of a region in southeast Alberta and determine the processes that produced the landform assemblage. The study area is located towards the maximum southwestern position of the Laurentide Ice Sheet at circa. 18 ka BP and, hence, records landscape development in a sub-marginal setting. Also, the field area forms part of the proposed Livingstone Lake flood path (Rains *et al.*, 1993) and, if the meltwater hypothesis is correct, then floodwaters must have crossed southeast Alberta. Therefore, both the bed deformation and meltwater hypotheses for subglacial landscape development can be tested within the field area and the origin of the landform assemblage determined. The ultimate aims of the research are to:

- 1) Develop a generalised model of subglacial processes for southeast Alberta,
- 2) Evaluate the existing models of subglacial landform evolution,
- 3) Develop a one-dimensional, hydraulic model of flow through a tunnel channel network in southeast Alberta.



## **Rationale of study**

There has been recent interest in modelling past and present ice sheets with a view to understanding Quaternary climate change (e.g., Huybrechts, 1990; Huybrechts *et al.*, 1991; Boulton *et al.*, 1995; Huybrechts and T'Siobell, 1995; Marshall *et al.*, 1996). Landforms are generally used as ice flow indicators and for reconstructing the extent, profile and hydrology of the Laurentide Ice Sheet (e.g., Dyke and Prest, 1987a; Boulton and Clark, 1990b; Clark, 1993). Hence, a correct interpretation of the geomorphology is essential to the model assumptions.

However, the two main theories proposed for subglacial landscape development imply dominance of quite different processes in the subglacial environment. With regard to the theoretical basis of glacial geomorphology, Shaw (1996, p. 183) notes, "The actualistic approach has been most influential in recent years. In its most conservative form, actualism holds that only processes that are observed directly give acceptable explanations". However, we cannot directly observe the processes which produced subglacial landforms beneath the Laurentide Ice Sheet and modern glaciers may not be suitable analogues for Laurentide processes. Geomorphology is, by definition, a deductive science where past forms can only be approached by fantasy and induction unless formal mathematics can be applied to the problem. Therefore, observations of landforms in deglaciated areas provide the main approach for determining the subglacial processes of past ice sheets. Thus, it is necessary to further investigate subglacial geomorphology to gain a better understanding of how ice sheets and glaciers operate.

## **Study Area**

The study area is located south and southwest of the Cypress Hills in southeast Alberta, and borders Saskatchewan to the east and Montana to the south (Figs. 1-1, 1-2). It lies within the limit of the Late Wisconsinan glaciation (e.g., Dyke and Prest, 1987a, b). The study area straddles the preglacial drainage divide that separates northeasterly drainage into Hudson Bay and the Beaufort Sea from southerly drainage into the Mississippi system and the Gulf of Mexico. Modern drainage in the area has been

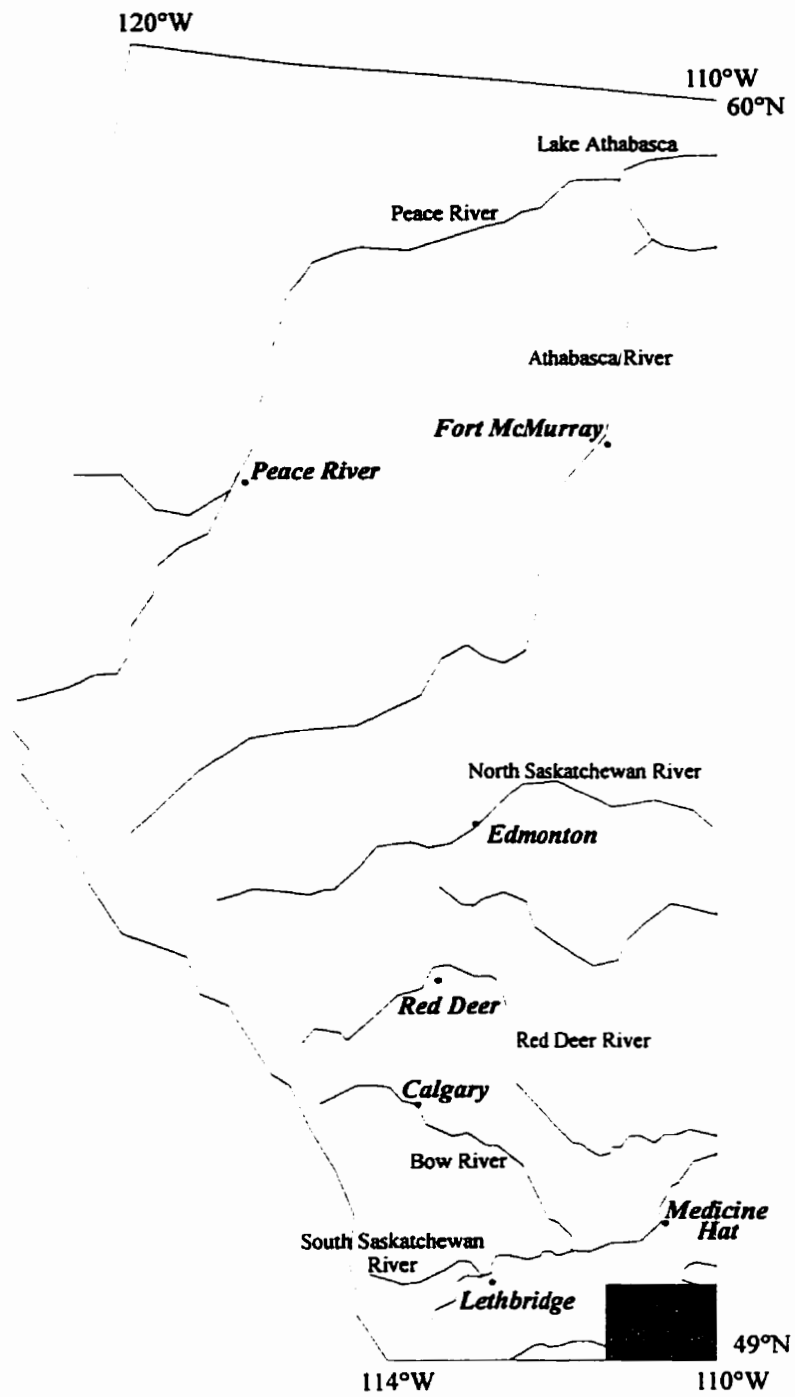


Figure 1-1. Map of Alberta, Canada, showing the location of the study area in southeast Alberta in relation to major cities and rivers in the province.

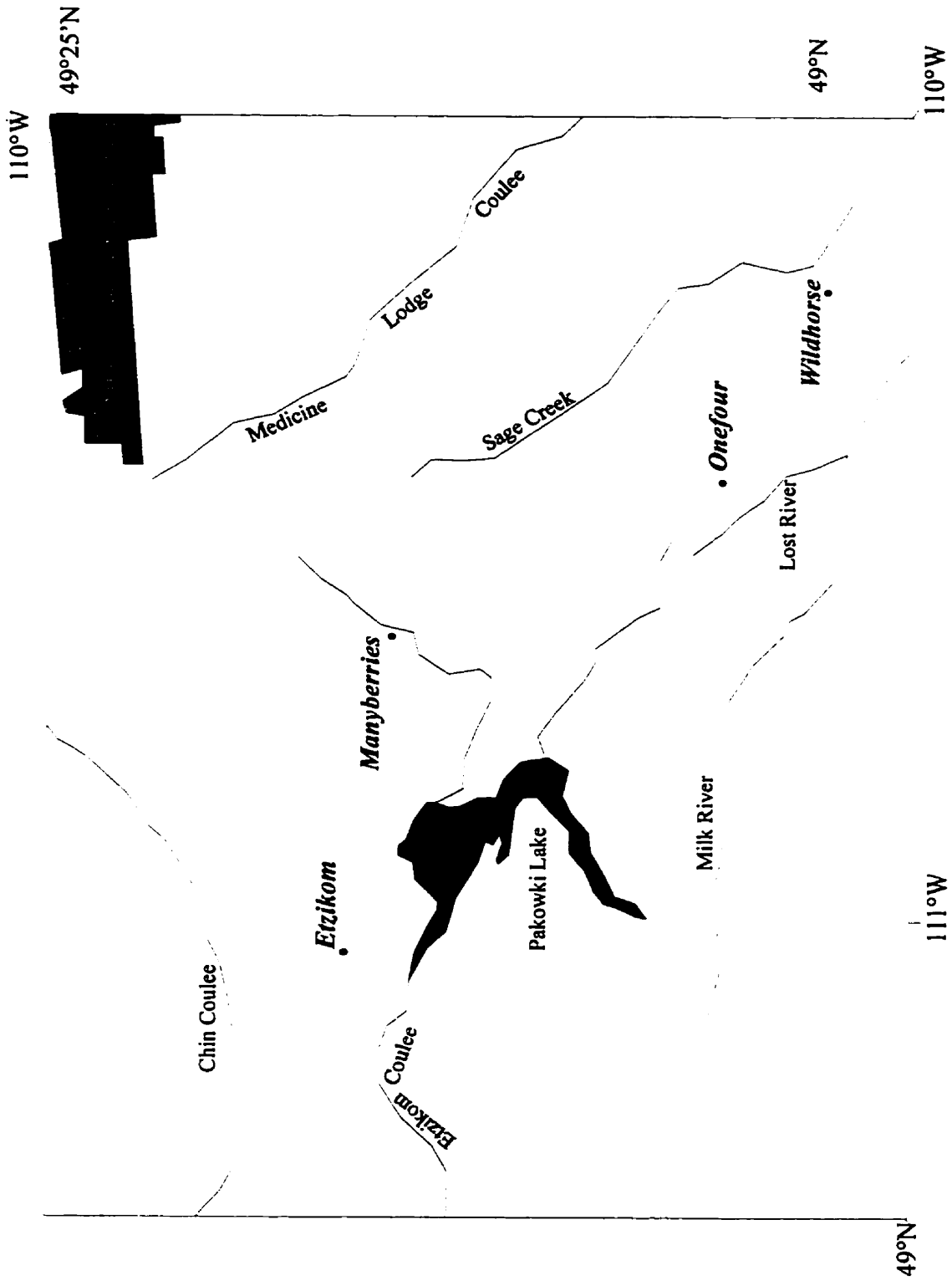


Figure 1-2. Detailed map of the study area in southeast Alberta showing major locations referred to in the study.

modified by glaciation (Westgate, 1968) with the Milk River now draining across the preglacial divide.

The area comprises a gently undulating relief with a number of major coulees dissecting the region. Pakowki Lake, to the northwest of the preglacial divide, forms an internal drainage basin representing the lowest point in the region. Maximum elevations are found on the Cypress Hills and the Sweet Grass Hills which were partly nunataks during the Late Wisconsinan glaciation where maximum ice thickness locally was approximately 500 m (Stalker, 1965; Catto, 1983).

### **Bedrock Geology**

Earlier work on the bedrock geology of the study area was reviewed by Westgate (1968). Apart from the Tertiary conglomerate and sandstone of the Cypress Hills, exposed bedrock in the study area comprises Late Cretaceous sandstone and shale, with minor bentonite layers (Table 1-1; Fig. 1-3). It is poorly lithified and friable. Hence, the fine-grained glacial deposits mainly reflect local bedrock sources, although they contain Shield erratics, indicative of Laurentide glaciation (Bayrock, 1962; Westgate, 1968). The marine bedrock, where it is close to the surface, results in solonchic soils (e.g., Rains *et al.*, 1993).

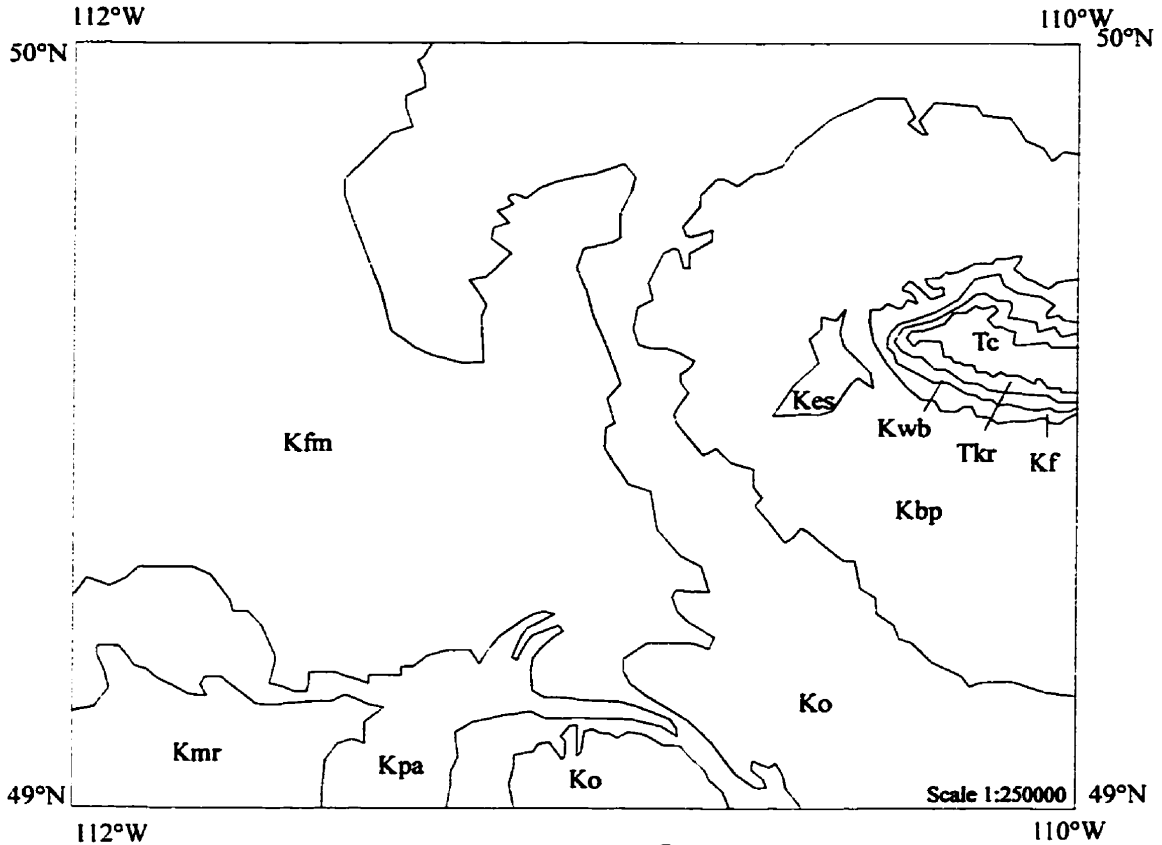
The southern Alberta Plains are situated on a broad, northerly plunging anticline known as the Sweet Grass Arch (Westgate, 1968). In the study area, which lies to the east of the fold axis, beds dip to the east and northeast. Some minor structural control of the surficial geology is noted by Westgate (1968).

### **Surficial Geology**

The established surficial geology of southeast Alberta identifies a range of glacial and deglacial landforms interpreted as evidence for multiple glacial events in the region (Fig. 1-4; Westgate, 1968; Kulig, 1996). Identification of end moraine sequences based on existing theories of landform development leads to these conclusions.

ERA	PERIOD	EPOCH	FORMATION	MAP KEY	MAIN LITHOLOGY
CENOZOIC	Quaternary	Holocene	Alluvium, aeolian		
		Pleistocene	Glacial deposits Saskatchewan sands & gravels		
	Tertiary	Pliocene Miocene	Flaxville		quartzose gravels
		Oligocene	Cypress Hills	Tc	conglomerate w/ minor sand and bentonite
		Paleocene	Ravenscrag	Tkr	non-marine, thin-bedded, fine grained sandstone, siltstone & shale
MESOZOIC	Cretaceous	Upper	Frenchman	Kf	thick, massive or coarsely cross-bedded medium grained sandstone
			Battle	Kwb	dark bentonite shale w/ thin tuff beds
			Whitemud	Kwb	sandstone & white clay w/ shale and lignite
		Cretaceous	Eastend	Kes	massive, medium grained sandstone, shale & carbonaceous beds
			Bearpaw	Kbp	fissile, marine shale w/ some sandy beds w. bentonite & ironstone concretions
			Oldman	Ko	continental origin, argillaceous sandstone with shale
			Foremost	Kfm	arenaceous shale, freshwater shaly siltstone, sandstone & coal
			Pakowki	Kpa	dark grey marine shale w/ thin sandstone, siltstone, bentonite
			Milk River	Kmr	massive sandstone grading into freshwater shales w/ coal and bentonite
			Lower Cretaceous	Alberta	

Table 1-1. Bedrock exposed at the surface in southeast Alberta (modified from Westgate, 1968, p. 10).



- |                 |                   |                   |                     |
|-----------------|-------------------|-------------------|---------------------|
| <u>Tertiary</u> |                   | <u>Cretaceous</u> |                     |
| Tc              | Cypress Hills Fm. | Kf                | Frenchman Fm.       |
| Tkr             | Ravenscrag Fm.    | Kwb               | Battle/Whitemud Fm. |
|                 |                   | Kes               | Eastend Fm.         |
|                 |                   | Kbp               | Bearpaw Fm.         |
|                 |                   | Ko                | Oldman Fm.          |
|                 |                   | Kfm               | Foremost Fm.        |
|                 |                   | Kpa               | Pakowki Fm.         |
|                 |                   | Kmr               | Milk River Fm.      |

Figure 1-3. Bedrock geology map of southeast Alberta showing major formations exposed at the surface. Units are Cretaceous and Tertiary in age (modified from Westgate, 1968, Fig. 4).

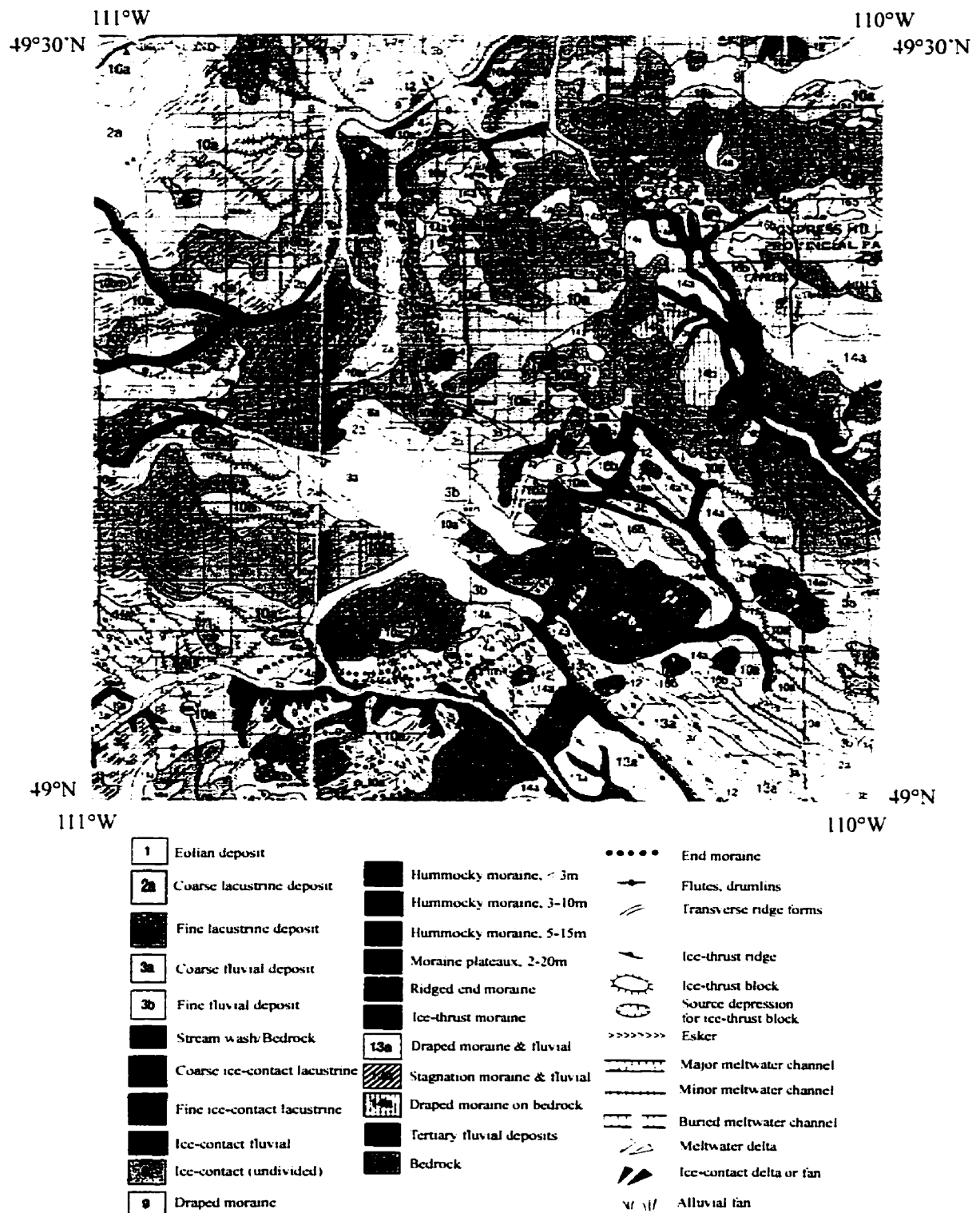


Figure 1-4. Surficial geology map of southeast Alberta showing major landforms and drift sheets associated with early studies of the glacial geomorphology in the region (modified from Shetsen, 1987). Scale 1:500,000.

The surficial geology of the Foremost-Cypress Hills region of Alberta was first documented by Dawson (1885) in which he noted the extent to which glaciation modified the preglacial landscape. This early work advocated that a 'glacial sea' was responsible for the observed landforms. Later workers advocated erosion and deposition from a 'Glacial Ice Sheet' (e.g., Dowling, 1917; Alden, 1924; Williams, 1929; Williams and Dyer, 1930). These later researchers described the distribution of ice-marginal channels and glacial landforms. More detailed analyses of glacial features were conducted by Johnston and Wickenden (1931), who delineated moraines and glacial lake deposits in southern Saskatchewan and Alberta that became progressively younger to the northeast and had a northwest-southeast trend. Wickenden (1937) also observed a major end moraine sequence that was later correlated with the Lethbridge moraine of Stalker (1977).

The most detailed investigation of this region was conducted by Westgate (1964, 1968) with reinterpretation by Kulig (1996). Westgate (1968) identified various glacial landforms and interpreted them as evidence of five glacial advances into the study area (Fig. 1-5). Westgate (1968) identified extensive areas of ground moraine and hummocky terrain of various relief, flutes, eskers, meltwater channels, thrust ridges, and minor transverse ridges. Surficial sediments include lodgement till, melt-out till, ice-disintegration sediment and glacial lake deposits. The earliest event identified by Westgate (1968) is an Early Wisconsinan advance extending into Montana. Subsequent advances occurred during the Late Wisconsinan but were less extensive. Landforms and sediments in southeast Alberta occurred in a predominately depositional environment. Major meltwater channels dissecting the region were interpreted as proglacial or ice-marginal channels which formed during deglaciation (Westgate, 1968).

Kulig (1996) reinterpreted the glacial stratigraphy and geomorphology in southeast Alberta and southwest Saskatchewan, and proposed a 5-stage sequence in the region (Fig. 1-6). In comparison to earlier researchers, Kulig (1996) did not identify any deposits of pre-Late Wisconsinan age. Kulig (1996) used drift sheets and inferred moraine limits to delineate multiple Late Wisconsinan glacial events in southeast Alberta.

Thus, the conventional interpretations of glacial stratigraphy and history of the study area invoke multiple glacial events, separated by complete or partial deglaciation,



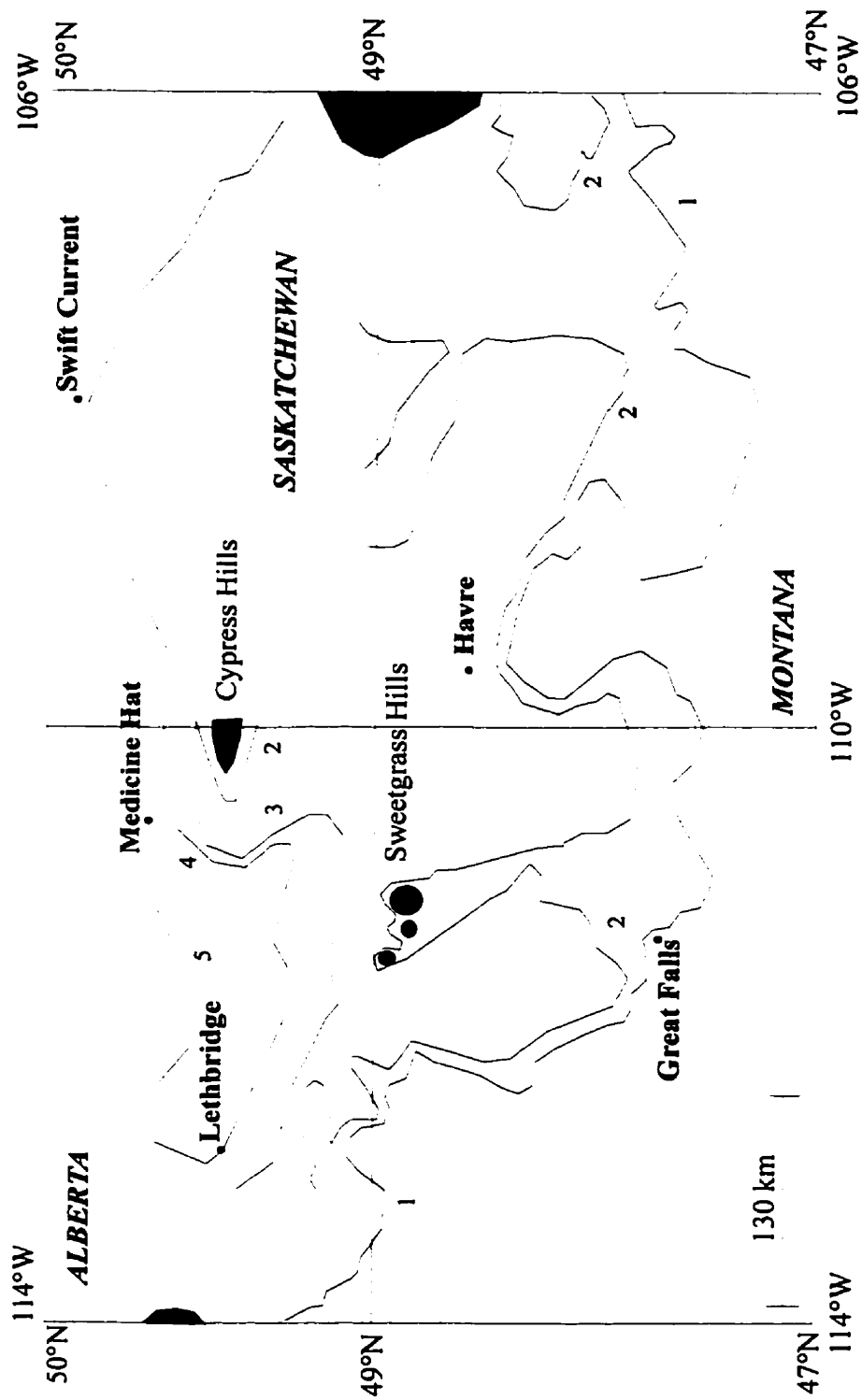


Figure 1-5. Reconstructed ice margins for multiple Wisconsinian glacial events in southeast Alberta and Montana based on end moraine sequences and drift sheet identification (modified from Westgate, 1968, p.74). Legend - 1. Elkwater event; 2. Wild Horse event; 3. Pakowki event; 4. Etzikom event; 5. Oldman event.

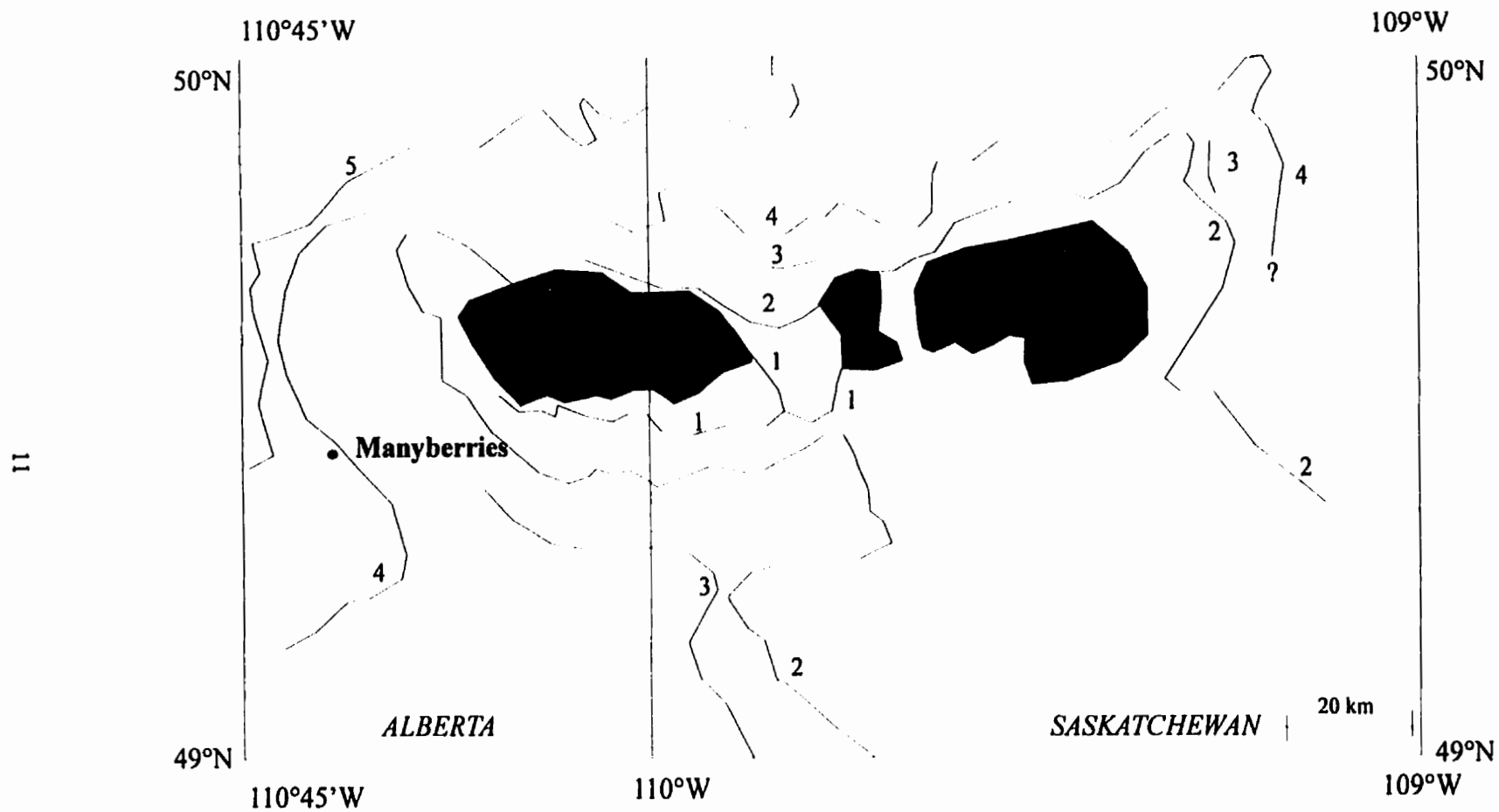


Figure 1-6. Reconstructed ice margins for multiple Late Wisconsin glacial advances in southeast Alberta (modified from Kulig, 1996, F.g. 3). Legend - 1. Underahl advance; 2. Middle Creek advance; 3. Altawan advance; 4. Pakowki advance; 5. Etzikom advance.

with ice stagnation becoming more important between younger glacial episodes. However, recent studies have shown that the Western Plains were subject to a single, Late Wisconsinan glaciation (e.g., Liverman *et al.*, 1989; Young *et al.*, 1994; Jackson *et al.*, 1996), and not to multiple glaciations. The Late Wisconsinan, Laurentide Ice Sheet reached southern Montana during glacial maximum and did not terminate at the Lethbridge moraine as previously supposed (c.f., Stalker, 1977; Dyke and Prest, 1987; Christiansen and Sauer, 1988; Kulig, 1996).

However, the glacial stratigraphy of the study area is unimportant for this particular study and it is provided here only for completeness. Field observations are at odds with widespread glacial deposition, instead reflecting an erosional, subglacial environment formed during the Late Wisconsinan glacial “maximum” and prior to widespread deglaciation of the region. Also, recent work has shown that traditional hypotheses for landform development may not adequately explain all glacial landform assemblages in Alberta (e.g., Rains *et al.*, 1993; Sjogren and Rains, 1995; Shaw, 1996; Munro and Shaw, 1997). Thus, previous interpretations of the glacial landscape in southeast Alberta should be re-evaluated. This study aims to determine the origin for the glacial landform assemblage observed in southeast Alberta and is independent of previous studies in the region.

## References

- Alden, W.C. 1924. Physiographic development of the Northern Great Plains. *Bulletin, Geological Society of America*, **35**, 385-424.
- Bayrock, L.A. 1962. Heavy minerals in till of central Alberta. *Journal of Alberta Society of Petroleum Geology*, **10**, 171-184.
- Benn, D.I. 1994a. Fluted moraine formation and till genesis below a temperate glacier: Slettmarkbreen, Jotunheimen, Norway. *Sedimentology*, **41**, 279-292.
- Boulton, G.S. 1979. Processes of glacier erosion on different substrata. *Journal of Glaciology*, **23**, 15-37.
- Boulton, G.S. 1987. A theory of drumlin formation by subglacial sediment deformation. In Menzies, J. and Rose, J. (eds) *Drumlin Symposium*. Balkema, Rotterdam, 25-80.
- Boulton, G.S. and Clark, C.D. 1990b. The Laurentide ice sheet through the last glacial cycle: the topology of drift lineations as a key to the dynamic behaviour of former ice sheets. *Transactions of the Royal Society of Edinburgh: Earth Sciences*, **81**, 327-347.
- Boulton, G.S., Hulton, N.J. and Vautrevers, M. 1995. Ice sheet models as tools for paleoclimatic analysis: the example of the European ice sheet through last glacial cycle. *Annals of Glaciology*, **21**, 103-110.
- Boyce, J.I. and Eyles, N. 1991. Drumlins carved by deforming till streams below the Laurentide Ice Sheet. *Geology*, **19**, 787-790.
- Brennand, T.A. 1994. Macroforms, large bedforms and rhythmic sedimentary sequences in subglacial eskers: genesis and meltwater regime. *Sedimentary Geology*, **91**, 9-55.
- Brennand, T.A. and Shaw, J. 1994. Tunnel channels and associated bedforms, south-central Ontario: their implications for ice sheet hydrology. *Canadian Journal of Earth Sciences*, **31**, 505-522.
- Catto, N.R. 1983. Loess in the Cypress Hills, Alberta, Canada. *Canadian Journal of Earth Sciences*, **20**, 1159-1167.
- Christiansen, E.A. and Sauer, E.K. 1988. Age of the Frenchman Valley and associated drift south of the Cypress Hills, Saskatchewan, Canada. *Canadian Journal of Earth Sciences*, **25**, 1703-1708.

- Clark, C.D. 1993. Mega-scale lineations and cross-cutting ice-flow landforms. *Earth Surface Processes and Landforms*, **18**, 1-29.
- Dardis, G.F. and McCabe, A.M. 1994. Subglacial processes, sediments and landforms - an introduction. *Sedimentary Geology*, **91**, 1-8.
- Dawson, G.M. 1885. Report on the vicinity of the Bow and Belly Rivers. *Geological Survey of Canada, Report of Progress 1882-83-84*, pt. C, 168pp.
- Dowling, D.B. 1917. The southern plains of Alberta. *Geological Survey of Canada, Memoir*, **93**, 200pp.
- Dyke, A.S. and Prest, V.K. 1987a. Late Wisconsinan and Holocene history of the Laurentide ice sheet. *Geographie physique et Quaternaire*, **41**, 237-263.
- Dyke, A.S. and Prest, V.K. 1987b. The Late Wisconsinan Maximum. *GSC Map 1702a* (1:5,000,000).
- Eklund, A. and Hart, J.K. 1996. Glaciotectonic deformation within a flute from the Isfallsglaciären, Sweden. *Journal of Quaternary Science*, **11**, 299-310.
- Hart, J.K. 1995a. Drumlin formation in southern Anglesey and Arvon, north west Wales. *Journal of Quaternary Science*, **10**, 3-14.
- Hart, J.K. 1997. The relationship between drumlins and other forms of subglacial glaciotectonic deformation. *Quaternary Science Reviews*, **16**, 93-107.
- Huybrechts, P. 1990. The Antarctic ice sheet during the last glacial-interglacial cycle: a 3-D experiment. *Annals of Glaciology*, **14**, 115-119.
- Huybrechts, P., Letreguilly, A. and Reeh, N. 1991. The Greenland Ice Sheet and greenhouse warming. *Palaeogeography, Palaeoclimatology, Palaeoecology*, **89**, 399-412.
- Huybrechts, P. and T'Siobell, S. 1995. Thermomechanical modelling of Northern hemisphere ice sheets with a 2-level mass balance parameterisation. *Annals of Glaciology*, **21**, 111-116.
- Jackson, L.E., Little, E.C., Leboe, E.R. and Holme, P.J. 1996. A re-evaluation of the paleogeography of the maximum continental and montane advances, southwestern Alberta. *Geological Society of Canada, Current Research 1996-A*, 165-173.

- Johnston, W.A. and Wickenden, R.T.D. 1931. Moraines and glacial lakes in southern Saskatchewan and southern Alberta. *Transactions, Royal Society of Canada, Series 3, sec. IV, 25, 29-44.*
- Kor, P.S.G., Shaw, J. and Sharpe, D.R. 1991. Erosion of bedrock by subglacial meltwater, Georgian Bay, Ontario: a regional view. *Canadian Journal of Earth Sciences, 28, 623-642.*
- Kulig, J.J. 1996. The glaciation of the Cypress Hills of Alberta and Saskatchewan and its regional implications. *Quaternary International, 32, 53-77.*
- Liverman, D.G.E., Catto, N.R. and Rutter, N.W. 1989. Laurentide glaciation in west-central Alberta: a single (Late Wisconsinan) event. *Canadian Journal of Earth Sciences, 26, 266-274.*
- Marshall, S.J., Clarke, G.K.C., Dyke, A.S. and Fisher, D.A. 1996. Geologic and topographic controls on fast flow in the Laurentide and Cordilleran Ice Sheet. *Journal of Geophysical Research, 101, 17827-17839.*
- Menzies, J. and Rose, J. 1989. Subglacial bedforms - an introduction. *Sedimentary Geology, 62, 117-122.*
- Munro, M.J. and Shaw, J. 1997. Erosional origin of hummocky terrain in south-central Alberta, Canada. *Geology, 25, 1027-1030.*
- Piotrowski, J.A. 1997. Subglacial environments - an introduction. *Sedimentary Geology, 111, 1-7.*
- Rains, R.B., Shaw, J., Skoye, R., Sjogren, D. and Kvill, D. 1993. Late Wisconsinan subglacial megaflood paths in Alberta. *Geology, 21, 323-326.*
- Shaw, J. 1983. Drumlin formation related to inverted melt-water erosional marks. *Journal of Glaciology, 29, 461-479.*
- Shaw, J. 1996. A meltwater model for Laurentide subglacial landscapes. In McCann, S.B. and Ford, D.C. (eds) *Geomorphology Sans Frontieres*. Wiley, Chichester, 181-236.
- Shaw, J., Kvill, D. and Rains, R.B. 1989. Drumlins and catastrophic floods. *Sedimentary Geology, 62, 177-202.*
- Shaw, J., Rains, R.B., Eyton, R. and Weissling, L. 1996. Laurentide subglacial outburst floods: landform evidence from digital elevation models. *Canadian Journal of Earth Sciences, 33, 1154-1168.*

- Shetsen, I. 1987. Quaternary Geology, southern Alberta. *Alberta Research Council Map* (1:50,000).
- Sjogren, D. and Rains, R.B. 1995. Glaciofluvial erosional morphology and sediments of the Coronation-Spondin Scabland, east-central Alberta. *Canadian Journal of Earth Sciences*, **32**, 565-578.
- Stalker, A. MacS. 1965. Pleistocene ice surface, Cypress Hills area. Alberta Society of Petroleum Geologists, Calgary, Alberta. 15<sup>th</sup> Annual Conference Guidebook, part 1, 142-161.
- Stalker, A. MacS. 1977. The probable extent of Classical Wisconsinan ice in southern and central Alberta. *Canadian Journal of Earth Sciences*, **14**, 2614-2619.
- Westgate, J.A. 1964. *Surficial Geology of the Foremost-Cypress Hills area*. PhD thesis, Department of Geology, University of Alberta, 209pp.
- Westgate, J.A. 1968. Surficial Geology of the Foremost - Cypress Hills area, Alberta. *Research Council of Alberta, Bulletin*, **22**, 121pp.
- Williams, M.Y. 1929. The physiography of the southwestern plains of Canada. *Transactions of Royal Society of Canada, Series 3*, **23**, 61-69.
- Williams, M.Y. and Dyer, W.S. 1930. Geology of southern Alberta and southwestern Saskatchewan. *Geological Survey of Canada, Memoir*, **163**, 160pp.
- Wickenden, R.T.D. 1937. Age relations of glacial deposits in southeastern Alberta and southwestern Saskatchewan (abs). *Royal Society of Canada, Series 3*, **31**, p.cxlirii.
- Young, R.R., Burns, J.A., Smith, D.G, Arnold, L.D. and Rains, R.B. 1994. A single Late Wisconsinan, Laurentide glaciation, Edmonton area and southwestern Alberta. *Geology*, **22**, 683-686.

## **CHAPTER 2: THE ORIGIN OF SUBGLACIAL LANDFORMS IN SOUTHEAST ALBERTA, CANADA**

### **Introduction**

Boulton (1986) advocated “a paradigm shift in glaciology” (p.18) whereby subglacial deformation could explain glacier dynamics and landform associations. However, recent research in Alberta and elsewhere in Canada by Shaw and co-workers challenges this assertion. There is no consensus on the origin of subglacial landforms (e.g., Menzies and Rose, 1989; Dardis and McCabe, 1994; Piotrowski, 1997). The two main competing hypotheses explaining subglacial landforms are: 1) the bed deformation hypothesis (e.g., Boulton, 1974, 1987, 1996a; Boulton and Hindmarsh, 1987), and 2) the meltwater hypothesis (e.g., Shaw, 1983, 1996; Shaw *et al.*, 1989). Sound interpretations of subglacial processes as obtained from landform studies have implications for glacier dynamics and ice sheet morphology (e.g., Boulton and Jones, 1979; Alley *et al.*, 1986; Shoemaker, 1991, 1992a, b; Boulton *et al.*, 1995b), and subglacial hydrology and thermal regime (Boulton and Dobbie, 1993; Walder and Fowler, 1994; Boulton and Caban, 1995; Boulton *et al.*, 1995b). These hypotheses are discussed below.

Studies by Boulton (1979), Alley *et al.*, (1986), Boulton and Hindmarsh (1987) and Clarke (1987) have shown that where glacially induced shear stresses deform sediment at the ice bed there is a resulting increase in ice velocity. Such sediment deformation is known as subglacial glaciotectionic deformation (Hart and Boulton, 1991). Identification of subglacially deformed sediment leads to connections between landforms, subglacial deformation processes and zones of fast glacier movement (e.g., Boulton and Clark, 1990a, b; C.D. Clark, 1993; P.U. Clark, 1994; Evans, 1996).

Direct observations of subglacial deformation were made by Boulton and co-workers at Breidamerkurjökull, Iceland (e.g., Boulton, 1974; Boulton and Jones, 1979; Boulton and Hindmarsh, 1987). Segmented dowels placed in subglacial sediments were displaced by strain within the sediment, and calculations show that this deformation accounted for 80-95 % of glacier motion (Boulton and Hindmarsh, 1987). Other



examples of *in situ* deformation of subglacial sediments have been obtained for Trapridge Glacier, Yukon, and Storglaciären, Sweden (Blake *et al.*, 1992; Iverson *et al.*, 1995).

The deformation of subglacial sediments is primarily controlled by the strength of the material as determined by Coulomb's law. Provided that there is a free drainage system, sediments with high permeability and porosity allow water to drain quickly, thus, maintaining sediment strength and limiting deformation. Sediment with low effective pressure has reduced strength and is more conducive to deformation. Bed deformation causes erosion, when immobile sediment beneath the base of the deforming layer is set in motion. Deposition occurs when all or some of the deforming layer comes to rest (Alley, 1989; Hart and Boulton, 1991; Hart, 1995a; Boulton, 1996a).

Studies suggest that deformed sediment is expected where a glacier has moved over a soft bed (Boulton and Hindmarsh, 1987). However, the destruction of primary structures in highly strained sediment makes identification of deformation tills problematic (Boulton, 1987; Hart *et al.*, 1990). Thus, similar deposits may be identified as deformation tills (Boulton and Jones, 1979; Alley, 1991; Hicock and Dreimanis, 1992a), or melt-out tills (Clayton *et al.*, 1989; Mickelson *et al.*, 1992; Ronnert and Mickelson, 1992). Grain-size and clast-fabric analyses are commonly used in till identification (Dowdeswell and Sharp, 1986). However, grain-size distribution in deformation tills can differ dramatically (Benn, 1995, 1996a; Hooke and Iverson, 1995) while clast a-axis fabrics can vary in orientation from strong to weak (Dowdeswell and Sharp, 1986; Benn, 1994b, 1995; Hart, 1994). The difficulty of deformation till identification based on accepted criteria, leads to concerns over misidentification of sediment and subsequent misinterpretation of process.

Despite difficulties in identification, deformed sediments have been observed in many subglacial landforms. Most emphasis has been placed on the implication of these sediments for the origin of drumlins. Observations of deformed sediments within drumlins has led to the conclusion that they, too, are products of subglacial glaciotectionic deformation (Hart, 1997). Figure 2-1 (Boulton, 1987) shows the evolution of drumlins involving deformation processes. Similarly, Hart (1997) identifies three types of drumlins; erosional, deformational, and depositional forms, (Fig. 2-2) that represent a

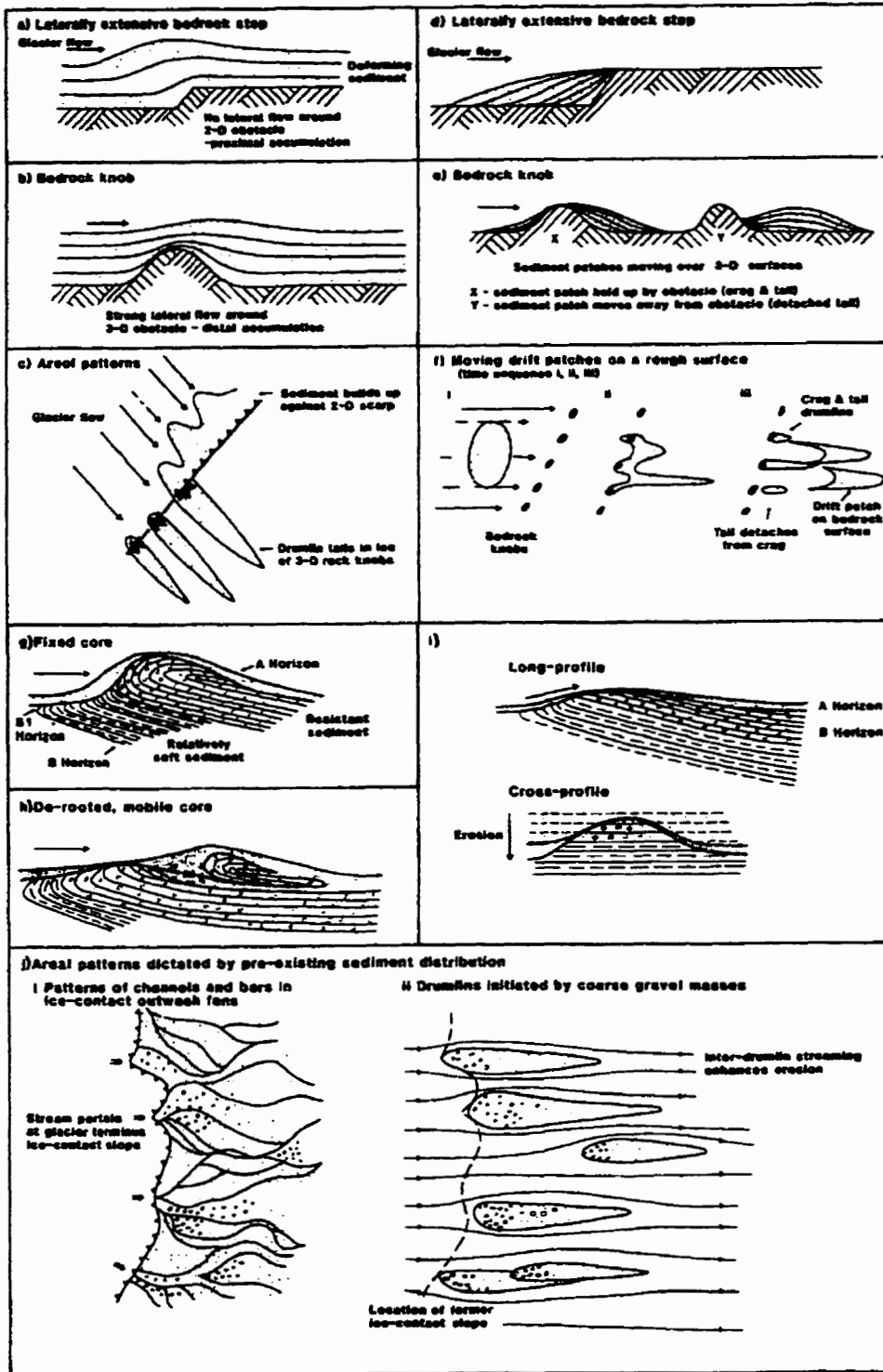


Figure 2-1. Drumlin formation showing internal structures and distribution patterns according to the bed deformation hypothesis (from Boulton, 1987, Fig. 27).

continuum of bed deformation, where local factors determine whether sediment is being removed or deposited.

From direct observation of deformed sediments in drumlins, some workers have determined that drumlins and other streamlined features are evidence of fast moving glacier ice (e.g., Boulton and Clark, 1990a, b; C.D. Clark, 1993; P.U. Clark, 1994; Evans, 1996). This assertion is linked to observations of deforming layers beneath Ice Stream B, Antarctica, and Columbia Glacier, Alaska, where glacier velocities are in excess of 800  $\text{myr}^{-1}$  and 4  $\text{kmyr}^{-1}$ , respectively (Alley *et al.*, 1986, 1987a, b; Blankenship *et al.*, 1986, 1987; Krimmel and Vaughn, 1987; Whillans *et al.*, 1987; Humphrey *et al.*, 1993; Whillans and van der Veen, 1995). However, it is not known if basal motion is solely due to bed deformation or if sliding is also significant (e.g., Iverson *et al.*, 1995). Studies have suggested that flutes may be forming on bedrock beneath the deforming layer at Ice Stream B (Alley *et al.*, 1986). However, no direct observations have been made, and it is unclear whether till deformation is the eroding mechanism. Nor, is it clear that these types of subglacial forms forming on the bedrock surface will create landforms following deglaciation.

In addition, the shapes of drumlin fields may be transverse or longitudinal. Transverse fields may have formed behind former ice margins, while longitudinal fields may represent the paths of former ice streams or glacier lobes (e.g., Wright, 1957, 1962; Rose and Letzer, 1977; Jones, 1982; Piotrowski and Smalley, 1987; Rose, 1987b; Dyke and Morris, 1988; Goldstein, 1989; Patterson and Hooke, 1996). It is important to note, however, that with the exception of small flutes in front of modern glaciers, no drumlins have been directly observed during formation. Consequently, the bed deformation hypothesis is based largely on circular arguments: suggestions that ice streams may move by bed deformation and observations of deformed sediments in some drumlins lead to the conclusion that drumlins are formed by ice streams.

Despite observations of bed deformation processes beneath modern glaciers, and the occurrence of deformed sediments within landforms, the relative importance of this process for landform genesis remains unclear. Landforms that are morphologically similar to drumlins and flutes also contain undisturbed fluvial sediments (e.g., Dardis and

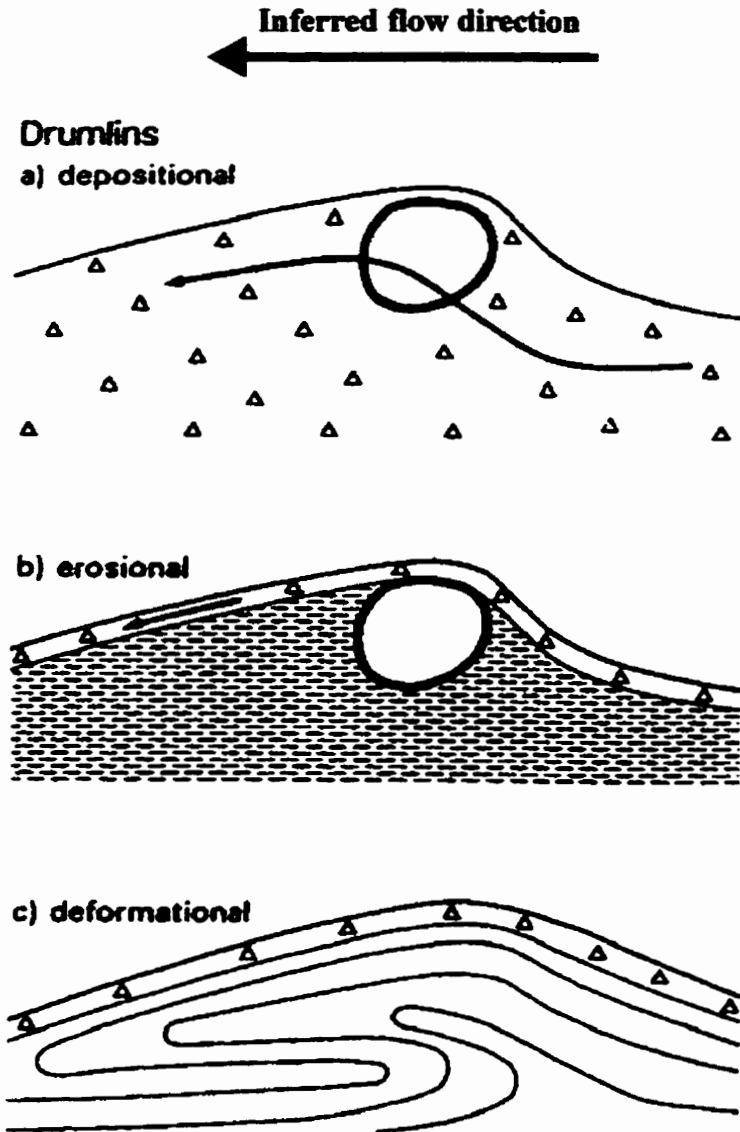


Figure 2-2. Three theoretical types of drumlins produced by bed deformation - a) depositional, b) erosional, and 3) deformational (modified from Hart, 1997, Fig. 2). Ice flow from right to left.

McCabe, 1983, 1987; Shaw, 1983; Shaw and Kvill, 1984; Hanvey, 1987, 1989; McCabe and Dardis, 1989, 1994; Dardis and Hanvey, 1994) and intact bedrock (e.g., Shaw and Sharpe, 1987; Shaw *et al.*, 1989). Thus, some “drumlins” cannot be easily explained by the bed deformation hypothesis. Subglacial processes invoked from field studies should explain all characteristics of a landform including morphology, sedimentology and stratigraphy.

The main alternative theory to the bed deformation hypothesis is the meltwater hypothesis (e.g., Shaw, 1983, 1996). The basic premise of this hypothesis is that turbulent, subglacial sheet flows create erosional and depositional drumlin types and an array of associated landforms (Fig. 2-3; e.g., Shaw, 1983, 1988; Shaw and Kvill, 1984; Shaw and Sharpe, 1987; Sharpe and Shaw, 1989; Shaw *et al.*, 1989; Kor *et al.*, 1991; Fisher and Shaw, 1992; Rains *et al.*, 1993; Brennand, 1994; Brennand and Shaw, 1994; Sjogren and Rains, 1995; Grant, 1997; Munro and Shaw, 1997; Sawagaki and Hirakawa, 1997).

Small-scale imagery of Alberta and northern Saskatchewan reveals broad tracts of eroded bedrock that strongly resemble an anastomosing river system, although their physical scales are very different. This system connects northern Alberta with the study area in southeast Alberta (Fig. 2-4). Coherent fields of landforms up to 100 km wide have been documented (Fig. 2-5; e.g., Shaw, 1983; Shaw and Kvill, 1984; Shaw *et al.*, 1989; Rains *et al.*, 1993; Shaw *et al.*, 1996), and suggest contemporaneous formation by sheet flows operating beneath the Laurentide Ice Sheet. Such observations at a variety of scales have suggested that erosion occurred as a result of meltwater storage and subsequent “catastrophic” release as large meltwater sheets.

Coherent landform assemblages are often dissected by tunnel channels and overlain by eskers, which are held to represent the eventual concentration of sheet flow into, first, large channels and, then, smaller subglacial conduits (e.g., Brennand and Shaw, 1994). Inherent instability within broad sheet flows leads to this progressive channelisation of flow (Shoemaker, 1992a, b; Brennand and Shaw, 1994; Sjogren and Rains, 1995). While Walder (1982) argued that sheet flows are unstable, his analysis was concerned with non-turbulent flow, where “water flow is steady, one-dimensional, and

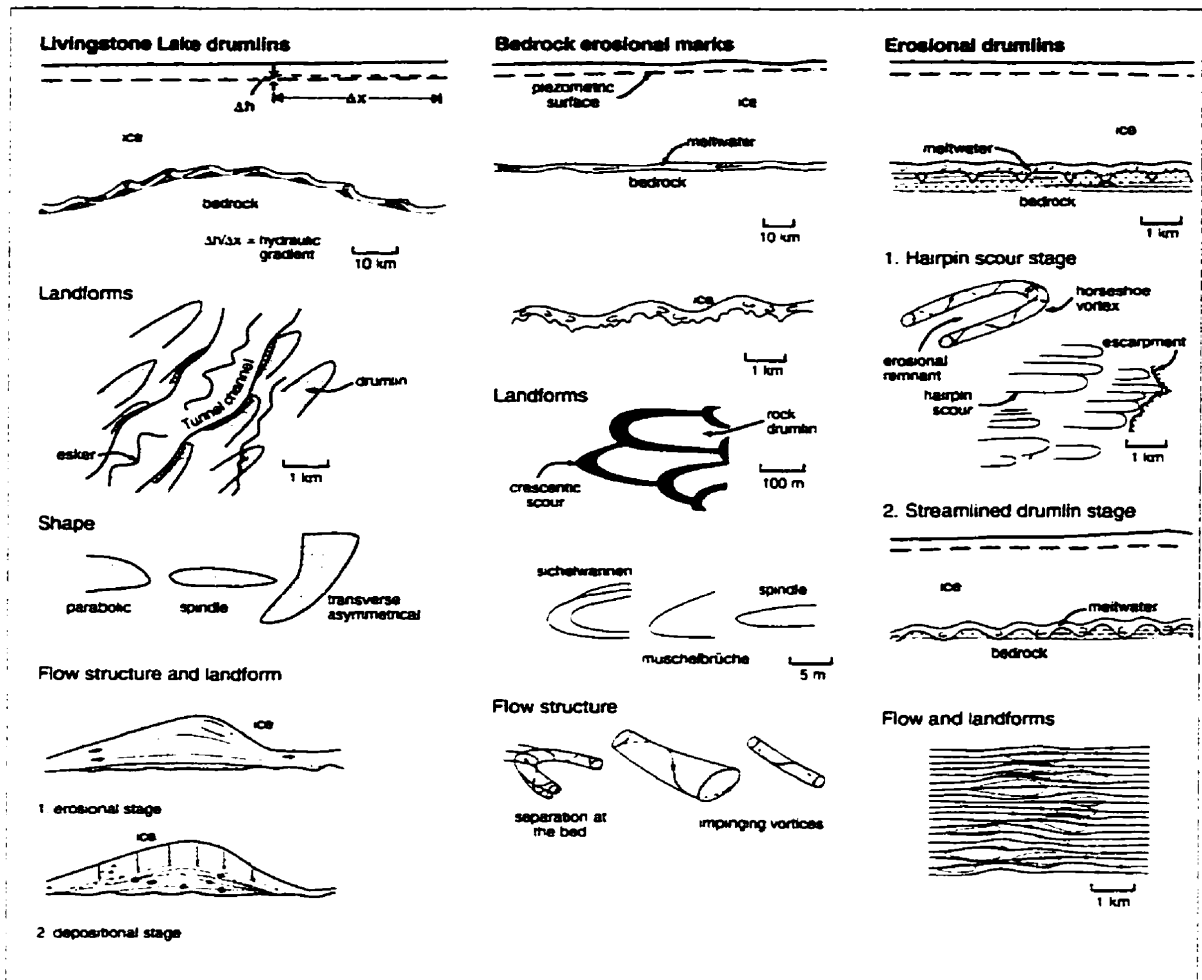


Figure 2-3. Observations and interpretations for the formation of selected subglacial landforms describing erosional and depositional landforms (from Shaw *et al.*, 1996, Fig. 1).

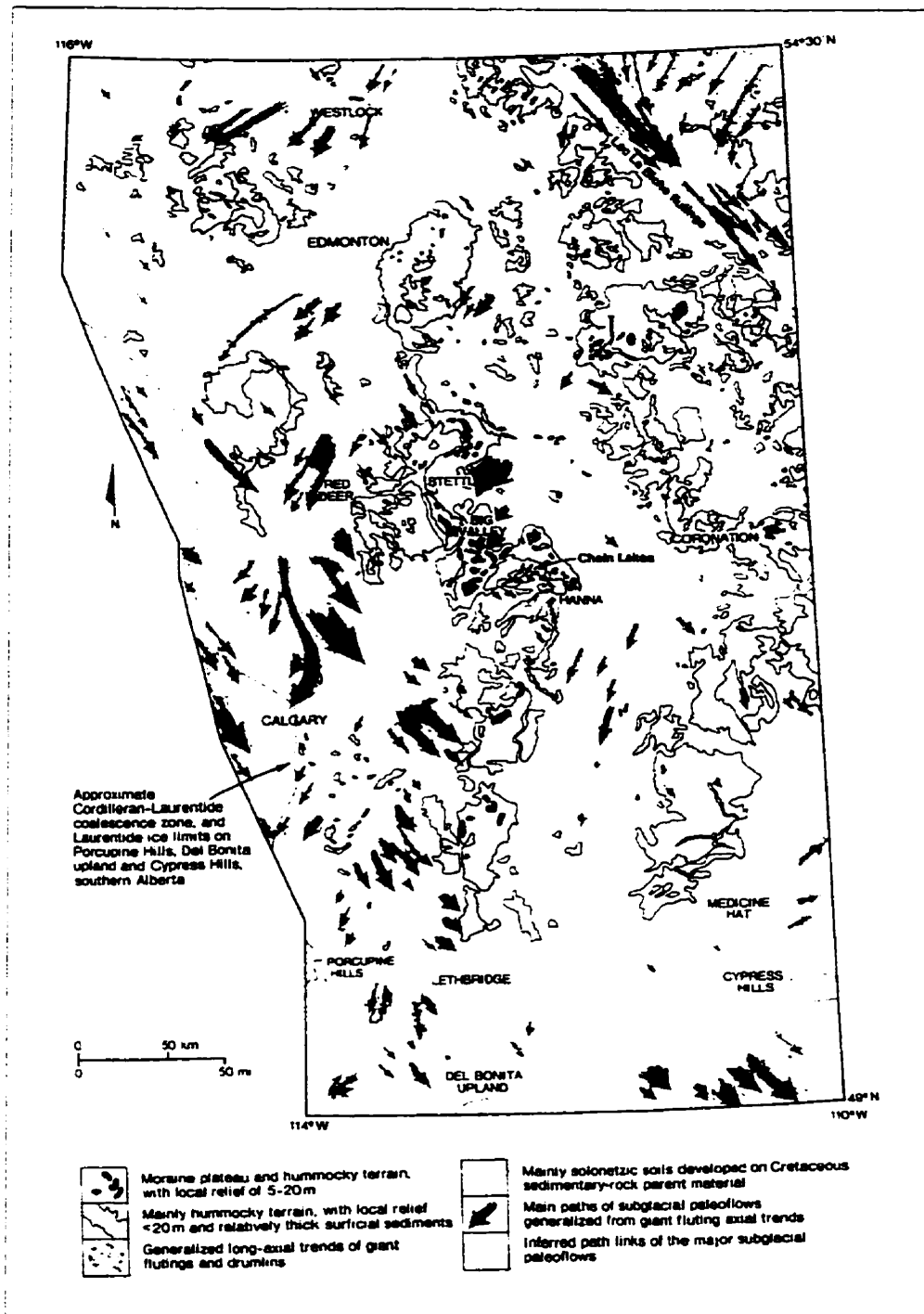


Figure 2-4. Map showing main components of subglacial landform assemblages associated with sheet flow erosion by the Livingstone Lake flood event, central and southern Alberta (modified from Rains *et al.*, 1993, Fig. 2).

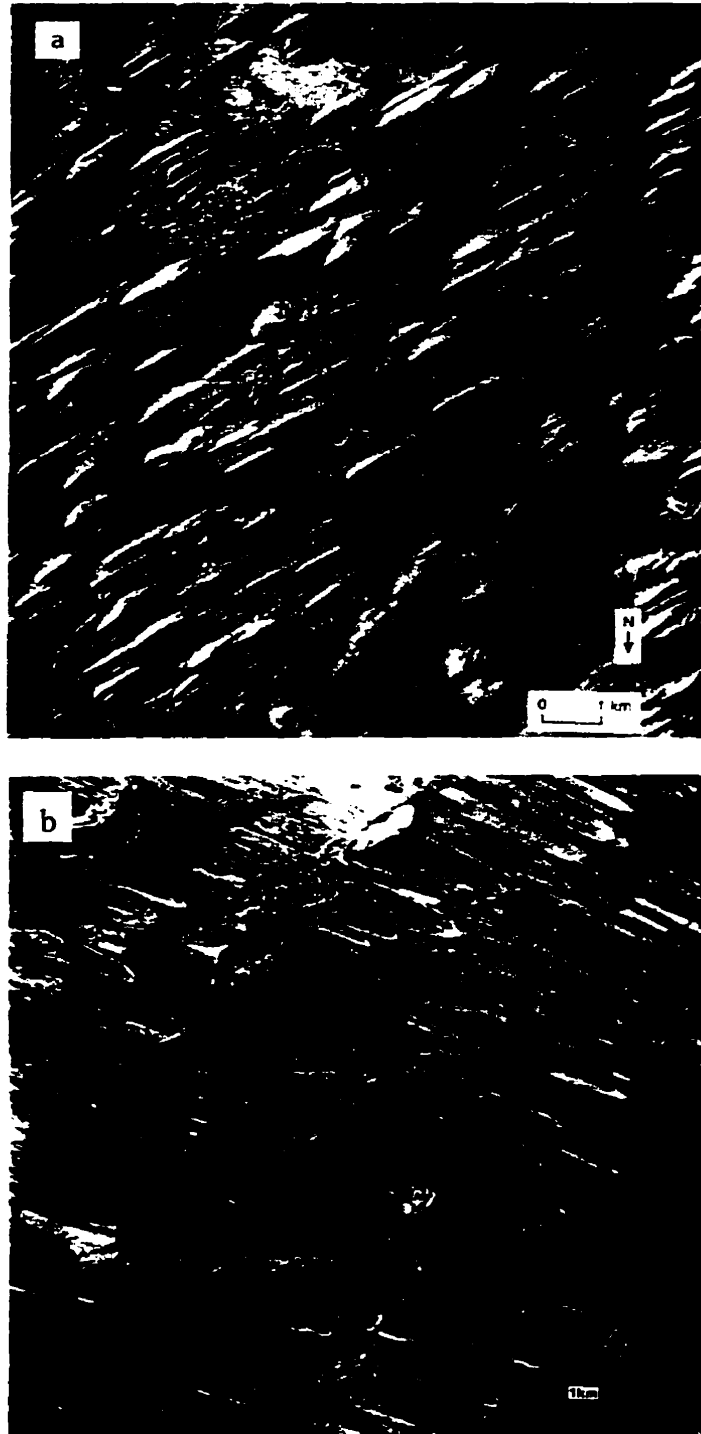


Figure 2-5. Depositional and erosional drumlin types formed by subglacial meltwater processes: a) parabolic and spindle drumlins at Livingstone Lake, north Saskatchewan produced by deposition in subglacial cavities (from Shaw, 1996, Fig. 7.30a); b) Classical drumlin types eroded by subglacial meltwater and left as remnants, Beverly Lake, NWT (from Shaw, 1996, Fig. 7.29).



parallel to ice flow” (p. 275). In contrast, subglacial meltwater flows were most likely highly transient (Shaw, 1996). Shoemaker (1992a, 1994) showed that flow in an outburst flood is best explained as a two-phase event with a laminar phase followed by a turbulent phase. Providing the surface slope of the ice sheet is less than  $3 \times 10^{-3}$ , the sheet flow remains quasi-stable, allowing it to become turbulent, at which stage landforms may be produced (Shoemaker, 1991). The friction factor decreases less rapidly in turbulent flow than in laminar flow and, hence, although sheet flow in subglacial meltwater is inherently unstable, where the ice surface slope is small, sheet flows can theoretically exist to a depth of 100 m for a duration of weeks (Shoemaker, 1991).

Decreasing discharge over time leads to flow being concentrated in pre-existing channels, or new channels scoured during the waning flow stage (Brennand and Shaw, 1994). Thus, while some workers argue that sheet flows are unstable and could not have produced the observed landforms, such flow instability is recorded by sequences of subglacial landforms, reflecting both sheet and channelised flow.

Another major question asked of the meltwater hypothesis is the meltwater source. Estimated discharges for the Livingstone Lake event ( $6 \times 10^7 \text{ m}^3 \text{ s}^{-1}$ ), are based on a mean velocity of  $10 \text{ ms}^{-1}$ , an average flow depth of 40 m and a minimum flow width of 150 km (Shaw, 1996). The total volume of meltwater required is  $8.4 \times 10^4 \text{ km}^3$  (Shaw *et al.*, 1989; Shaw, 1996), although Shoemaker (1991) suggested that abrasion may considerably reduce this estimate. The difficulty of accounting for a meltwater source should not automatically discredit the hypothesis, in the way that Bretz’s flood hypothesis was opposed because for a time he did not know the source of the Scabland Flood (Bretz, 1969). The evidence presented to support a meltwater origin for subglacial landforms is taken here as evidence that such a reservoir must have existed (Shaw, 1996).

One possible meltwater source is a large supraglacial lake situated on an ice sheet with a very low surface gradient (Shaw, 1996). A nearly flat ice sheet profile may be the product of surging, possibly by bed deformation (Boulton *et al.*, 1985; Clayton *et al.*, 1985, 1989; Fisher *et al.*, 1985; MacAyeal, 1993b; Marshall *et al.*, 1996) and in combination with a warming climate, would extend the ablation zone over a large proportion of the ice sheet. Small, supraglacial lakes are observed on modern glaciers

with low-angle profiles (e.g., Mellor and McKinnon, 1960; Echelmeyer and Harrison, 1990; Russell, 1993), and there is no physical reason why large lakes could not form. If such a supraglacial lake connected abruptly with the bed then the related high hydraulic head may have been sufficient to drive meltwater beneath the ice sheet.

Field evidence in Alberta suggests an alternate source for this meltwater. Complex lacustrine and till sequences in hummocky terrain at McGregor Lake, Alberta, are thought to have resulted from repeated infill and drainage of a subglacial lake located in the preglacial Bow River valley (Munro-Stasiuk, submitted). Preglacial valleys in Alberta are broad and shallow and provide natural depressions in the landscape. These depressions would have provided sites for subglacial meltwater reservoirs. Large volumes of subglacial meltwater could have been stored in preglacial valleys, other natural depressions, and even over higher ground beneath the Laurentide Ice Sheet in Alberta (Munro-Stasiuk, submitted). It is unclear what might trigger the catastrophic release of these subglacial lakes, but it is possible that a trigger may occur at the ice margin. Alternatively, a trigger towards the ice sheet centre, causing a sudden connection of a large supraglacial lake with the bed, may best explain the distribution of proposed flood paths (Shaw, 1996).

The source of subglacial meltwater capable of the geomorphic work required by the meltwater hypothesis is an important consideration. However, this hypothesis should not be rejected solely because little is known about the meltwater reservoir.

Benn and Evans (1998, p. 446) referred to the meltwater hypothesis as “an example of an unfalsifiable hypothesis: no matter what the evidence, a way can be found to explain it in terms of the flood. As such, it is not a testable scientific theory, but a body of ideas that could conceivably have produced drumlins, Rogen moraine and other landforms.” Although, as is the case with all landforms of past ice sheets, there are no actualistic observations, the meltwater hypothesis cannot be so readily discounted. Subglacial lakes have been identified beneath the East Antarctic ice sheet (Oswald and Robin, 1973; Cudlip and McIntyre, 1987; Ellis-Evans and Wynn-Williams, 1996; Kapitsa *et al.*, 1996), though they are in rock basins and unlikely to drain catastrophically. The recent jökulhlaup from Vatnajökull, Iceland, was one of the largest observed and may

provide a study site for future subglacial, morphological and sedimentary investigations. Indeed, evidence for jökulhlaups occurring from beneath modern glaciers and ice sheets may be applied to Pleistocene landscapes to support the role of meltwater in their evolution (Clarke, 1986).

It is also suggested that the megaflood hypothesis “relies on form analogies and largely untested numerical modelling” (Benn and Evans, 1998, p. 448). Form analogy is the basis of the science of geomorphology whereby landform identification is largely based on morphological criteria. Such identification then allows processes to be interpreted from analogous forms. Identification of drumlins is, in the first instance, based on qualitative recognition of form and pattern. Subsequently, comparison of internal structural relationships with the external form may be used to test hypotheses. Such observations are used to discriminate between erosional and depositional drumlins, and to suggest details of drumlin formation. However, the identification of features by purely descriptive terminology, e.g., drumlin or flute, has often been extended to imply process and, therefore, genesis. This has generated some misunderstanding within glacial geomorphology where it is essential to separate observation from interpretation. Nonetheless, both the subglacial deformation and the meltwater hypotheses are ultimately tested against field evidence. If one of these hypotheses is untestable, so too is the other.

Numerical modelling of unsteady, turbulent sheet flow is complex and has not yet been attempted for drumlin formation. However, the processes within turbulent flow are well understood qualitatively. Concepts of fluid dynamics (e.g., Yalin, 1972; Allen, 1982) can be applied to such qualitative models to better understand the morphology, internal structure and patterns of many subglacial landforms. The explanation of landform evolution using accepted fluid dynamic principles places the meltwater hypothesis on a strong empirical and theoretical foundation. The meltwater hypothesis is, therefore, grounded in physics and hydraulic theory, by which it is ‘falsifiable’, and the hypothesis has already been tested against theoretical expectations (e.g., Shaw *et al.*, 1989; Shoemaker, 1992b; Pollard *et al.*, 1996; Szilder *et al.*, submitted).

## **Geomorphology**

Hill-shaded digital elevation models (DEMs) of southeast Alberta illustrate a complex subglacial landscape (Figs. 2-6, 2-7) which was studied by air photo analysis and field work to investigate the origin of the glacial landscape in the region. Westgate (1968) and Kulig (1996) reconstructed glacial environments from observations of ground and hummocky moraine, flutes, eskers, glaciotectonic ridges, and meltwater channels. Surficial sediments were inferred to include lodgement till, ice-disintegration sediment, and glaciolacustrine deposits. The suite of landforms was interpreted by Westgate and Kulig as evidence for multiple advance and retreat cycles of the Laurentide Ice Sheet. It has since been established that there was only a single glaciation, the Late Wisconsinan, of the western part of the Alberta Plains (e.g., Christiansen and Sauer, 1988; Liverman *et al.*, 1989; Young *et al.*, 1994; Jackson *et al.*, 1996). Thus, the age and origin of the glacial landscape of southeast Alberta is open to question, but probably formed during Late Wisconsinan time.

Research in Alberta and elsewhere has shown that many subglacial landforms may be explained by predominately erosional, subglacial meltwater processes (e.g., Shaw, 1983; Shaw *et al.*, 1989; Rains *et al.*, 1993; Sjogren and Rains, 1995; Shaw, 1996; Shaw *et al.*, 1996; Munro and Shaw, 1997). The subglacial landscape of southeast Alberta is approached here in light of that new research.

### *Description*

A northwest to southeast tract of eroded, Late Cretaceous bedrock characterises much of the study area (Figs. 2-6, 2-7). The local bedrock comprises marine sandstone and shale, with minor bentonite layers. Ironstone nodules are also observed in the bedrock, which is poorly lithified and friable. This tract has an average width of at least 80 km and crosses the preglacial divide between the Cypress Hills and the Sweet Grass Hills. Channels dissect this erosion surface. The northwest extent of this eroded zone is masked by small transverse ridges, interpreted as end moraines which are believed to relate to deglaciation (Westgate, 1968; Kulig, 1996). Where local bedrock is exposed at

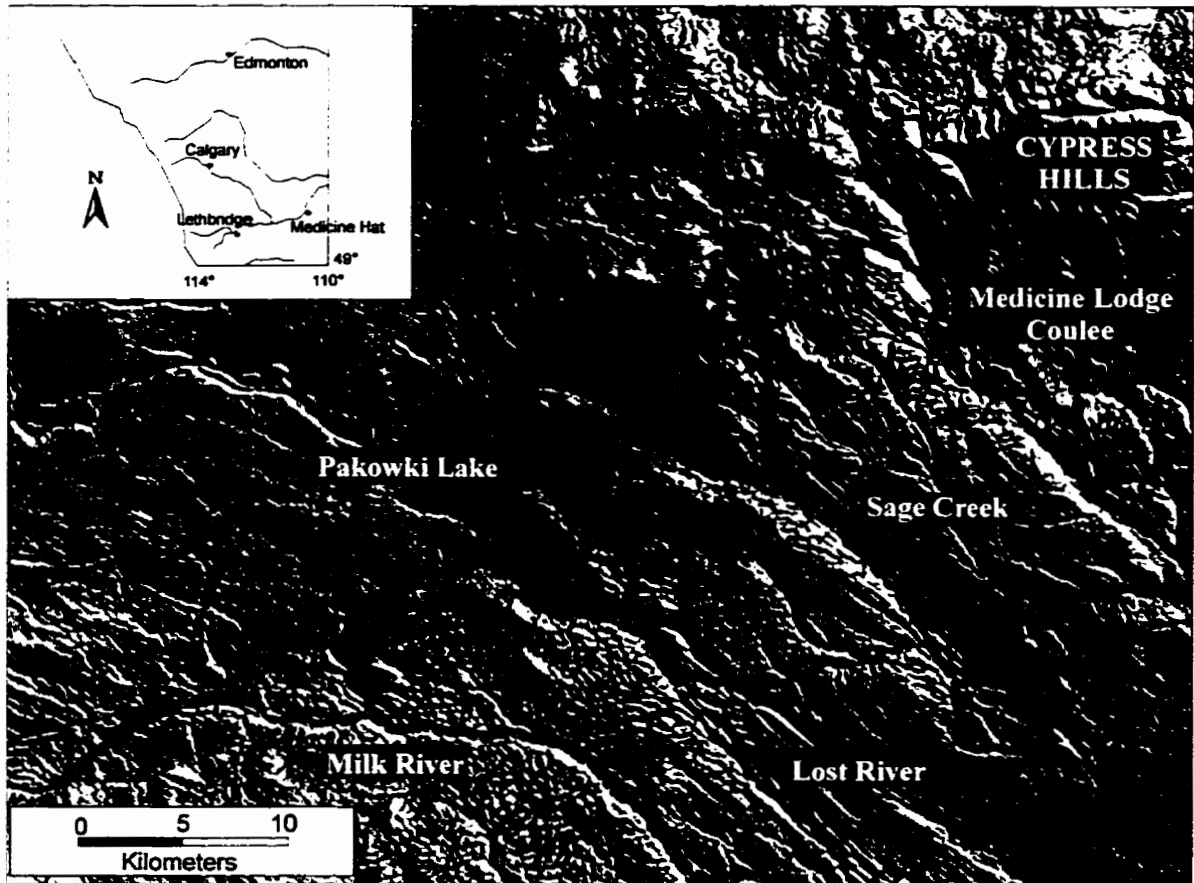


Figure 2-6. Hill-shaded digital elevation model of southeast Alberta showing assemblage of subglacial landforms (sun angle at 45°N, 25° elevation).

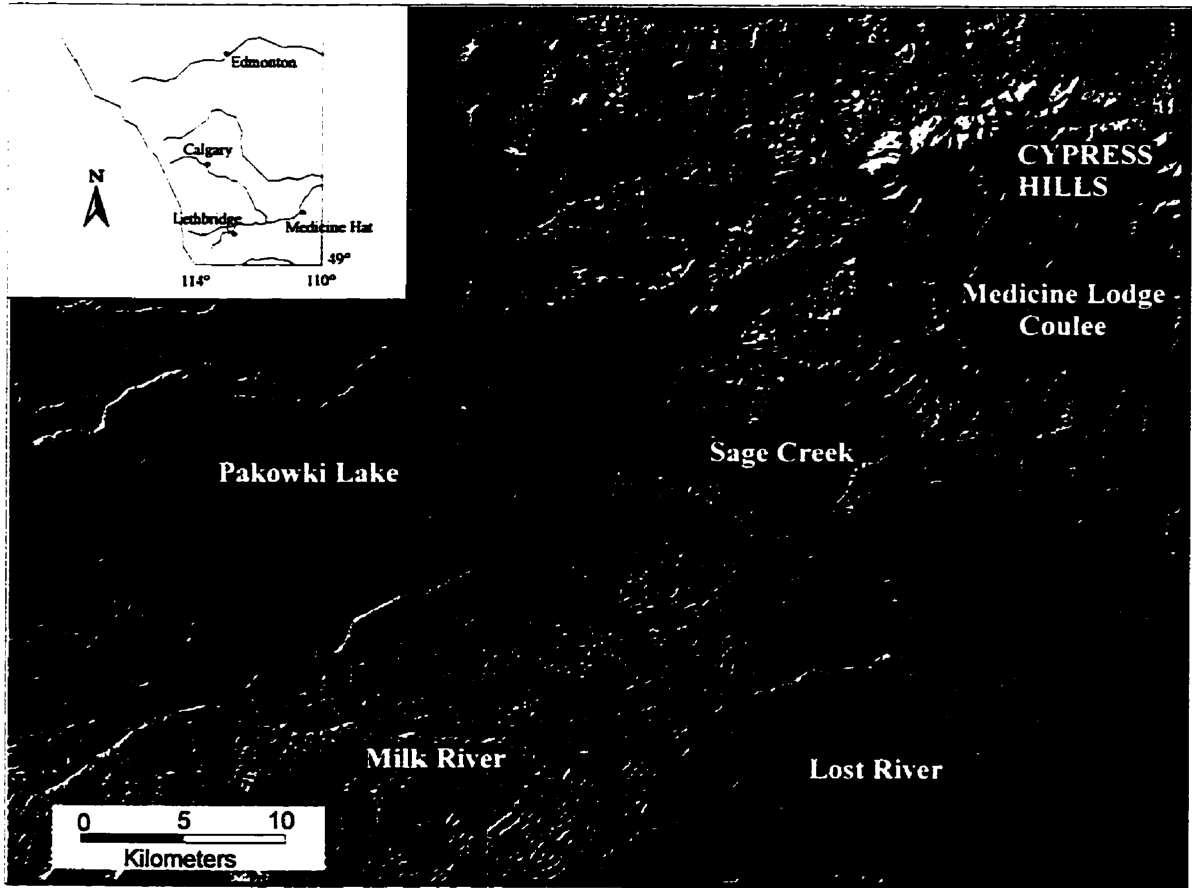


Figure 2-7. Hill-shaded digital elevation model of southeast Alberta showing assemblage of subglacial landforms (sun angle at 315°N, 25° elevation).

the surface it is generally undisturbed, with the preservation of primary bedding structures, although there is some evidence of glaciotectonic deformation involving folding (Fig. 2-8).

Diamicton and sorted, stratified deposits are spatially restricted. They are poorly-sorted, fine-grained clays and silts, relating to local bedrock characteristics, and contain dispersed Shield clasts. Glacial diamicton is massive, and shows no evidence of pervasive deformation. Lower contacts tend to be conformable although small rip-up clasts were noted along the contact with bedrock in some instances. At one site, diamicton conformably overlies channel-fill deposits containing cross-laminated sand and fine gravel.

Remnants of current-bedded sediments include cross-laminated sands with Type A climbing ripples, indicating relatively high deposition from bedload. Infilled channels containing cross-bedded sands with variable flow directions are also noted (Fig. 2-9). It is not clear if these glaciofluvial deposits rest on till or directly on the bedrock surface. They are, however, truncated at the ground surface.

Numerous exposures along cut banks reveal a regional-scale erosional surface truncating glacial sediment and/or Late Cretaceous bedrock (Fig. 2-10). Bedding structures within the substrate can be traced across the erosion surface. This truncation surface is either relatively flat or forms hummocky terrain (c.f., Munro and Shaw, 1997). Hummocky terrain is directly underlain by diamicton, and/or preglacial gravels, and/or bedrock. Solonchic soils on the surface of eroded bedrock are similar to those developed on scoured bedrock tracts elsewhere in southern Alberta (Rains *et al.*, 1993), and indicate marine bedrock at, or close to, the ground surface.

Boulders and cobbles, ranging in size from 0.2 m to > 2.5 m in diameter, are scattered on the eroded bedrock surface (Fig. 2-11). These large clasts are mainly erratics of igneous, metamorphic and sedimentary rocks from the Canadian Shield, although there are also some local sandstone clasts. Shield clasts are subrounded to rounded, reflecting a relatively long transport history. Local bedrock clasts are more angular, having travelled only short distances. The poorly lithified, local clasts are susceptible to comminution and would not have survived long transport distances. Patches of preglacial gravels on the

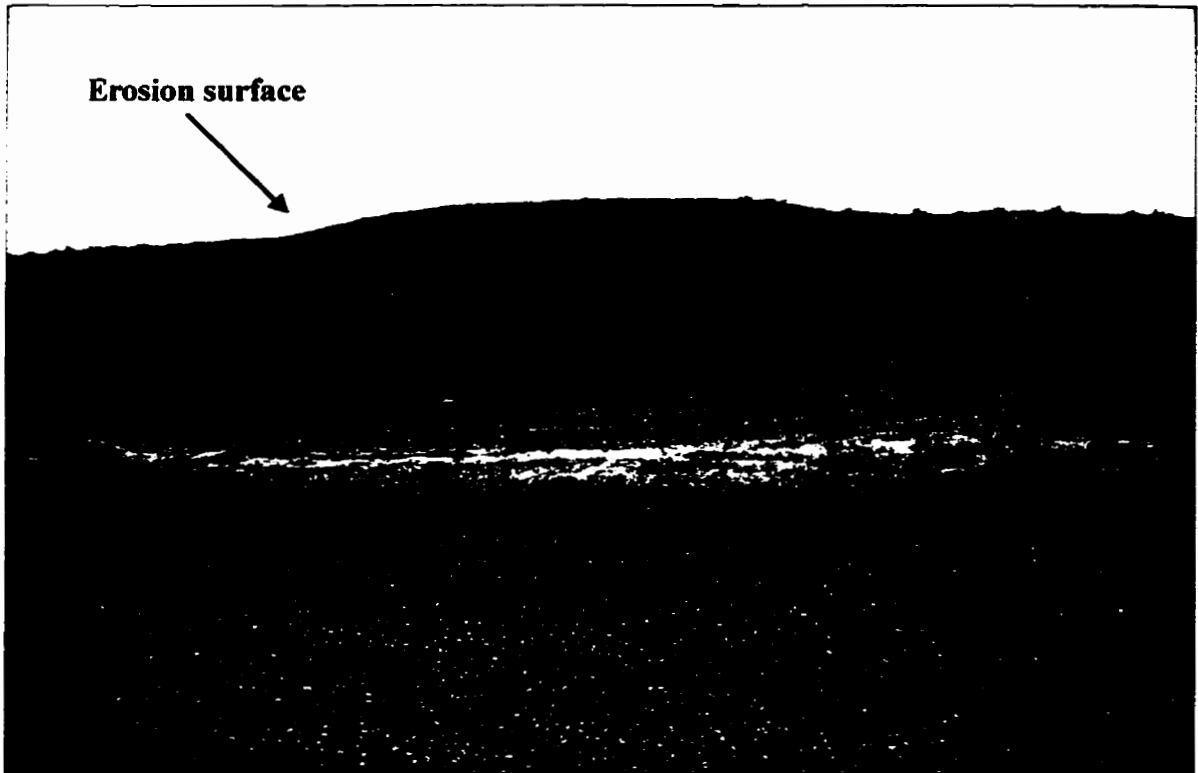


Figure 2-8. Glaciotectonically deformed bedrock in transverse ridge on the preglacial divide showing a truncated surface.



**A**



**B**

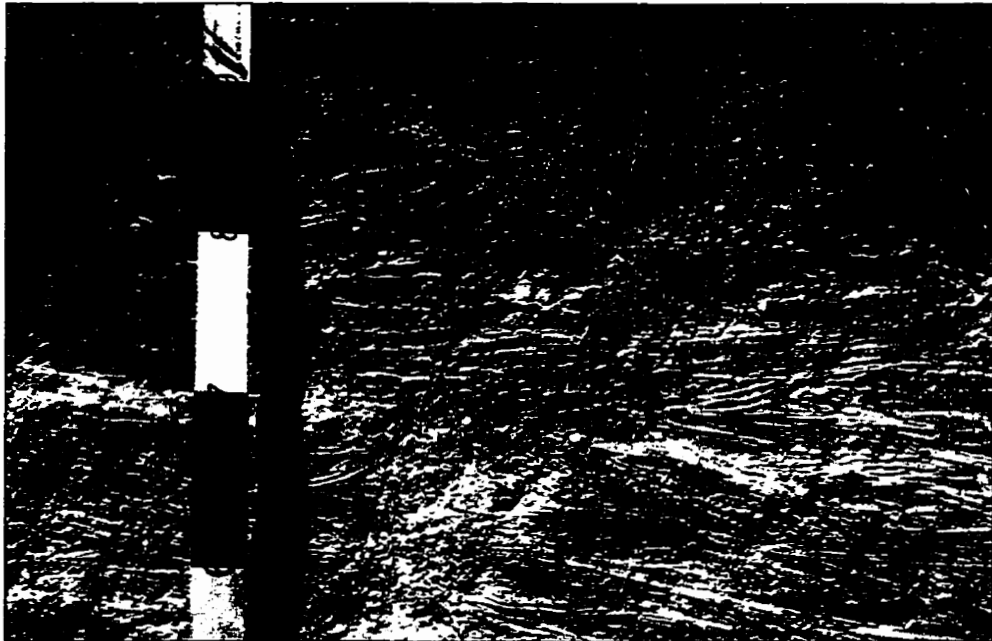


Figure 2-9. a) Channel scour and infill in glaciofluvial sediments, b) Glaciofluvial sands with climbing ripples and cross-bedding, exposed at surface at Pinhorn Grazing Reserve (south of Milk River) and preserved within scoured bedrock tract. Flow from left to right.

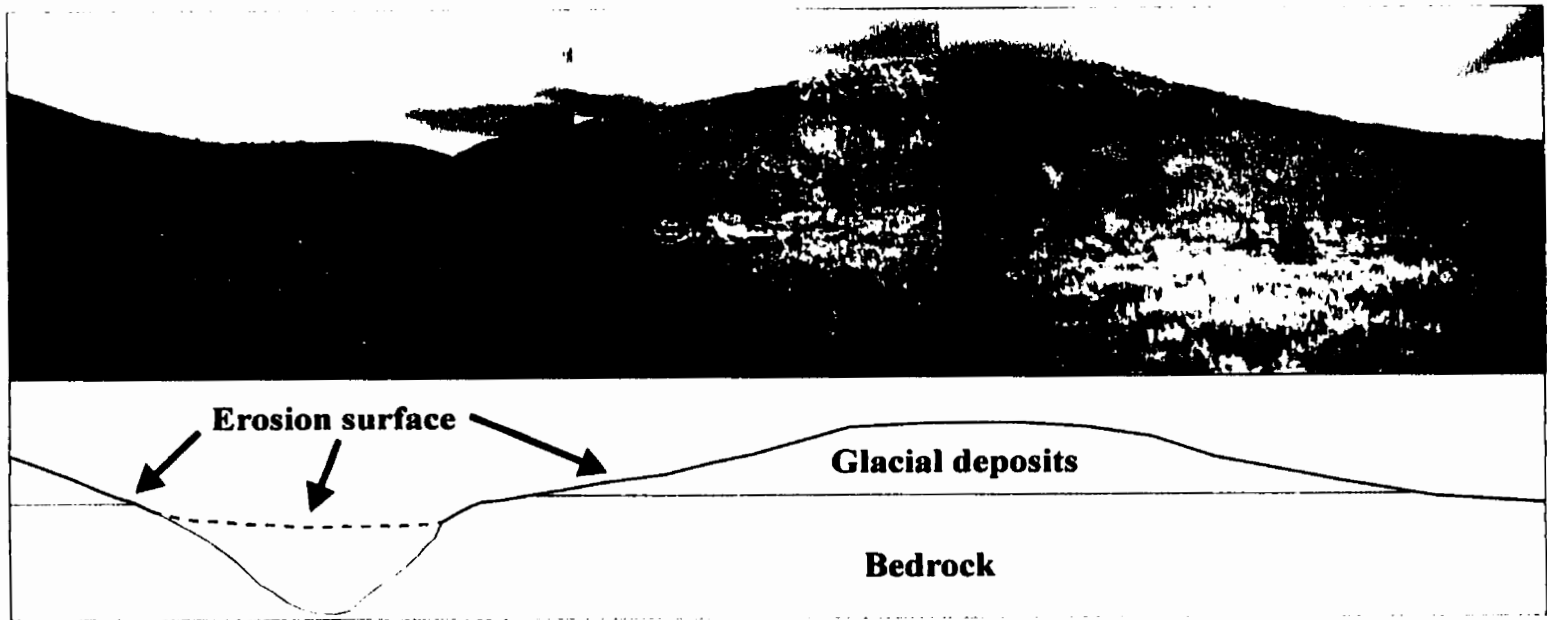


Figure 2-10. Photo mosaic showing an undulating erosion surface at Sage Creek. Erosion surface truncates Late Cretaceous sandstone and shale, and glacial deposits producing hummocky terrain. There is no evidence of deformation within this section. Regional-scale erosion also produces flat topography where flow velocities are increased.



**Figure 2-11. Boulder lags comprising mainly Shield clasts resting directly on the bedrock surface indicate deposition and subsequent removal of glacial sediment by erosion capable of moving all but the largest boulders.**

bedrock surface are restricted to the southern slope of the Cypress Hills. Faceted and bullet-shaped boulders were observed at the ground surface (Fig. 2-12), and indicate transportation and deposition at the base of a sliding ice sheet (e.g., Clark and Hansel, 1989).

Parts of the bedrock tract show flutings which cross the preglacial divide and continue to the southeast. Flutings are defined as fields of ridges and troughs arranged parallel with flow. These forms are oriented northwest to southeast, are generally < 5 m in height and may be tens of metres to kilometres in length (Fig. 2-13). Intact bedrock was observed within ridges. Other flutings contain bedded surficial sediment, showing primary bedding, which is truncated at the landform surface. These surficial sediments include undisturbed, rippled sand and silt overlying gravel resting directly on bedrock (Fig. 2-14). Consequently, the forms are independent of the material within them. Crescentic-shaped depressions are present at their northwest ends and lateral grooves parallel most flutings (Fig. 2-13). Boulders are also common.

Shallow depressions (< 2 m deep) on the scoured bedrock tract to the southeast of the preglacial divide also trend northwest to southeast (Fig. 2-15). These erosional forms, cut into Late Cretaceous bedrock, are associated with flutings and commonly contain boulders within the depressions.

An anabranching network of channels starts and ends abruptly and is confined to the preglacial divide (Figs. 2-6 and 2-7). The channels are mainly aligned northwest to southeast and have trapezoidal cross sections, steep sides and nearly flat floors. They are up to 100 m deep and 5 km wide (Fig. 2-16). Most modern streams are underfit within these channels. The channels are incised entirely into Late Cretaceous bedrock, with no evidence of glacial sediment on the uppermost surfaces. Scoured bedrock with Shield erratics was noted on interfluvies between channels. Glacial sediment is sparse in this area.

With the exception of the Milk River Canyon, major channels in the study area have convex-up long profiles (Fig. 2-17). Modern drainage, with divides within channels and with streams flowing in opposite directions, confirms this convexity. In addition, channel bed slope is partly against the regional gradient and channels were eroded



**Figure 2-12. Bullet-shaped boulders with faceted faces are observed on the bedrock surface indicating active basal transport and possible lodgement below the Laurentide Ice Sheet during ice advance.**

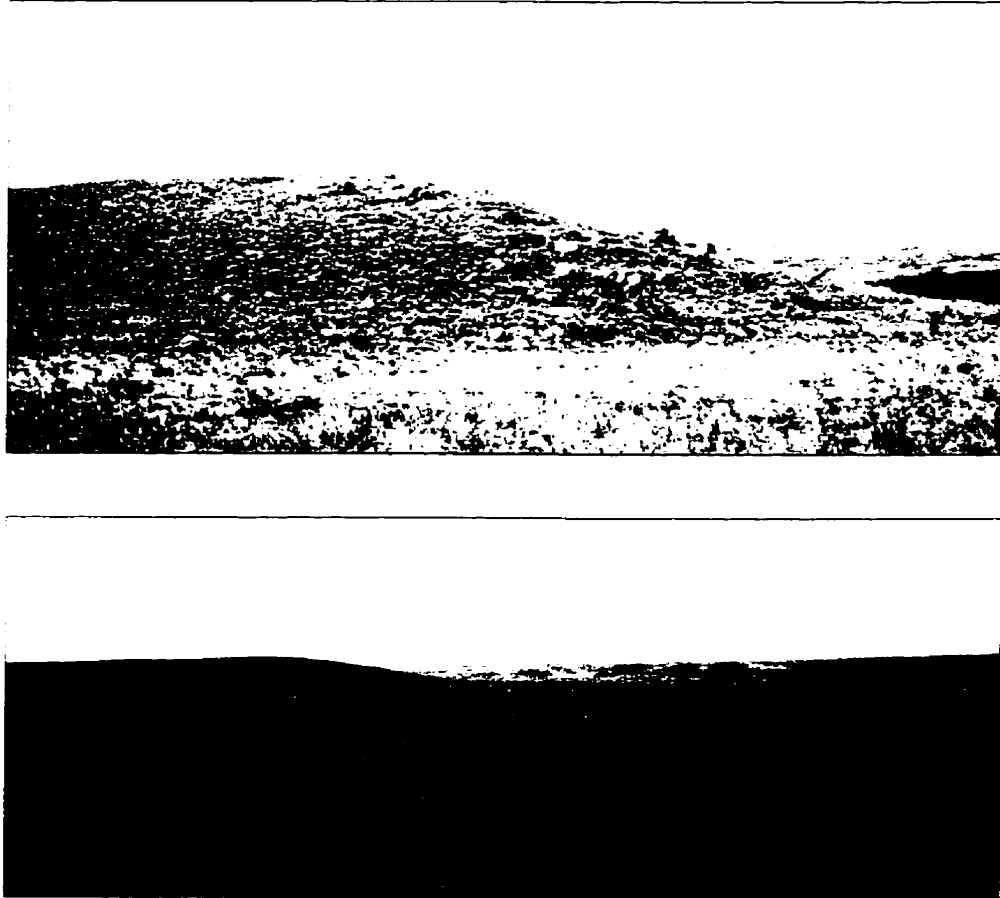


Figure 2-13. Photographs showing remnant ridges within the main scoured tract showing characteristic proximal scours at upstream end of ridges. Ridges are composed of Late Cretaceous bedrock in these examples. Flow is from right to left.

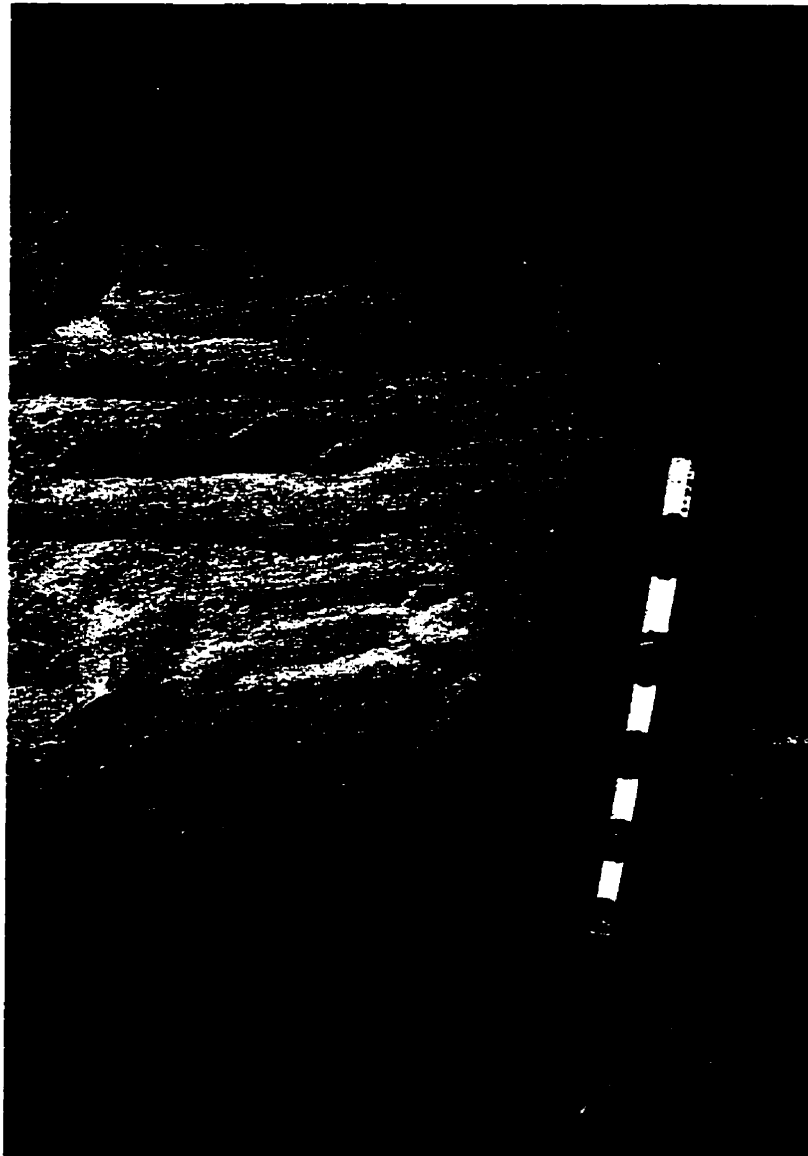


Figure 2-14. Glaciofluvial sands with Type A climbing ripples and plane bedded sands preserved in remnant ridge at Onefour within main scoured zone. Sands unconformably overlie massive gravels (not seen in photo) which rest directly on bedrock.

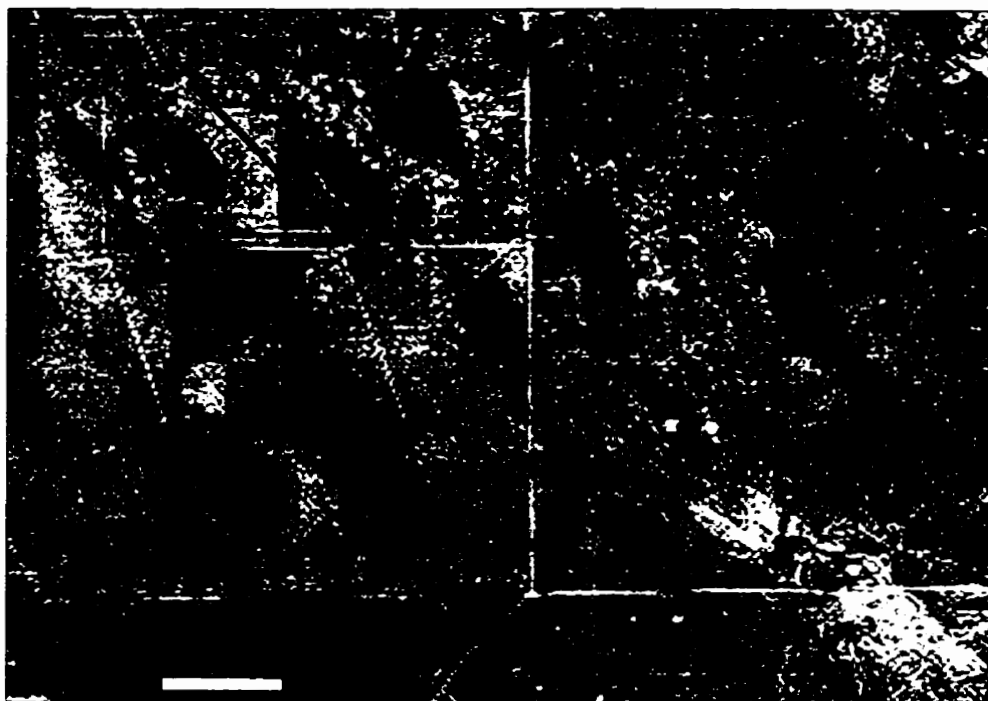


Figure 2-15. Eroded depressions (s-forms), oriented NW-SE, superimposed on scoured bedrock tract at Onefour.





Figure 2-16. Lost River channel showing characteristic tunnel channel morphology and Late Cretaceous bedrock exposed along valley walls.

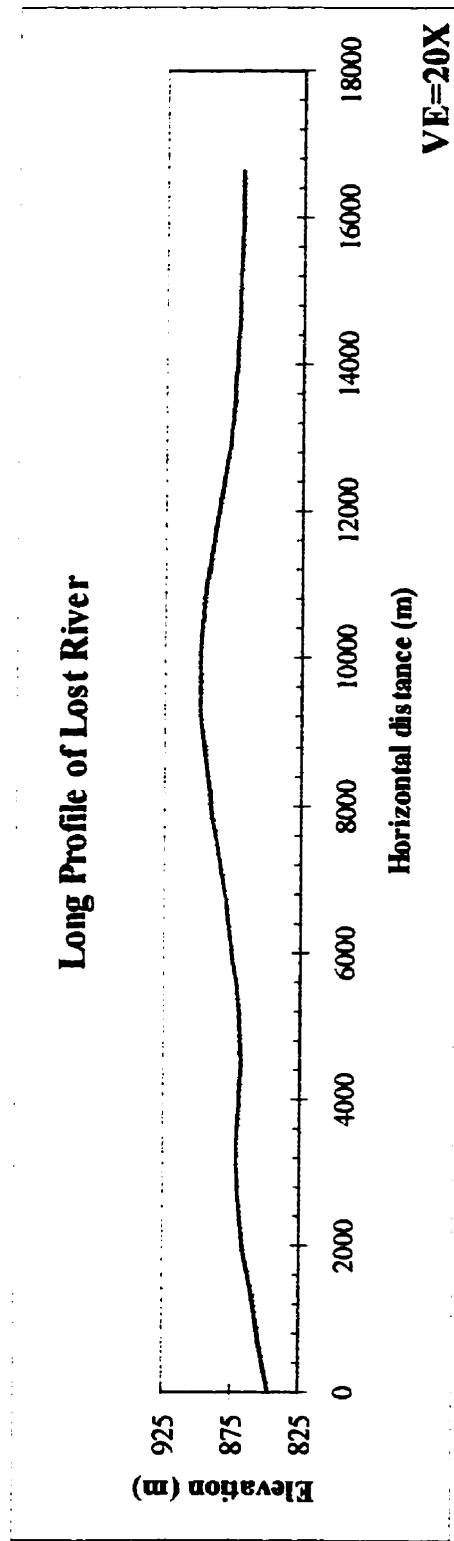
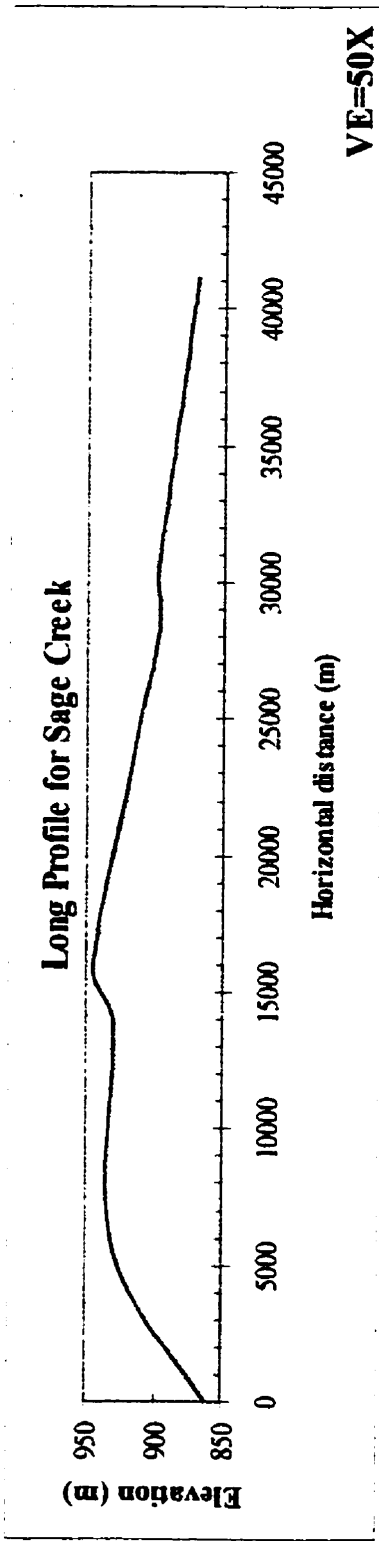


Figure 2-17. Long profiles for Lost River and Sage Creek showing convex-up profiles indicative of subglacial meltwater erosion across the preglacial divide.

through the preglacial divide indicating flow against an adverse slope. No evidence of glacial erosion (e.g., striae, glacial sediment) was noted within the channels.

Transverse ridges, with crests running northeast to southwest, are superimposed on the preglacial divide (Fig. 2-7). These bedforms are defined as ridges and troughs arranged transverse with flow. They are confined to the preglacial divide suggesting that this ridge was a significant factor in their formation. Bedforms are approximately 25 m high in the southwestern part of the study area, decreasing to a minimum relief of 1-2 m in the northeast. Wavelengths (measured from ridge crest to ridge crest) also decrease from 1300 m in the southwest to 405 m in the northeast. The transverse ridges contain deformed bedrock dipping towards the northwest which, in some instances, is truncated at the surface (Fig. 2-8). Glacial sediment was not observed within the transverse ridges, though there are boulders at the surface. Flutings, oriented northwest to southeast, are superimposed on ridge crests. The troughs between transverse ridges contain wetlands and elongated lakes. Since the transverse ridges are truncated by major channels, they pre-date channel incision. Three types of ridge morphology are identified: a) Type 1, three-dimensional wave forms, b) Type 2, two-dimensional nested wave forms and c) Type 3, rhomboidal interfering forms (Fig. 2-18).

### *Interpretation*

Most landforms in the study area are part of an erosion surface that cross-cuts bedrock and surficial sediments, and indicates flow from northwest to southeast. These occurrences of glacial sediments provide evidence for glacial erosion and deposition beneath the Laurentide Ice Sheet. These sediments are not, however, related to landform evolution. Thus, sediment deposition pre-dated erosion. The landform assemblage may be explained by two alternative hypotheses as discussed above: 1) bed deformation, or 2) subglacial meltwater erosion. Field evidence supports an origin for the features by subglacial meltwater erosion.

The absence of subglacial and supraglacial sediment sequences on the ground surface suggests that erosion at the base of a deforming layer is unlikely (e.g., Hart, 1997). Subglacial fluvial erosion, in comparison, could erode the area, removing glacial

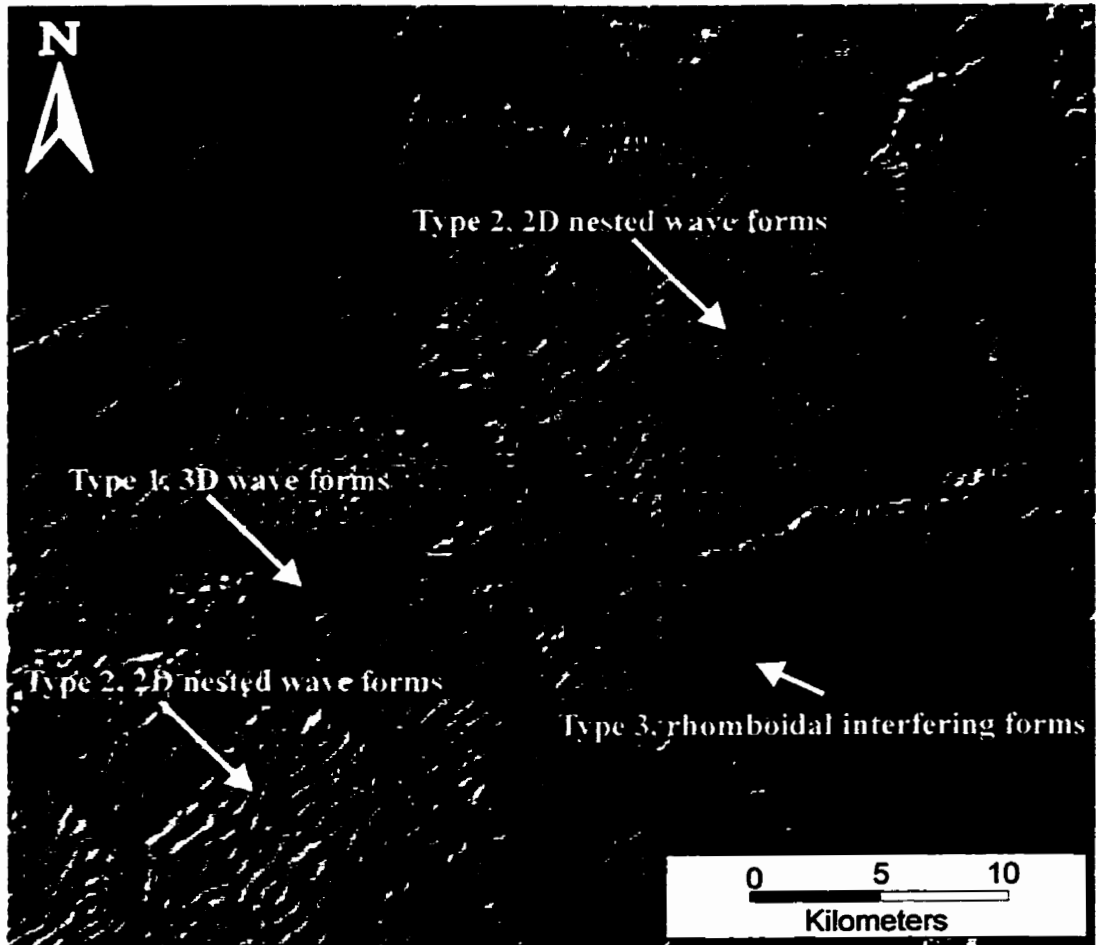


Figure 2-18. Transverse ridges observed on the preglacial divide showing Type 1, 3D wave forms; Type 2, 2D nested wave forms; and, Type 3, rhomboidal interfering forms.

sediments previously deposited by ice in the region. Fluvial erosion of the preglacial divide would require subglacial meltwater flow. Flow of subglacial meltwater is driven by the hydraulic gradient, where head is measured relative to the hydrostatic head (Shreve, 1972). In zones of high hydraulic head (i.e., where water pressure is close to the overburden pressure), flow may have been driven against the regional gradient and across the preglacial divide. Remnants of glacial sediment and extensive scoured bedrock are explained by differential erosion whereby sediment was retained in some places but was completely removed in others. This erosion produced hummocky terrain in zones of relatively low flow velocities along the margins of broad sheet flows. More complete erosion in the main scoured tracts is taken to indicate more powerful meltwater flows. It is unclear how direct erosion by ice or deformational processes could have differentially eroded the substrate and preserve undisturbed glaciofluvial sediments. Also, erosion by active ice would have incorporated sediment into basal ice. During melting, this would have been deposited at the surface forming thick sediment sequences. Such sequences were not observed in the study area.

Shield clasts resting on the eroded bedrock surface form a discontinuous boulder lag. Remnants of glacial sediment contain similar Shield clasts suggesting that the lag boulders were left behind as finer sediment was eroded. The lags are unlikely to have been formed by subaerial processes, since they are not associated with eolian or sheetwash deposits (c.f., Munro and Shaw, 1997). Boulder lags indicate that glacial sediment was largely removed by a widespread erosional process incapable of carrying boulders. Since ice does not preferentially transport small grain sizes while leaving large material behind, transport was most likely in a high velocity, turbulent fluid flow (e.g., Kor *et al.*, 1991; Munro and Shaw, 1997). Movement of boulders from underlying till to the surface by frost heave cannot account for the boulder lag as till is generally absent from the study area. Rounded boulders may also result from erosion of saprolites (Patterson and Boerboom, 1998). However, the local bedrock does not comprise crystalline rocks and the soft Cretaceous bedrock is unlikely to form saprolites and corestones. Therefore, surface boulders are interpreted as a fluvial lag.

Differential transport of fine-grained sediment by ice should result in deposition of this material at the ice margin. Large accumulations of glacial sediment are not observed in Montana, indicating that eroded rock and sediment was transported well beyond the Laurentide ice margin. Differential fluvial transport of fine-grained material could account for the absence of large glacial deposits in marginal locations. These flows would have been capable of transporting sediment far beyond the ice, much of it possibly into the Gulf of Mexico (Shaw *et al.*, 1996). Therefore, turbulent, sediment-laden meltwater flowing beneath the Laurentide Ice Sheet, with the competency to erode and transport all sediment sizes except the largest boulders, is required. The occurrence of boulders across the preglacial divide indicates that subglacial, pressurised flow was needed. It is inferred that the boulder lags formed contemporaneously across the whole area.

Crescentic scours and lateral grooves parallel to flutings, are typical of analogous forms produced by meltwater and wind (e.g., Shaw, 1994a). The crescentic and lateral grooves combine to form hairpin scours related to horseshoe vortices around obstacles (Shaw, 1994a). Dreimanis (1993) noted proximal scours and lateral grooves around small-scale ridges in the forefield of Breidamerkurjökull, Iceland, which he attributed to meltwater erosion in subglacial cavities. Similar features are also observed on bedrock around Georgian Bay, Ontario (Kor *et al.*, 1991) and around large-scale remnant ridges in Alberta (Rains *et al.*, 1993) and Saskatchewan (Grant, 1997). Their form is scale-independent.

Flow across the preglacial divide would have accelerated, due to a reduced gap width between the ice and bed, causing increased erosion and enhancing the strength of horseshoe vortices around obstacles (Shaw, 1994a). Characteristic scour patterns seen around flutes, similar to those seen in the study area, are only attained where Reynolds Numbers (Re) are  $> 10^4$  (Allen, 1982; Shaw, 1994a). These Reynolds Numbers are commonly achieved by flowing water and wind, but are orders of magnitude too large for flows in high viscosity ice (Shaw, 1994a).

Eroded depressions in the scoured bedrock tract are interpreted as *sculpted forms* (s-forms) (Kor *et al.*, 1991), that may also be explained by subglacial meltwater erosion.

This term is preferred over *p-forms* (Dahl, 1965), which infers abrasion by plastically deforming ice. The term *s-form* was adopted by Kor *et al.*, (1991) as a non-genetic alternative. These *s-forms* may result from a variety of vortices in turbulent flows, some impinging on the bed and some generated by the bedform itself (Allen, 1982). Their orientation is consistent with flutes in the study area suggesting that they were all formed contemporaneously by broad sheet flows. Kor *et al.*, (1991) drew similar conclusions from erosional forms at Georgian Bay, Ontario.

The landforms described above are best explained through erosion by subglacial meltwater flowing in broad sheets. Formation was more or less contemporaneous. Rains *et al.*, (1993) noted extensive tracts of scoured bedrock elsewhere in Alberta, which contain large-scale *s-forms* and flutings (Fig. 2-4) that are attributed to sheet flow during the Livingstone Lake flood event. Kor *et al.*, (1991) documented large-scale bedrock erosion in Georgian Bay, Ontario, which resulted in bedforms that are best explained by subglacial sheet flow erosion.

The extensive erosion surface and associated landforms discussed above are dissected by a number of large channels. Their convex-up long profiles could only have been formed by pressurised meltwater. Therefore, subglacial channelised flow is required. This is supported by the evidence for subglacial fluvial erosion discussed above.

However, other processes might possibly account for these channels. These alternatives are discussed below to show why a subglacial meltwater origin is most likely.

1. Channels may be excavated along preglacial fluvial valleys. Westgate (1968) noted that the ancestral Milk River was diverted to the northeast by the preglacial divide. Thus, no evidence suggests that these tunnel channels existed prior to the onset of glaciation in the region. As well, evidence for a single glaciation in western Alberta, the Late Wisconsinan, (e.g., Liverman *et al.*, 1989; Young *et al.*, 1994; Jackson *et al.*, 1996) precludes antecedent tunnel channels.
2. Tunnel channels could also be structurally controlled, yet no structures in the underlying bedrock are known to coincide with channel locations (Westgate,

1968). Thus, structural control is rejected as a principal element of tunnel channel formation in southeast Alberta.

3. Grübe (1983) attributed tunnel channels in northern Europe to glacial erosion. Yet, tunnel channels in southeast Alberta show no evidence of ice abrasion, and their complex, anabranching patterns are difficult to explain by glacial erosion (c.f., Sjogren and Rains, 1995).
4. Westgate (1968) considered some channels to be ice-marginal (Milk River) and used them as evidence for successive positions of retreating ice. He interpreted other channels (Lost River and Sage Creek) as spillways from glacial lakes such as Glacial Lake Pakowki (Westgate, 1968). However, the convex-up long profiles of tunnel channels and the upflow-sloping regional gradient preclude a subaerial origin for these features. Subglacial, pressurised, conduit flow was necessary to form these channels.

Thus, these channels are inferred to be subglacial in origin, and were formed by meltwater erosion. They are interpreted as tunnel channels. Various subglacial processes might account for these channels (c.f., O'Cofaigh, 1996). Tunnel channels may be eroded by steady-state discharges flowing in Nye channels and accompanied by channel ward creep of deforming sediment (Boulton and Hindmarsh, 1987). However, under unsteady conditions, high pressure within Nye channels would drive sediment away from conduits and cause decoupling of the ice from its bed (Brennand, 1994). Drainage conditions may also limit the rate and spatial extent of till deformation towards a subglacial conduit (Alley, 1992). The tunnel channels described here are incised into bedrock and the interfluves are largely devoid of surficial sediment. Sediment removal likely occurred prior to channel formation. Steady-state drainage and time-transgressive channel evolution are discounted because of the short time available for erosion. Erosion could only have occurred between about 18 ka and 14 ka BP. Also, the absence of channel-ward deformation along subglacial bedrock channels rules out subglacial deformation as a general explanation for the tunnel channels in southeast Alberta.



Time-transgressive tunnel channels might have been eroded close to the ice margin by jökulhlaups (Wingfield, 1990) or by seasonal, supraglacial drainage reaching the bed (Mooers, 1989). There are no large-scale, outwash fans at the ends of tunnel channel segments in the study area that would support marginal zone or time-transgressive formation. Similarly, the complex anabranching network is difficult to explain by time-transgressive formation (e.g., Sjogren and Rains, 1995). Contemporaneous erosion by a single flow event best explains this complex network.

Consequently, tunnel channels in southeast Alberta are taken to record catastrophic, subglacial drainage under high pressure gradients beneath the Laurentide Ice Sheet (c.f., Brennand and Shaw, 1994). Channels operated as Nye channels, or as combinations of Nye and Röthlisberger channels, and carried meltwater southeast towards the ice margin. Convex-up, channel long profiles and their crossing of the preglacial divide could not have been produced by subaerial flows. Only subglacial meltwater flow with a high hydraulic gradient can account for this phenomenon (Shreve, 1972). The interconnected channel network suggests the contemporaneous operation of subglacial channels that required high-magnitude flows of short duration (c.f., Wright, 1973; Brennand and Shaw, 1994; Sjogren and Rains, 1995).

A remarkable suite of transverse bedforms is superimposed on the preglacial divide and is cross-cut by tunnel channels. The transverse bedforms show some evidence of glaciotectionic processes although the ridge morphology is primarily erosional. The inferred origin for these ridges is largely based on the conclusions discussed above. A subglacial meltwater origin for flutings elsewhere in the study area suggest that fluvial processes may have been significant for ridge formation. The origin of these features is discussed in Chapter 3, but the alternative hypotheses are introduced here.

There are two possible hypotheses for the origin of transverse ridges in southeast Alberta:

1. Transverse ridges may be primary glaciotectionic features with minor modification by subsequent subglacial meltwater flows producing the superimposed streamlined forms.

2. Ridges may be primary fluvial bedforms, e.g., antidunes, produced by stationary waves in subglacial meltwater flows.

The large-scale, transverse ridges were previously interpreted as glaciotectionic thrust ridges (e.g., Westgate, 1968; Shetsen 1987), and are morphologically somewhat similar to transverse ridge forms described by Bluemle and Clayton (1984) and Tsui *et al.*, (1989). Ridge formation was considered by those authors to result from detachment, transport and imbricate stacking of the substrate. Fold noses or upturned ends of thrust blocks were implied to form the ridges. In this case, deformation requires that the strength of the material, which is reduced by high pore water pressure, is less than the shear stresses generated by overriding ice. Glaciotectionic ridges are generally concave upglacier, and are thought to parallel the former ice margin (Aber *et al.*, 1989). However, ridges observed in the study area do not correspond to reconstructed ice-margins. Nevertheless, deformed bedrock within some ridges makes it likely that the Laurentide Ice Sheet displaced subsurface material and glaciotectionic deformation might well have partially contributed to ridge formation.

Scoured bedrock, boulder lags and flutings on transverse ridges support their modification by subglacial meltwater erosion. Thus, although the ridge morphology may have been partly the result of glaciotectionic processes, their final forms owe much to meltwater erosion. This view is strengthened by the complex ridge morphology and in particular, Type 2 and Type 3 wave forms. These patterns have not been noted in glaciotectionic ridges. Tunnel channel incision across the transverse ridges by channelised subglacial flows further supports a fluvial component to ridge formation.

Alternatively, the transverse ridges may be primary bedforms resulting from erosion beneath stationary waves in subglacial meltwater sheet flows. If so, they are interpreted as erosional antidunes. They are analogous to transverse s-forms in bedrock (Kor *et al.*, 1991), erosional megaripples in the Eastern Channel of the Laurentian Fan (Hughes Clarke *et al.*, 1990) and antidune bedforms in rivers (Shaw and Kellerhals, 1977; Allen 1982). The complex ridge morphology (Fig. 2-18) is similar to features commonly observed in antidunes formed by fluvial processes, suggesting that similar processes may

have produced these transverse bedforms. These features may be part of a family of erosional bedforms (s-forms) including non-directional, undulating beds (Kor *et al.*, 1991) and hummocky terrain (Munro and Shaw, 1997).

## **Conclusions**

Field observations in southeast Alberta support an erosional origin for a suite of subglacial landforms, including scoured bedrock zones, flutings, s-forms and tunnel channels. An extensive erosional surface and network of tunnel channels truncate bedrock and surficial sediments with no evidence of pervasively deformed substrate materials. The erosional landscape evolved subglacially, most likely by meltwater scour.

Landform relationships record meltwater sheets, at least 80 km wide, flowing from the northwest, parallel to remnant ridges and tunnel channels, which subsequently became concentrated in channels. The inferred sequence of events was as follows:

1. Advancing Laurentide ice across southeastern Alberta brought erratics from the Shield, eroded local bedrock and deposited fine-grained tills, and provided sediment to streams and lakes in which glaciofluvial and glaciolacustrine deposits accumulated. Glaciotectonic processes at the ice margin and beneath the advancing ice sheet, deformed bedrock and may have produced thrust ridges of various scales.
2. Widespread scouring of glacial sediment and underlying bedrock by a subglacial outburst flood, flowing in enormous sheets, left large erosional tracts on the landscape. These tracts are characterised by flat terrain and hummocky terrain. Boulder lags on the scoured surface are remnants of glacial sediments deposited by Laurentide ice and subsequently eroded by fluvial processes. The floods took place some time between glacial “maximum” and deglaciation of the area, roughly in the period between 18 ka and 14 ka BP.
3. Impinging vortices and horseshoe/longitudinal vortices in turbulent meltwater flowing over the preglacial divide, eroded flutings and s-forms into the

scoured bedrock tract, and modified glaciotectonic ridges. If the transverse ridges are primary fluvial bedforms, they were probably formed beneath internal stationary waves in subglacial sheet flows at this time. These forms were produced during regional-scale erosion of bedrock and surficial sediment.

4. Progressive channelisation of the sheet flow across the preglacial divide during waning discharges, resulted in partial ice-bed recoupling, flow concentration, increased meltwater flow velocities and preferential incision in areas of deeper flow. Channels operated synchronously and eventually carried all the flow after the ice sheet recoupled with its bed on interfluves. The absence of channels downglacier of the preglacial divide marks flow divergence and decreasing velocities. Low gradient ice sheet profiles led to minimal ice flow as the ice settled to its bed following flood release. Thus, an almost pristine subglacial environment is preserved today on the Western Plains.
5. Only minor landscape modification of the area occurred during deglaciation, including the formation of small eskers, the establishment of glacial lakes, rivers, creeks, and eolian dune fields.

Potential meltwater sources for large subglacial floods have been discussed by Shaw (1996) and Munro-Stasiuk (submitted) although direct evidence for a supraglacial lake source is unlikely to be found. The Pakowki basin immediately behind the preglacial divide is a probable location for subglacial meltwater storage. Munro-Stasiuk (submitted) finds evidence upglacier from the study area, from tills and glaciolacustrine deposits, for deposition in a subglacial reservoir that drained repeatedly. Similar drainage from many subglacial reservoirs may have ultimately reached a reservoir located at Pakowki Lake. Drainage of subglacial and, possibly, supraglacial reservoirs along the Livingstone Lake flood path may have eventually penetrated an ice-marginal seal, causing catastrophic release of the stored meltwater. Field evidence suggests that such drainage did occur, first as a sheet and, later, in tunnel channels. Release of meltwater

over the Milk River divide may have allowed the release of subglacial lakes all the way to Keewatin. Thus, the drainage event described in this paper, would have carried much of the flood water of the proposed Livingstone Lake event.

The total amount of material eroded by the subglacial meltwater flows cannot be accurately determined, although tunnel channel depth provides a minimum measure. Sediment carried in suspension by subglacial flows to the ice margin may have been carried by proglacial rivers and deposited well beyond the limit of Late Wisconsinan glaciation, partly in the Gulf of Mexico (Shaw *et al.*, 1996). Such transport would account for the absence of major deposits at the former ice margins in Montana. Geomorphic evidence suggests a flow at least 80 km wide, and between 10 and 60 m deep, with a conservative velocity of  $10 \text{ ms}^{-1}$ . Instantaneous discharges of  $10^6$ - $10^7 \text{ m}^3\text{s}^{-1}$  are estimated that are similar to estimates obtained elsewhere (c.f., Shaw, 1996). It is proposed that the scoured zone of southeast Alberta must have been of regional extent and is a part of the Livingstone Lake megaflood path recognised in Alberta (Rains *et al.*, 1993).

The observed landforms show a consistent pattern that may be interpreted as part of a continuum of subglacial environments. They largely record erosion by subglacial meltwater flows following glacial erosion, transport and deposition of sediment. As only one medium is required, a less complex subglacial system is proposed than hypotheses requiring multiple processes to account for the subglacial landforms. Conclusions from this study support a genesis of many subglacial landforms by subglacial fluvial erosion.

## References

- Aber, J.S., Croot, D.G. and Fenton, M.M. 1989. *Glaciotectonic Landforms and Structures*. Kluwer Academic Publishers, Dordrecht, 201 pp.
- Allen, J.R.L. 1982. *Sedimentary structures. Developments in Sedimentology* 30A. Elsevier, Amsterdam, vol.2, 593 pp.
- Alley, R.B. 1989. Water pressure coupling of sliding and deformation: 1. Water system. *Journal of Glaciology*, **35**, 108-118.
- Alley, R.B. 1991. Deforming-bed origin for southern Laurentide till sheets? *Journal of Glaciology*, **37**, 67-76.
- Alley, R.B. 1992. How can low-pressure channels and deforming tills coexist subglacially? *Journal of Glaciology*, **38**, 200-207.
- Alley, R.B., Blankenship, D.D., Bentley, C.R. and Rooney, S.T. 1986. Deformation of till beneath Ice Stream B, west Antarctica. *Nature*, **322**, 57-59.
- Alley, R.B., Blankenship, D.D., Bentley, C.R., and Rooney, S.T. 1987a. Till beneath Ice Stream B: 3, Till deformation: Evidence and implications. *Journal of Geophysical Research*, **92**, 8921-8929.
- Alley, R.B., Blankenship, D.D., Bentley, C.R., and Rooney, S.T. 1987b. Till beneath Ice Stream B: 4. A coupled ice-till flow model. *Journal of Geophysical Research*, **92**, 8931-8940.
- Benn, D.I. 1994b. Fabric shape and the interpretation of sedimentary fabric data. *Journal of Sedimentary Research*, **A64**, 910-915.
- Benn, D.I. 1995. Fabric signature of subglacial till deformation, Breidamerkurjokull, Iceland. *Sedimentology*, **42**, 735-747.
- Benn, D.I. 1996a. Subglacial and subaqueous processes near a grounding line: sedimentological evidence from a former ice-dammed lake, Achnasheen, Scotland. *Boreas*, **25**, 23-36.
- Benn, D.I. and Evans, D.J.A. 1998. *Glaciers and Glaciation*. Arnold, London, 734pp.
- Blake, E., Clarke, G.K.C. and Gerin, M.C. 1992. Tools for examining subglacial bed deformation. *Journal of Glaciology*, **38**, 388-396.

- Blankenship, D.D., Bentley, C.R., Ronney, S.T. and Alley, R.B. 1986. Seismic measurements reveal a saturated porous layer beneath an active Antarctic ice stream. *Nature*, **322**, 54-57.
- Blankenship, D.D., Bentley, C.R., Ronney, S.T. and Alley, R.B. 1987. Till properties beneath ice stream B. 1. Properties derived from seismic travel times. *Journal of Geophysical Research*, **92**, 8903-8911.
- Bluemle, J.P. and Clayton, L. 1984. Large-scale thrusting and related processes in North Dakota. *Boreas*, **13**, 279-299.
- Boulton, G.S. 1974. Processes and patterns of glacial erosion. In Coates, D.R. (ed) *Glacial Geology*. State University of New York, Binghamton, pp. 41-87.
- Boulton, G.S. 1979. Processes of glacier erosion on different substrata. *Journal of Glaciology*, **23**, 15-38.
- Boulton, G.S. 1986. A paradigm shift in glaciology. *Nature*, **322**, 18.
- Boulton, G.S. 1987. A theory of drumlin formation by subglacial deformation. In Menzies, J. and Rose, J. (eds) *Drumlin Symposium*. Balkema, Rotterdam, 25-81.
- Boulton, G.S. 1996a. Theory of glacial erosion, transport and deposition as a consequence of subglacial sediment deformation. *Journal of Glaciology*, **42**, 43-62.
- Boulton, G.S. and Caban, P. 1995. Groundwater flow beneath ice sheets: Part 2 - Its impact on glacier tectonic structures. *Quaternary Science Reviews*, **14**, 563-588.
- Boulton, G.S., Caban, P.E. and van Gijssel, K. 1995b. Groundwater flow beneath ice sheets: Part 1 - Large scale patterns. *Quaternary Science Reviews*, **14**, 545-562.
- Boulton, G.S. and Clark, C.D. 1990a. A highly mobile Laurentide Ice sheet revealed by satellite images of glacial lineations. *Nature*, **346**, 813-817.
- Boulton, G.S. and Clark, C.D. 1990b. The Laurentide Ice sheet through the last glacial cycle: drift lineations as a key to the dynamic behaviour of former ice sheets. *Transactions of the Royal Society of Edinburgh, Earth Sciences*, **81**, 327-347.
- Boulton, G.S. and Dobbie, K.E. 1993. Consolidation of sediments by glaciers: relations between sediment geotechnics, glacier dynamics and subglacial groundwater flow. *Journal of Glaciology*, **39**, 26-44.

- Boulton, G.S. and Hindmarsh, R.C.A. 1987. Sediment deformation beneath glaciers: rheology and geological consequences. *Journal of Geophysical Research*, **92**, 9059-9082.
- Boulton, G.S., Hulton, N.J. and Vautravers, M. 1995a. Ice sheet models as tools for paleoclimatic analysis: the example of the European ice sheet through the last glacial cycle. *Annals of Glaciology*, **21**, 103-110.
- Boulton, G.S. and Jones, A.S. 1979. Stability of temperate ice caps and ice sheets resting on beds of deformable sediment. *Journal of Glaciology*, **24**, 29-43.
- Boulton, G.S., Smith, G.D., Jones, A.S. and Newsome, J. 1985. Glacial geology and glaciology of the last mid-latitude ice sheets. *Geological Society of London Journal*, **142**, 447-474.
- Brennand, T.A. 1994. Macroforms, large bedforms and rhythmic sedimentary sequences in subglacial eskers: genesis and meltwater regime. *Sedimentary Geology*, **91**, 9-55.
- Brennand, T.A. and Shaw, J. 1994. Tunnel channels and associated landforms, south-central Ontario: their implications for ice sheet hydrology. *Canadian Journal of Earth Sciences*, **31**, 505-522.
- Bretz, J.H. 1969. The Lake Missoula floods and the Channeled Scabland. *Journal of Geology*, **77**, 505-543.
- Christiansen, E.A. and Sauer, E.K. 1988. Age of the Frenchman Valley and associated drift south of the Cypress Hills. *Canadian Journal of Earth Sciences*, **25**, 1703-1708.
- Clark, C.D. 1993. Mega-scale lineations and cross-cutting ice-flow landforms. *Earth Surface Processes and Landforms*, **18**, 1-29.
- Clark, P.U. 1994. Unstable behaviour of the Laurentide Ice sheet and its implications to ice sheet dynamics. *Quaternary Research*, **41**, 19-25.
- Clark, P.U. and Hansel, A.K. 1989. Till lodgement, clast ploughing and glacier sliding over a deformable glacier bed. *Boreas*, **18**, 201-207.
- Clarke, G.K.C. 1986. Professor Mathews, outburst floods, and other glaciological disasters. *Canadian Journal of Earth Sciences*, **23**, 859-868.
- Clarke, G.K.C. 1987. Subglacial till: a physical framework for its properties and processes. *Journal of Geophysical Research*, **92**, 8942-8984.



- Clayton, L., Mickelson, D.M. and Attig, J.W. 1989. Evidence against pervasively deformed bed material beneath rapidly moving lobes of the southern Laurentide Ice sheet. *Sedimentary Geology*, **62**, 203-208.
- Clayton, L., Teller, J.T. and Attig, J.W. 1985. Surging of the southwestern part of the Laurentide Ice sheet. *Boreas*, **14**, 235-241.
- Cudlip, W. and McIntyre, N.F. 1987. Seasat altimeter observations of an Antarctic "lake". *Annals of Glaciology*, **9**, 55-59.
- Dahl, R. 1965. Plastically sculptured detail forms on rock surfaces in northern Nordland, Norway. *Geografiska Annaler, Series A*, **47**, 3-140.
- Dardis, G.F. and Hanvey, P.M. 1994. Sedimentation in a drumlin lee-side wave cavity, northwest Ireland. *Sedimentary Geology*, **91**, 97-114.
- Dardis, G.F. and McCabe, A.M. 1983. Facies of subglacial channel sedimentation in late Pleistocene drumlins, Northern Ireland. *Boreas*, **12**, 263-278.
- Dardis, G.F. and McCabe, A.M. 1987. Subglacial sheet-wash and debris flow deposits in late Pleistocene drumlins, Northern Ireland. In Menzies, J. and Rose, J. (eds) *Drumlin Symposium*. Balkema, Rotterdam, 225-240.
- Dardis, G.F. and McCabe, A.M. 1994. Subglacial processes, sediments and landforms - an introduction. *Sedimentary Geology*, **91**, 1-8.
- Dowdeswell, J.A. and Sharp, M. 1986. Characterisation of pebble fabrics in modern glacial sediments. *Sedimentology*, **33**, 699-710.
- Dreimanis, A. 1993. Water-eroded crescentic scours and furrows associated with subglacial flutes at Breidamerkurjökull, Iceland. *Boreas*, **22**, 110-112.
- Dyke, A.S. and Morris, T.F. 1988. Drumlin fields, dispersal trains and ice streams in Arctic Canada. *The Canadian Geographer*, **32**, 86-90.
- Echelmeyer, K. and Harrison, W.D. 1990. Jacobshavns Isbrae, west Greenland, seasonal variations in velocity - or lack thereof. *Journal of Glaciology*, **36**, 82-88.
- Ellis-Evans, C.J. and Wynn-Williams, D. 1996. A great lake under the ice. *Nature*, **381**, 644-646.
- Evans, D.J.A. 1996. A possible origin for a mega-fluting complex on the southern Alberta prairies, Canada. *Zeitschrift für Geomorphologie, Supplement Band 106*, 125-148.

- Fisher, D.A., Reeh, N. and Langley, K. 1985. Objective reconstructions of the Late Wisconsinan Laurentide Ice sheet and the significance of deformable beds. *Geographie physique et Quaternaire*, **39**, 229-238.
- Fisher, T.G. and Shaw, J. 1992. A depositional model for Rogen moraine, with examples from the Avalon Peninsula, Newfoundland. *Canadian Journal of Earth Sciences*, **29**, 669-686.
- Goldstein, B. 1989. Lithology, sedimentology, and genesis of the Waden drumlin field, Minnesota, USA. *Sedimentary Geology*, **62**, 241-277.
- Grant, N.M. 1997. *Genesis of the North Battleford Fluting Field, West-Central Saskatchewan*. MSc thesis, University of Alberta, Edmonton.
- Grübe, F. 1983. Tunnel valleys. In Ehlers, J. (ed) *Glacial deposits in north-west Europe*. Balkema, Rotterdam, 257-258.
- Hanvey, P.M. 1987. Sedimentology of lee-side stratification sequences in late Pleistocene drumlins, north-west Ireland. In Menzies, J. and Rose, J. (eds) *Drumlin Symposium*. Balkema, Rotterdam, 241-253.
- Hanvey, P.M. 1989. Stratified flow deposits in a late Pleistocene drumlin in northwest Ireland. *Sedimentary Geology*, **62**, 211-221.
- Hart, J.K. 1994. Till fabric associated with deformable beds. *Earth Surface Processes and Landforms*, **19**, 15-32.
- Hart, J.K. 1995a. Drumlin formation in southern Anglesey and Arvon, north west Wales. *Journal of Quaternary Science*, **10**, 3-14.
- Hart, J.K. 1997. The relationship between drumlins and other forms of subglacial glaciotectionic deformation. *Quaternary Science Reviews*, **16**, 93-107.
- Hart, J.K. and Boulton, G.S. 1991. The interrelationships between glaciotectionic deformation and glaciodeposition within the glacial environment. *Quaternary Science Reviews*, **10**, 335-350.
- Hart, J.K., Hindmarsh, R.C.A. and Boulton, G.S. 1990. Different styles of subglacial glaciotectionic deformation in the context of the Anglian ice sheet. *Earth Surface Processes and Landforms*, **15**, 227-241.
- Hicock, S.R. and Dreimanis, A. 1992. Deformation till in the Great Lakes region: implications for rapid flow along the south-central margin of the Laurentide Ice sheet. *Canadian Journal of Earth Sciences*, **29**, 1565-1579.

- Hooke, R.Le B. and Iverson, N.R. 1995. Grain-size distribution in deforming subglacial tills, role of grain fracture. *Geology*, **23**, 57-60.
- Hughes Clarke, J.E., Shor, A.N., Piper, D.J.W. and Mayer, L.A. 1990. Large-scale current-induced erosion and deposition in the path of the 1929 Grand Banks turbidity current. *Sedimentology*, **37**, 613-629.
- Humphrey, N.F., Kamb, B., Fahnestock, M. and Engelhardt, H. 1993. Characteristics of the bed of the lower Columbia Glacier, Alaska. *Journal of Geophysical Research*, **98**, 837-846.
- Iverson, N.R., Hanson, B., Hooke, R.LeB. and Jansson, P. 1995. Flow mechanism of glaciers on soft beds. *Science*, **267**, 80-81.
- Jackson, L.E. Jr., Little, E.C., Leboe, E.R. and Holme, P.J. 1996. A re-evaluation of the paleogeography of the maximum continental and montane advances, southwestern Alberta. *Geological Survey of Canada, Current Research 1996-A*, 165-173.
- Jones, N. 1982. The formation of giant flutings in east-central Alberta. In Davidson-Arnott, R., Nickling, W. and Fahey, B.D. (eds) *Research in Glacial, Glacio-fluvial and Glacio-lacustrine Systems*. Geo Books, Norwich, 49-70.
- Kapitsa, A.P., Ridley, J.K., Robin, G.deQ., Siegert, M.J. and Zotikov, I.A. 1996. A large deep freshwater lake beneath the ice of central East Antarctica. *Nature*, **381**, 684-686.
- Kor, P.S.G., Shaw, J. and Sharpe, D.R. 1991. Erosion of bedrock by subglacial meltwater, Georgian Bay, Ontario: a regional view. *Canadian Journal of Earth Sciences*, **28**, 623-642.
- Krimmel, R.M. and Vaughn, B.H. 1987. Columbia Glacier, Alaska: changes in velocity 1977-1986. *Journal of Geophysical Research*, **92**, 8961-8968.
- Kulig, J.J. 1996. The glaciation of the Cypress Hills of Alberta and Saskatchewan and its regional implications. *Quaternary International*, **32**, 53-77.
- Liverman, D.G.E., Catto, N.R. and Rutter, N.W. 1989. Laurentide glaciation in west-central Alberta: a single (Late Wisconsinan) event. *Canadian Journal of Earth Sciences*, **26**, 266-274.
- MacAyeal, D.R. 1993b. Binge/purge oscillations of the Laurentide ice sheet as a cause of the North Atlantic's Heinrich Events. *Paleoceanography*, **8**, 775-784.

- Marshall, S.J., Clarke, G.K.C., Dyke, A.S. and Fisher, D.A. 1996. Geologic and topographic controls on fast flow in the Laurentide and Cordilleran Ice sheet. *Journal of Geophysical Research*, **101**, 17827-17839.
- McCabe, A.M. and Dardis, G.F. 1989. Sedimentology and depositional setting of late Pleistocene drumlins, Galway Bay, western Ireland. *Journal of Sedimentary Petrology*, **59**, 944-959.
- McCabe, A.M. and Dardis, G.F. 1994. Glaciotectonically induced water-throughflow structures in a Late Pleistocene drumlin, Kanrawer, County Galway, western Ireland. *Sedimentary Geology*, **91**, 173-190.
- Mellor, M. and McKinnon, G. 1960. The Amery Ice Shelf and its hinterland. *Polar Record*, **10**, 30-34.
- Menzies, J. and Rose, J. 1989. Subglacial bedforms - an introduction. *Sedimentary Geology*, **62**, 117-122.
- Mickelson, D.M., Ham, N.R. and Ronnert, L. 1992. Comment on 'Striated clast pavements: products of deforming subglacial sediment?'. *Geology*, **20**, 285.
- Mooers, H.D. 1989. On the formation of the tunnel valleys of the Superior Lobe, central Minnesota. *Quaternary Research*, **32**, 24-35.
- Munro, M.J. and J. Shaw. 1997. Erosional origin of hummocky terrain in south-central Alberta, Canada. *Geology*, **25**, 1027-1030.
- Munro-Stasiuk, M.J. submitted. Erosional hummocky terrain: evidence for water storage and catastrophic drainage at the base of the Laurentide ice sheet, south-central Alberta. *Annals of Glaciology*, **28**.
- O'Cofaigh, C. 1996. Tunnel Valley Genesis. *Progress in Physical Geography*, **20**, 1-19.
- Oswald, G.K.A. and Robin, G.deQ. 1973. Lakes beneath the Antarctic Ice sheet. *Nature*, **245**, 251-254.
- Patterson, C.J. and T.J. Boerboom. 1998. The significance of pre-existing, deep weathering of crystalline rock in interpreting the effects of glaciation on the Canadian Shield, Minnesota. *Abstracts, International Symposium on Glaciers and Glaciated Landscapes*, Kiruna, Sweden, 20.
- Patterson, C.J. and Hooke, R.Le.B. 1996. Physical environments of drumlin formation. *Journal of Glaciology*, **41**, 30-38.

- Piotrowski, J.A. 1997. Subglacial environments - an introduction. *Sedimentary Geology*, 111, 1-7.
- Piotrowski, J.A. and Smalley, I.J. 1987. The Woodstock drumlin field, southern Ontario, Canada. In Menzies, J. and Rose, J. (eds) *Drumlin Symposium*. Balkema, Rotterdam, 309-322.
- Pollard, A., Wakarani, N. and Shaw, J. 1996. Genesis and morphology of erosional shapes associated with turbulent flow over a forward facing step. In Ashworth, P.J., Bennett, S.J., Best, J.L. and McLelland, S.L. (eds) *Coherent Flow Structures in Open Channels*. Wiley, Chichester, 249-265.
- Rains, R.B., Shaw, J., Skoye, R., Sjogren, D. and Kvill, D. 1993. Late Wisconsinan subglacial megaflood paths in Alberta. *Geology*, 21, 323-326.
- Ronnert, L. and Mickelson, D.M. 1992. High porosity of basal till at Burroughs Glacier, southeastern Alaska. *Geology*, 20, 849-852.
- Rose, J. 1987b. Drumlins as part of a glacier bedform continuum. In Menzies, J. and Rose, J. (eds) *Drumlin Symposium*. Balkema, Rotterdam, 103-116.
- Rose, J. and Letzer, J.M. 1977. Superimposed drumlins. *Journal of Glaciology*, 18, 471-480.
- Russell, A.J. 1993. Supraglacial lake drainage near Sondre Stromfjord, Greenland. *Journal of Glaciology*, 39, 431-433.
- Sawagaki, T. and Hirakawa, K. 1997. Erosion of bedrock by subglacial meltwater, Soya Coast, East Antarctica. *Geografiska Annaler*, 79A, 223-238.
- Sharpe, D.R. and Shaw, J. 1989. Erosion of bedrock by subglacial meltwater, Cantley, Quebec. *Geological Society of America Bulletin*, 101, 1011-1020.
- Shaw, J. 1983. Drumlin formation related to inverted meltwater erosional marks. *Journal of Glaciology*, 29, 461-479.
- Shaw, J. 1988. Subglacial erosional marks, Wilton Creek, Ontario. *Canadian Journal of Earth Sciences*, 25, 1256-1267.
- Shaw, J. 1994a. Hairpin erosional marks, horseshoe vortices, and subglacial erosion. *Sedimentary Geology*, 91, 269-283.
- Shaw, J. 1996. A meltwater model for Laurentide subglacial landscapes. In McCann, B. and Ford, D.C. (eds) *Geomorphology Sans Frontiers*. Wiley, Chichester, 181-236.

- Shaw, J. and Kellerhals, R. 1977. Paleohydraulic interpretation of antidune bedforms with applications to antidunes in gravel. *Journal of Sedimentary Petrology*, **47**, 257-266.
- Shaw, J. and Kvill, D. 1984. A glaciofluvial origin for drumlins of the Livingstone Lake area, Saskatchewan. *Canadian Journal of Earth Sciences*, **12**, 1426-1440.
- Shaw, J. and Sharpe, D.R. 1987. Drumlin formation by subglacial meltwater erosion. *Canadian Journal of Earth Science*, **24**, 2316-2322.
- Shaw, J., Kvill, D. and Rains, R.B. 1989. Drumlins and catastrophic subglacial floods. *Sedimentary Geology*, **62**, 177-202.
- Shaw, J., Rains, R.B., Eyton, R. and Weissling, L. 1996. Laurentide subglacial outburst floods: landform evidence from digital elevation models. *Canadian Journal of Earth Sciences*, **33**, 1154-1168.
- Shetsen, I. 1987. Quaternary geology, southern Alberta. *Alberta Research Council Map*, scale 1:500000.
- Shoemaker, E.M. 1991. On the formation of large subglacial lakes. *Canadian Journal of Earth Sciences*, **28**, 1975-1981.
- Shoemaker, E.M. 1992a. Subglacial floods and the origin of low-relief ice sheets lobes. *Journal of Glaciology*, **38**, 105-112.
- Shoemaker, E.M. 1992b. Water sheet outburst floods from the Laurentide Ice sheet. *Canadian Journal of Earth Sciences*, **29**, 1250-1264.
- Shoemaker, E.M. 1994. Reply to comments on 'Subglacial floods and the origin of low-relief ice sheet lobes' by J.S. Walder. *Journal of Glaciology*, **40**, 201-202.
- Shreve, R.L. 1972. Movement of water in glaciers. *Journal of Glaciology*, **11**, 205-214.
- Sjogren, D. and Rains, R.B. 1995. Glaciofluvial erosional morphology and sediments of the Coronation-Spondin Scabland, east-central Alberta. *Canadian Journal of Earth Sciences*, **32**, 565-578.
- Szilder, K., Lozowski, E.P. and Shaw, J. submitted. Broad, subglacial outburst floods: a hydraulic model.
- Tsui, Po.C., Cruden, D.M. and Thomson, S. 1989. Ice-thrust terrains and glaciotectionic settings in central Alberta. *Canadian Journal of Earth Sciences*, **26**, 1308-1318.

- Walder, J.S. 1982. Stability of sheet flow of water beneath temperate glaciers and implications for glacier surging. *Journal of Glaciology*, **28**, 273-293.
- Walder, J.S. and Fowler, A. 1994. Channelized subglacial drainage over a deformable bed. *Journal of Glaciology*, **40**, 3-15.
- Westgate, J.A. 1968. Surficial geology of the Foremost-Cypress Hills area, Alberta. *Research Council of Alberta, Bulletin* 22.
- Whillans, I.M. and Veen, C.J. van der. 1995. New and improved determinations of velocity of Ice Stream B and C, West Antarctica. *Journal of Glaciology*, **39**, 483-490.
- Whillans, I.M., Bolzan, J. and Shabtaie, S. 1987. Velocity of Ice Streams B and C, Antarctica. *Journal of Geophysical Research*, **92**, 8895-8902.
- Wingfield, R. 1990. The origin of major incursions within the Pleistocene deposits of the North Sea. *Marine Geology*, **91**, 31-52.
- Wright, H.E. 1957. Stone orientation in Wadena drumlin field, Minnesota. *Geografiska Annaler*, **39**, 19-31.
- Wright, H.E. 1962. Role of the Wadena lobe in the Wisconsinan glaciation in Minnesota. *Bulletin of the Geological Society of America*, **73**, 73-100.
- Wright, H.E. 1973. Tunnel valleys, glacial surges, and subglacial hydrology of the Superior Lobe, Minnesota. In Black, R.F., R.P. Goldthwait and H.B. Willman., eds. The Wisconsinan Stage. *Geological Society of America Memoir*, **136**, 251-276.
- Yalin, M.S. 1972. *Mechanics of Sediment Transport*. Pergamon Press, Oxford, 290 pp.
- Young, R.R., Burns, J.A., Smith, D.G., Arnold, L.D. and Rains, R.B. 1994. A single Late Wisconsinan, Laurentide glaciation, Edmonton area and southwestern Alberta. *Geology*, **22**, 683-686.

## CHAPTER 3: TRANSVERSE BEDFORMS: GLACIOTECTONIC DEFORMATION OR FLUVIAL EROSION?

### Introduction

Ice-thrust features have been mapped extensively across the glaciated Great Plains of North America (Kupsch, 1962; Moran *et al.*, 1980; Bluemle and Clayton, 1984; Tsui *et al.*, 1989) and such thrusting may have been the single most important geomorphic process operating in some areas of North America (Bluemle and Clayton, 1984). Hill-shaded digital elevation models (DEMs) of southeast Alberta reveal transverse ridges superimposed on an upstanding ridge which forms the preglacial divide between the Cypress Hills and the Sweet Grass Hills (Fig. 3-1). These landforms are part of a complex subglacial environment formed during the Late Wisconsinan glaciation of the region and have been mapped as glaciotectionic ridges of thrust bedrock and till (Westgate, 1968; Shetsen, 1987).

Three main types of glacial thrust forms have been documented (Bluemle and Clayton, 1984; Tsui *et al.*, 1989): (1) *hill-depression forms* are equidimensional hills downglacier of a depression of similar dimensions (e.g., Bluemle, 1970; Clayton and Moran, 1974); (2) *transverse ridge forms* which tend to include overturned folds, or thrust faulted imbricate stacks (e.g., Rutten, 1960; Kupsch, 1962; Stalker, 1973b; Clayton *et al.*, 1980; Bluemle and Clayton, 1984; Oldale and O'Hara, 1984); and (3) *irregular forms* which are intermediate to the other forms and comprise irregularly located, closely-spaced hills, ridges and depressions (e.g., Fenton, 1983). These ice-thrust features can occur in 3 glaciotectionic settings (Tsui *et al.*, 1989): (1) escarpment setting; (2) valley setting; and (3) plains setting. Transverse ridges in the study area are most similar to transverse ridge forms (Bluemle and Clayton, 1984) and, from their association with the preglacial divide, correspond to the escarpment setting of Tsui *et al.*, (1989).

Transverse ridges in southeast Alberta are part of a predominately erosional, subglacial landscape with many features interpreted as products of subglacial meltwater erosion (Chapter 2). These ridges are mapped as glaciotectionic features (Shetsen, 1987), but their characteristics are not easily explained by glaciotectionic processes. Although



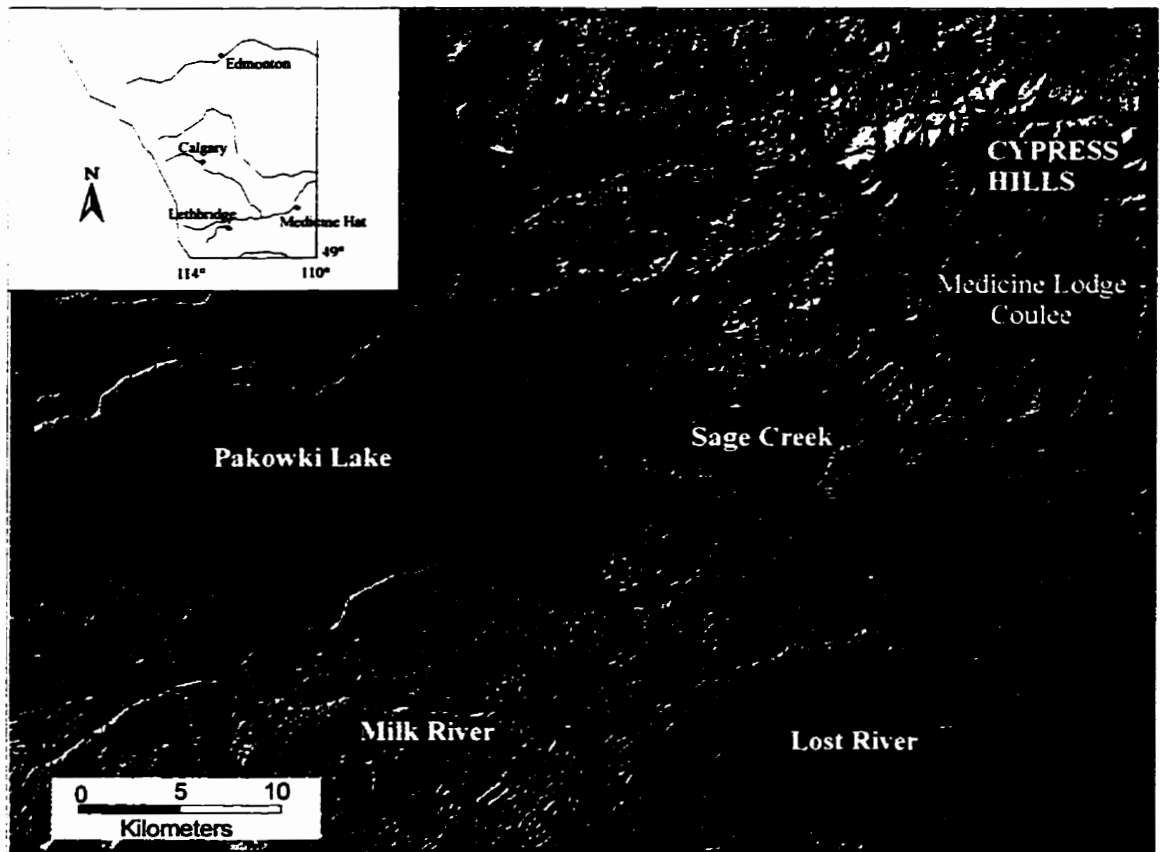


Figure 3-1. Hill-shaded DEM of southeast Alberta showing complex suite of transverse ridges on the preglacial divide (sun angle 315°N, elevation 25°).

morphologically similar to transverse ridge forms, they are also analogous to transverse s-forms in bedrock (Kor *et al.*, 1991), erosional megaripples in the Eastern Channel of the Laurentian Fan (Hughes Clark *et al.*, 1990) and antidunes formed in rivers (e.g., Shaw and Kellerhals, 1977; Allen, 1982). Thus, fluvial processes or turbidity currents created transverse ridges. This study investigates the pros and cons of glaciotectonism and fluvial erosion as explanations for the ridges.

In the absence of good exposures, ground penetrating radar (GPR) provides subsurface structural information. GPR has been successfully applied in investigations of geomorphic processes (e.g., Jol and Smith, 1991; Smith and Jol, 1992; Jol *et al.*, 1996); mapping soil stratigraphy, bedrock characteristics, subsurface topography and geological structures (e.g., Ulriksen, 1982; Worsfold *et al.*, 1986; Davis *et al.*, 1987; Annan, 1988; Annan *et al.*, 1988; Davis and Annan, 1989; Warner *et al.*, 1990); identification and thickness of permafrost (e.g., Pilon *et al.*, 1979, 1987; La Fleche *et al.*, 1987a, b, 1988; Dufour *et al.*, 1988); studies of groundwater depth (e.g., Annan and Davis, 1977); and in archaeological investigations (e.g., Vaughn, 1986). GPR has the potential to determine subsurface bedrock characteristics where lateral exposures and well-logs are limited. This technique is cost-effective, portable, easy to maintain and robust (Jol and Smith, 1991).

## **Methods**

GPR is based on the propagation and reflection of electromagnetic energy and is similar in principle to sonar and seismic reflection profiling (Jol and Smith, 1991). High frequency, electromagnetic pulses are emitted from the GPR unit which is capable of emitting energy in the 10-1000 MHz range. Energy is reflected back to a receiver from reflectors represented by changes in the bulk electrical properties of the substrate and by the character of the interface between different lithologies (Fig. 3-2). Two-way travel time is recorded and plotted against horizontal survey distance. The time taken for signals to be returned to the receiver is a function of the velocity of energy propagation through a medium and the depth of the reflectors (Jol and Smith, 1991; Jol *et al.*, 1996).

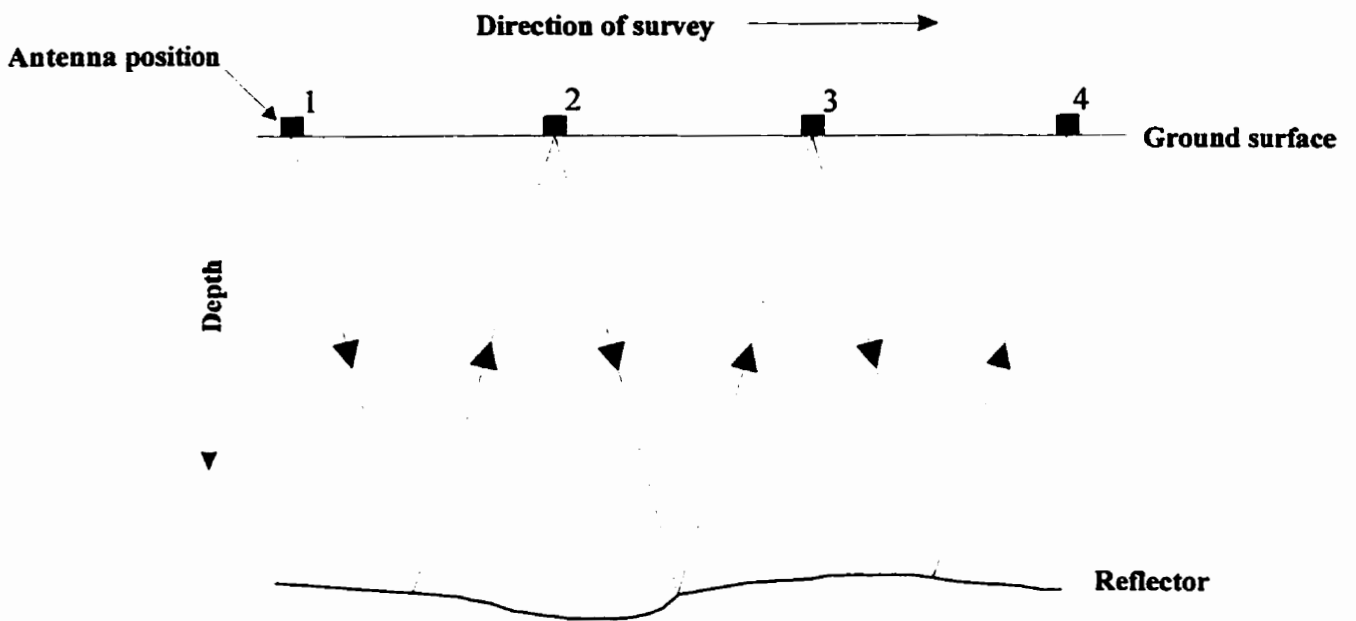


Figure 3-2. Principle of ground penetrating radar (GPR) based on propagation and reflection of electromagnetic energy from reflectors located beneath the surface. Depth of reflectors is a function of the two-way travel time of the signal and the near-surface velocity of the substrate material (modified from Jol and Smith, 1991, Fig. 3).

Depth (m) is determined from the propagation velocity ( $\text{mns}^{-1}$ ) for a medium and the recorded two-way travel time (ns).

Different lithologies and sediment types have different dielectric constants and, hence, propagation velocities that produce strong reflection from boundaries between units (Sheriff, 1984; Table 3-1). Differences in dielectric properties also attenuate the signal (Jol and Smith, 1991), allowing the character of the subsurface to be determined.

Material	Dielectric constant	Conductivity (mS/m)	Velocity (m/ns)	Attenuation (dB/m)
Air	1	0	0.3	0
Distilled water	80	0.01	0.033	0.002
Fresh water	80	0.5	0.033	0.1
Sea water	80	30000	0.01	1000
Dry sand	3-5	0.01	0.15	0.01
Saturated sand	20-30	0.1-1.0	0.06	0.03-0.3
Limestone	4-8	0.5-2.0	0.12	0.4-1.0
Shale	5-15	1-100	0.09	1-100
Silts	5-30	1-100	0.07	1-100
Clays	5-40	2-1000	0.06	1-300
Granite	4-6	0.01-1.0	0.13	0.01-1.0
Dry salt	5-6	0.01-1.0	0.13	0.01-1.0
Ice	3-4	0.01	0.16	0.01

Table 3-1. Dielectric properties for selected materials (from pulseEKKO IV software version 4.2).

GPR profiles were obtained using a 1000V transmitter and pulseEKKO IV software. Radar antenna with 25 MHz frequency were used to achieve maximum depth penetration although resolution was compromised. Near-surface velocities of  $0.15 \text{ mns}^{-1}$ , a sampling rate of 400 ps and 32 stacks per trace were used. Traces were taken at 1 m intervals with an antenna separation (transmitter-receiver) of 4 m (Fig. 3-3). Following data collection, profiles were plotted using pulseEKKO IV software with a trace-wiggle, automatic gain control, a trace stacking parameter of 2, and a point stacking parameter of 7. Topographic corrections were applied using profiles measured by dumpy level and staff.



**Figure 3-3. GPR unit in operation. 25 MHz antenna, showing transmitter/receiver units connected to two 6V batteries, are seen in foreground. A fibre optic cable carries signals from the transmitter/receiver units to the GPR console carried in a backpack. Console is powered by a 12V battery. Traces are collected at 1 m intervals and displayed and recorded on a laptop computer operated by field assistant.**

### **GPR investigation of transverse ridges**

A GPR profile was obtained across a transverse ridge on the preglacial divide, 10 km south of the Lost River channel (Fig. 3-1). The ridge is oriented northeast-southwest with a vertical relief of approximately 10 m and is composed entirely of Late Cretaceous sandstone and shale (Fig. 3-4). However, limited exposures did not allow description of the bedrock architecture. Ridge morphology shows an asymmetrical profile (Fig. 3-5) with the downstream side being slightly steeper. The profiled ridge is one of a series that are separated by depressions occupied by wetlands and elongated lakes. Traces were collected along a 200 m transect oriented at 180°N. Unfortunately, bad weather and problems with data retrieval allowed only part of the ridge to be successfully surveyed by GPR.

The GPR profile collected across the transverse ridge is shown in Figure 3-6. Information was obtained to a depth of approximately 15 m with a number of prominent reflectors being observed. The horizontal scale of all profiles is distance in metres, and the vertical scale is shown as both two-way travel time in nanoseconds, and depth in metres. The uppermost continuous reflector mirrors bed topography and represents a combination of the air-wave and ground-wave arrivals and should not be confused with deeper reflectors that record bedrock architecture (Jol and Smith, 1991).

Reflectors record changes in bedrock with depth and, hence, provide information on the character of that interface. Local bedrock comprises Late Cretaceous sandstone and shale of the Foremost Formation (Westgate, 1968). The prominent reflectors are likely shale beds where a higher dielectric constant, higher attenuation and lower velocity produce reflection and attenuation of the electromagnetic signal.

When plotted, the upper 15 m of the GPR profile reveals two seismic facies, identified by prominent reflectors (likely shale beds) at their base. These prominent reflectors dip northwest at 10-15°. The upper discontinuous reflector is first observed at 8 m depth and pinches out at 122 m along the profile. A lower discontinuous reflector is observed at 10-12 m depth and is observed between 35 m and 142 m. This reflector shows a similar angle of dip as the upper reflector. Between 142 m and 175 m, this lower



Figure 3-4. Late Cretaceous bedrock is exposed across the transverse ridge being profiled although structure cannot be discerned from limited surface exposures. Exposure is 75 cm high.

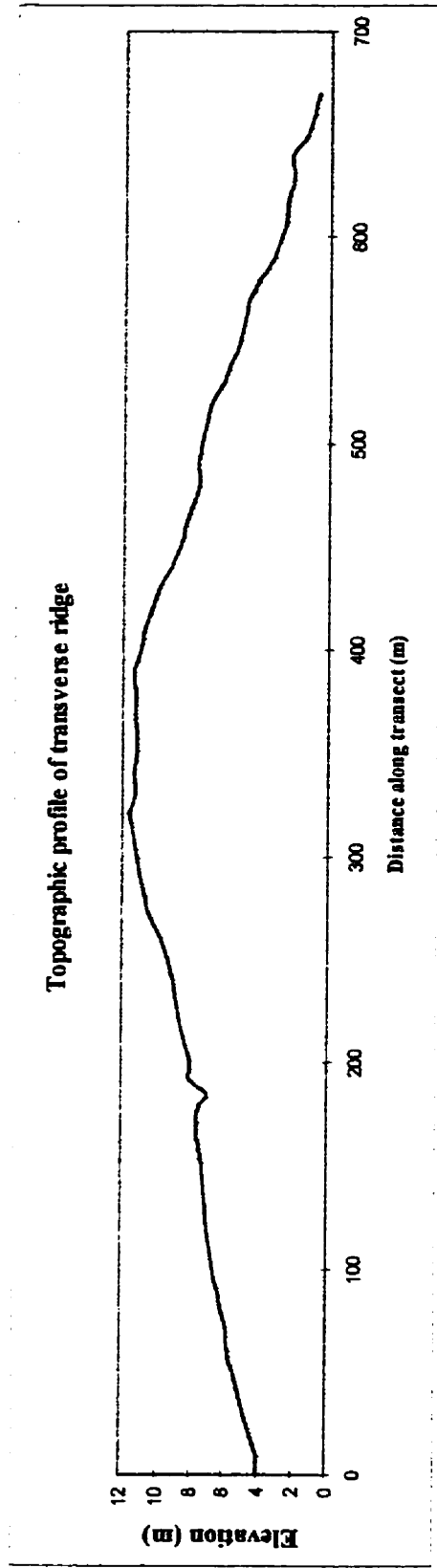


Figure 3-5. Topographic profile of transverse ridge profiled by GPR. VE=8X.



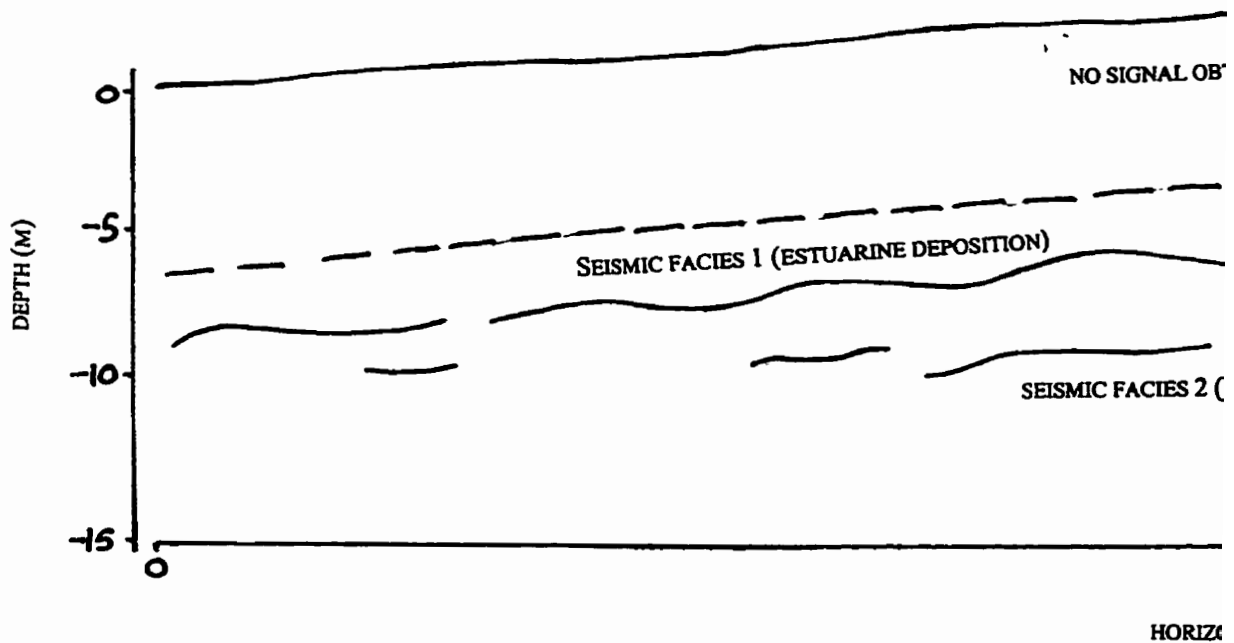
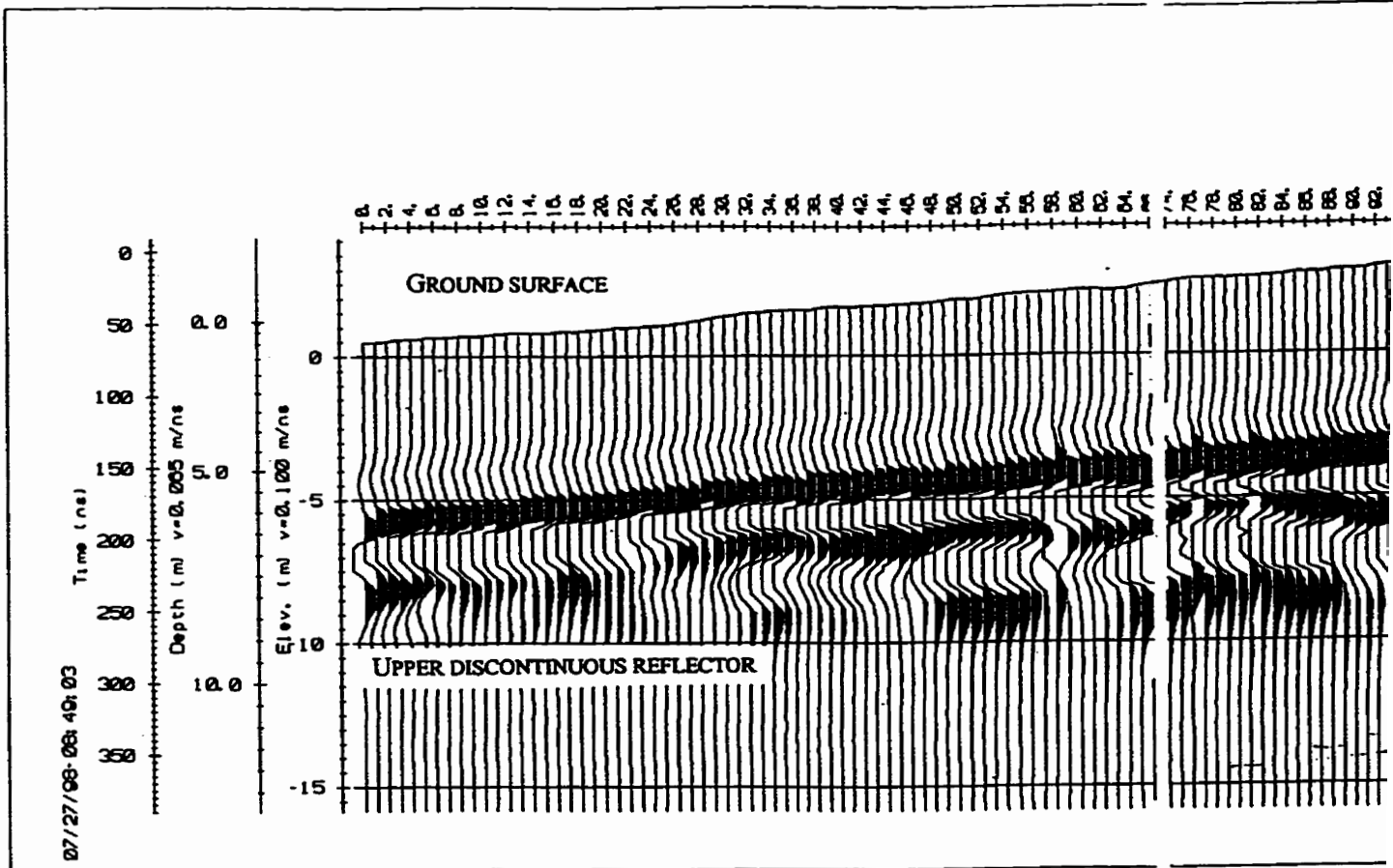
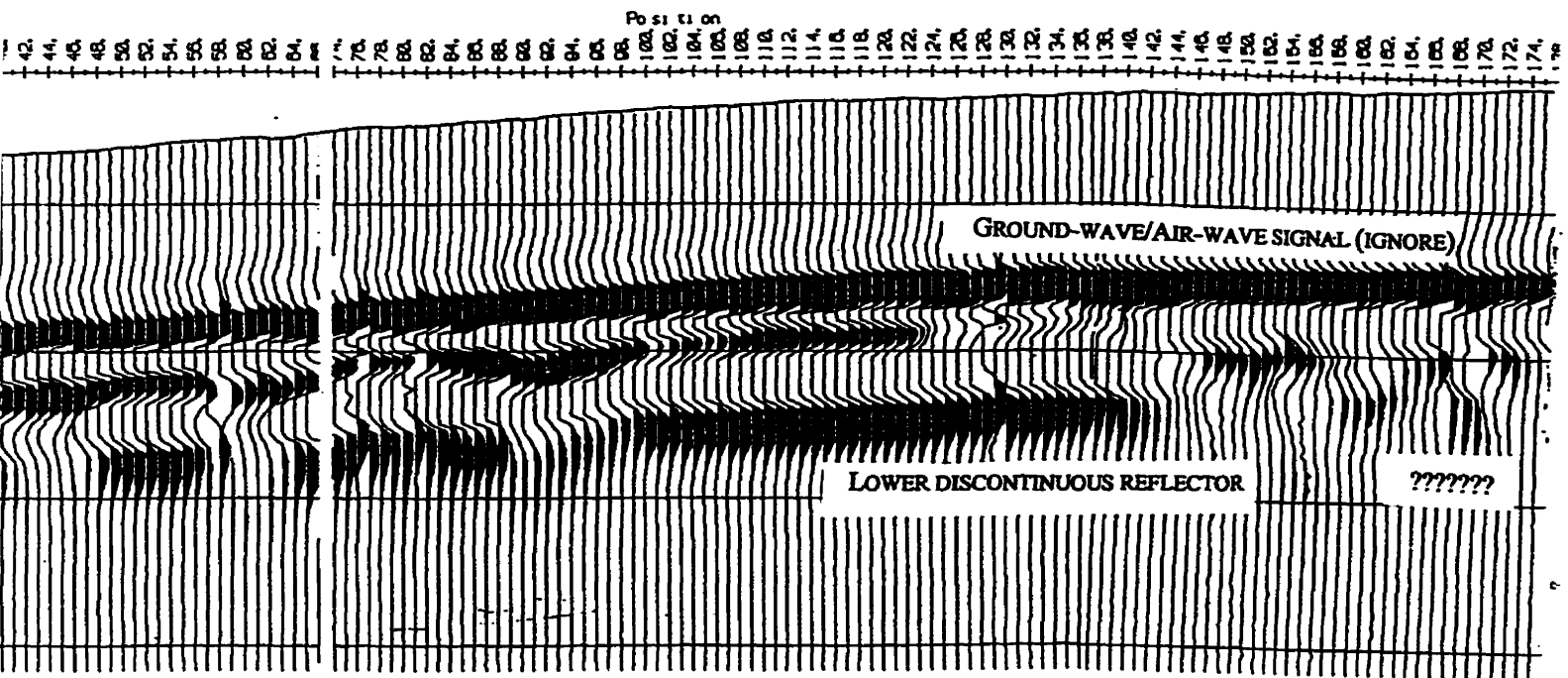


Figure 3-6. a) GPR profile obtained from reflection survey of transverse ridge.  
 b) Interpreted profile.





NO SIGNAL OBTAINED TO INFER STRUCTURE

FACIES 1 (ESTUARINE DEPOSITION)

? IRONSTONE CONCRETIONS ?

SEISMIC FACIES 2 (ESTUARINE DEPOSITION/CHANNEL SWITCHING)

100

175

HORIZONTAL DISTANCE (M)

transverse ridge.



reflector is discontinuous although the cause of this is uncertain. The character of the upper 8 m of the ridge cannot be resolved due to the GPR frequency used in the study where resolution was compromised to permit good penetration depth. The bedrock architecture observed by GPR may indicate either syn-depositional or post-depositional bedrock tectonics or rapid vertical and lateral changes in depositional style, perhaps associated with channel switching in a shallow marine or estuarine environment. These possibilities cannot be distinguished from the available information.

The bedrock architecture may reflect the depositional environment into which sediments were deposited during the Cretaceous. Inclined bedding may be epsilon cross-stratification associated with lateral accretion of point bars, or migrating channel-bar systems in an estuary environment (c.f., Reineck and Singh, 1980). Alternatively, deposition within tidal deltas or washover fans in a lagoonal setting may explain the coarse bedrock structure revealed by the radar survey (c.f., Reineck and Singh, 1980; Reinson, 1992). Following bedrock deposition and consolidation, the emplacement of the Sweet Grass Arch Pluton and associated volcanics may also have influenced the structure of the Cretaceous rocks (c.f., Westgate, 1968).

Post-depositional processes may also explain the observed bedrock structure. Dipping beds may have been produced by glaciotectonic thrusting of the bedrock producing ridges of unknown magnitude. This may have been associated with the advance of Laurentide ice into the region. However, shear planes associated with thrust faulting were not observed in the GPR profile. Evidence of deformed bedrock is noted elsewhere. Folded strata are observed in some ridges on the preglacial divide although this internal structure is truncated at the surface (Fig. 3-7). Glacial sediments are rarely observed within transverse ridges and Shield clasts commonly rest directly on the bedrock surface.

The important point to retain from the above discussion is that while many processes may account for the bedrock structure highlighted by the radar survey, this structure appears to be truncated at the surface. Hence, ridge form may be erosional and unrelated to the underlying bedrock.

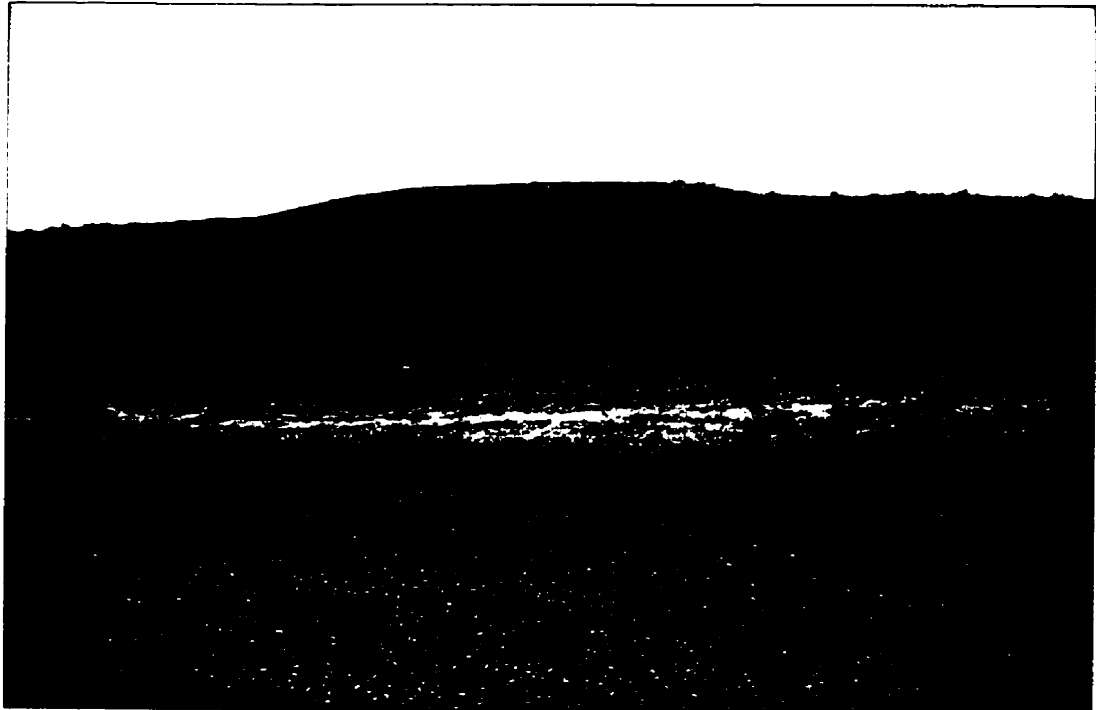


**Figure 3-7. Folded bedrock in transverse ridge possibly resulting from glaciotectonic thrusting from the northwest by the advancing Laurentide Ice Sheet. The ridge form is erosional with the syncline structure being truncated at the surface.**

### **Glaciotectonic deformation or fluvial erosion?**

Analysis of the GPR profile identifies an interesting bedrock structure that may be explained by various processes as discussed above. However, ridge morphology is unrelated to bedrock structure. Evidence from the GPR profile (Fig. 3-6) and observations of folded bedrock in other ridges across the preglacial divide (Fig. 3-7), indicate that glaciotectonic processes may have been at least partly responsible for producing the observed bedrock architecture. Thus, ridge formation may have been polygenetic with structure inherited from the initial depositional environments, a glaciotectonic component, and, last, an erosional component largely responsible for ridge and trough morphology.

A number of surface observations also provide information as to the probable origin of the transverse ridges in the study area. Flutings are superimposed on transverse ridges. They are less than 1 m high and tens of metres in length and are composed of intact bedrock (Fig. 3-8). These forms are restricted to ridge crests and do not cross intervening depressions. In the vicinity of the transverse ridges, flutings show poorly developed scours and furrows, but are nonetheless morphologically similar to flutings identified in the study area and elsewhere (c.f., Kor *et al.*, 1991; Rains *et al.*, 1993; Grant, 1997). Bedrock is exposed at the surface with only minor occurrences of glacial sediment. Shield clasts rest directly on the surface and are interpreted as discontinuous boulder lags.

Analysis of wavelength and amplitude of the transverse ridges across the preglacial divide reveals that wavelength decreases from 1300 m in the southwest to 400 m for smaller ridges in the northeast. Amplitude also decreases in the same direction from approximately 15 m to 1-2 m across the preglacial divide.

Three types of ridge patterns are observed (Fig. 3-9). These are described as: Type 1, three-dimensional wave forms, similar to hummocky terrain; Type 2, two-dimensional nested, and sometimes bifurcating, wave forms; and, Type 3, rhomboidal interfering forms. These forms are not described in other examples of ice-thrust ridges. This complex morphology occurs at the ridge scale and is not related to ice-marginal form (e.g., Aber *et al.*, 1989).

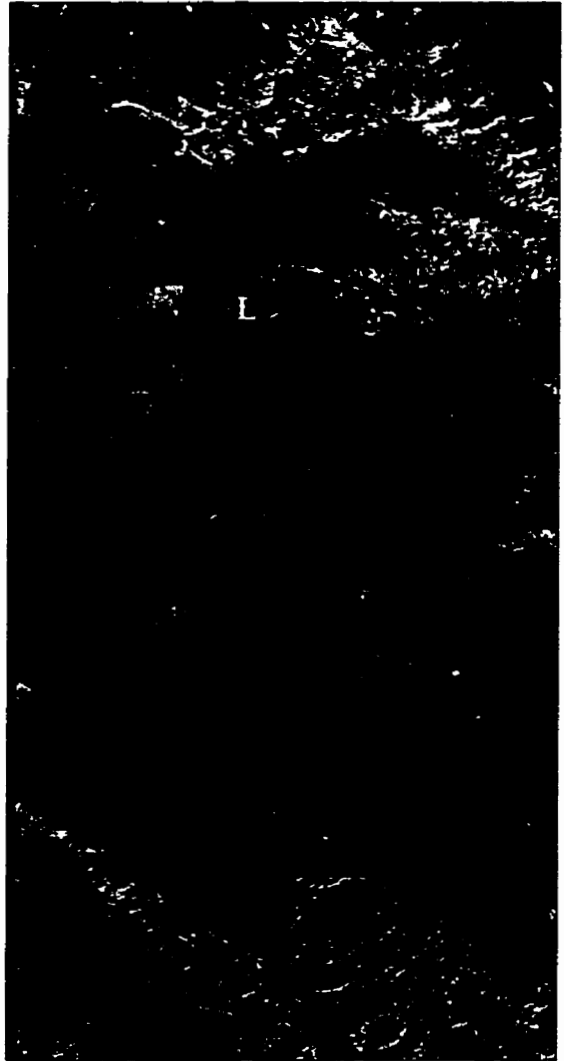
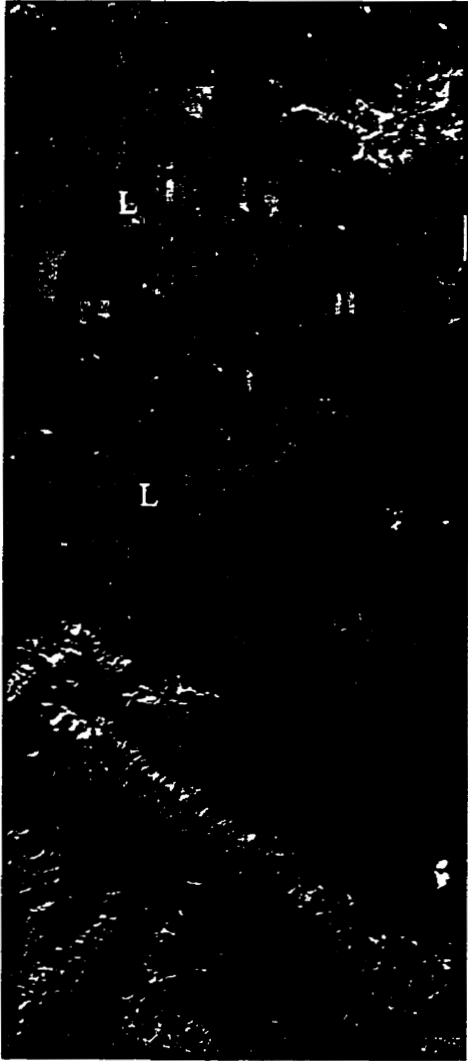


Figure 3-8. Stereopair showing transverse ridges at GPR study site with flutes superimposed on ridge surface. Scale 1:60,000. L refers to elongate lakes between ridges.



The preceding discussion has identified evidence for some glaciotectonic deformation of the local bedrock on the preglacial divide separating the Cypress Hills and the Sweet Grass Hills, although the extent of this deformation is not known. It is most likely to be Late Wisconsinan in age (c.f., Liverman *et al.*, 1989; Young *et al.*, 1994; Jackson *et al.*, 1996). However, superimposed on the ridge surfaces are features that are not explained by glaciotectonic deformation or depositional processes. Thus, two hypotheses are presented that may explain the landform assemblages located on the preglacial divide. First, transverse bedforms may be glaciotectonic ridges that were subsequently modified by the passage of subglacial meltwater. Second, these transverse features may be antidunes produced by erosion beneath stationary waves in subglacial meltwater flows.

*Hypothesis 1: Fluvially modified thrust bedforms*

Glaciotectonic deformation may be proglacial or subglacial and may arise during advance, maximal or recessional phases of glaciation (Aber *et al.*, 1989; Benn and Evans, 1998). It is difficult to distinguish which of these phases was responsible for glaciotectonic deformation in the study area, and it is possible that deformation occurred in all four. Lateral shear stress, related to resistance by local topography, is the fundamental cause of glaciotectonic deformation (Rotnicki, 1976; van der Wateran, 1985). Deformation of the substrate occurs when the stress transferred from the glacier exceeds the strength of the stressed material. Water pressure may play a significant part in determining the strength of the material (Aber *et al.*, 1989).

Glaciostatic pressure on the substrate is created by the overlying ice and is independent of ice movement. Differences in ice thickness, and, hence, vertical ice load, generate a lateral pressure gradient which is greatest at the ice margin. Thus, the lateral pressure gradient generates shear stresses that may produce glaciotectonic deformation in stationary ice. However, moving ice may substantially increase the shear stresses operating on the substrate (Aber *et al.*, 1989).

Thrusting of bedrock in southeast Alberta may have occurred as Laurentide ice advanced across the region. The upslope passage of ice in Alberta would have resulted in

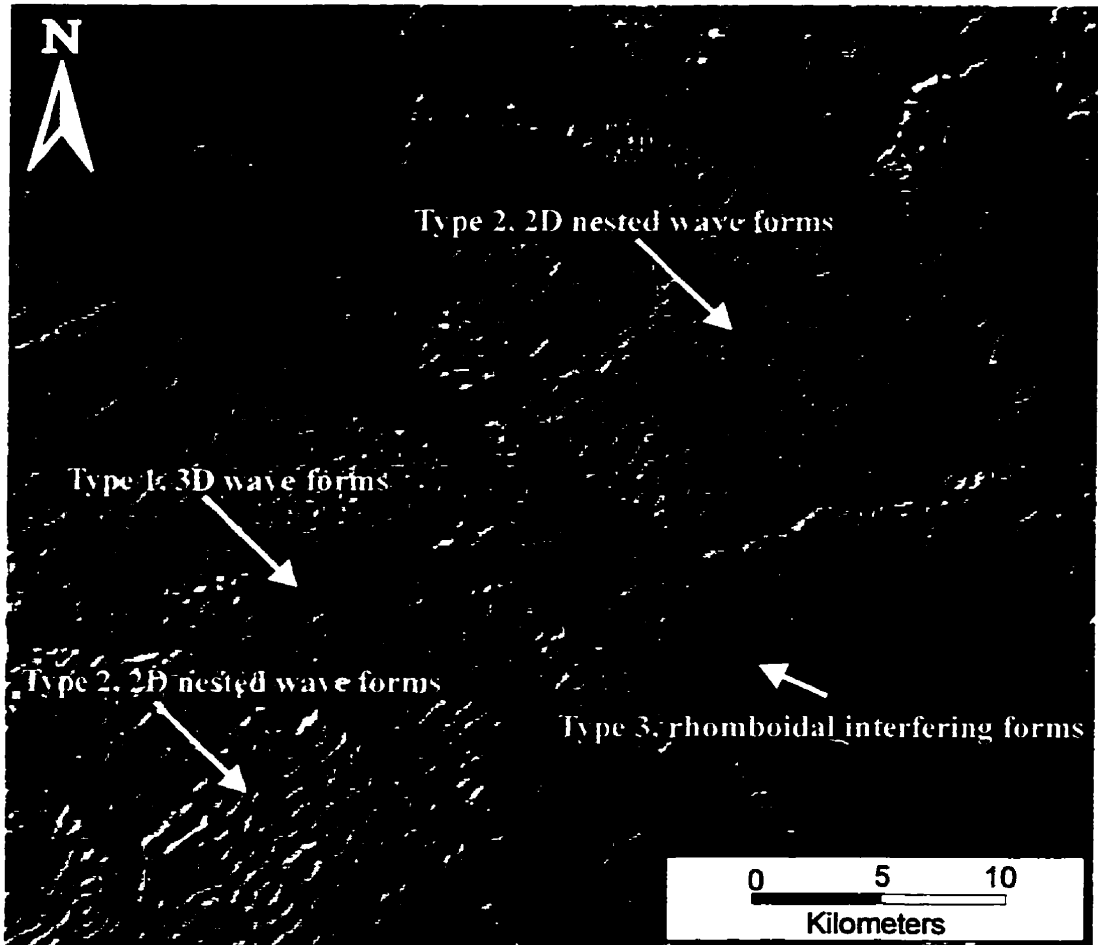


Figure 3-9. Hill-shaded DEM showing Type 1, Type 2 and Type 3 wave forms across the preglacial divide. These patterns may be controlled by flow characteristics associated with stationary waves within subglacial meltwater flows.

a steep ice front and high water pressure in groundwater which may have caused high glaciotectonic pressures that deformed the underlying bedrock (c.f., Aber *et al.*, 1989). Similarly, further ice advance across the region may have continued the deformation of substrate material subglacially. Deformed bedrock in some areas suggests thrusting from the northwest as a result of large shear stresses in the substratum. Thrusting produces stacking of inclined imbricate sheets which appear as repeated transverse ridges (Bluemle and Clayton, 1984; Tsui *et al.*, 1989).

Investigations of subglacial landforms in southeast Alberta have shown that they are most likely to have been the product of subglacial meltwater erosion (Chapter 2). The preglacial divide was probably a pinning point for Laurentide ice, and may have allowed subglacial meltwater to accumulate behind the divide in a large depression now occupied by Pakowki Lake. If sufficient volumes of subglacial meltwater were ponded behind the preglacial divide, ice may have separated from its bed in low-lying terrain. In this case, basal shear stresses formerly exerted in these areas would have been transferred to areas where the ice was in contact with its bed (Shaw, 1994a). Thus, increased shear stress across the preglacial divide may have been partly or wholly responsible for the glaciotectonics observed in bedrock on the preglacial divide.

Morphological and sedimentological evidence from flutings elsewhere in the study area, show that subglacial meltwater erosion was the most likely formation mechanism (c.f., Allen, 1982; Kor *et al.*, 1991; Shaw, 1994a; Munro and Shaw, 1997). Flutings superimposed on the transverse ridges may have been eroded by turbulent, sediment-laden meltwater containing horseshoe and other vortices. These vortices eroded crescentic scours and lateral furrows, leaving flutings superimposed on the ice-thrust ridges (Kor *et al.*, 1991; Shaw, 1994a). Impingement of vortices on the ridge surfaces caused erosion of ridge crests and an absence of flutes in the intervening depressions.

The movement of Laurentide ice across the preglacial divide would be expected to have eroded the substrate and deposited sediment on the surface (Benn and Evans, 1998). Accumulations of Shield clasts on the surface, some with faceted faces and striations, provide evidence for till deposition beneath moving ice (e.g., Clark and Hansel, 1989) although little till now remains. Removal of this material fits well with the hypothesis of

subglacial fluvial erosion (e.g., Munro and Shaw, 1997). It does not fit well with the glaciotectonic deformation hypothesis. If glacial processes were responsible for the removal of large quantities of glacial sediment, these would have been carried only as far as the ice margin. Large moraines or thick glacial deposits are not present along former Laurentide ice-margins in Montana. Thus, it is probable that the predominately fine-grained glacial sediment from the study area was transported well beyond the ice margin and possibly as far as the Gulf of Mexico (Shaw *et al.*, 1996).

It is hypothesised that the transverse ridges on the preglacial divide in the study area may have been formed by glaciotectonic processes, which produced imbricate stacking of bedrock along incompetent layers in the bedrock (e.g., Kupsch, 1962). Glaciotectonic deformation may be proglacial or subglacial in origin. Following ridge formation, large subglacial meltwater flows traversed the preglacial divide eroding bedrock flutes and removing much of the glacial sediment. Subsequent channelisation of sheet flow eroded tunnel channels that dissected the transverse bedforms. Subglacial meltwater erosion likely occurred at, or close to, the Late Wisconsinan "maximum". However, this hypothesis does not explain differences in wavelength and amplitude of transverse ridges across the preglacial divide, and does not account for the complex ridge morphology.

#### *Hypothesis 2: Erosional antidune formation*

Alternatively, transverse ridges may be antidunes associated with stationary waves in subglacial meltwater flows that were responsible for eroding flutes, scouring bedrock and producing boulder lags. Morphologically similar features have been observed in many environments associated with standing waves and turbulent flow (e.g., Yalin, 1972; Allen, 1982).

I have previously noted that glaciotectonic processes may have operated beneath the Laurentide Ice Sheet producing transverse thrust ridges and troughs. In addition, subglacial landforms in the study area have been explained by erosion beneath turbulent meltwater flows (Chapter 2). These conclusions may be extended to explain transverse ridges as a direct product of subglacial fluvial erosion. It should be noted that, while this

hypothesis is grounded in fluid theory, more detailed testing than that presented here is required.

Yalin (1972) described the processes by which antidunes are related to stationary waves on a water surface beneath air. Internal stationary waves may form antidunes or in-phase bedforms (Brennand, 1994). Antidunes are common beneath free surfaces with supercritical flow ( $Fr > 1$ ), although Shaw and Kellerhals (1977) observed antidunes in gravel to form in flows with Froude numbers of  $0.82 < Fr < 1.3$ .

Stationary waves are set up where there is a density interface within the flow (Fig. 3-10). In this case, the relevant densiometric Froude Number ( $Fr_d$ ) is required. This number is defined as:

$$Fr_d = V^2 / \{((\rho_d - \rho_f) / \rho_f) d g\} \quad (3.1)$$

where  $V$  is velocity ( $\text{ms}^{-1}$ ),  $\rho_d$  is the density of the hyperconcentrated layer,  $\rho_f$  is the density of the less dense layer,  $d$  is flow depth (m) and  $g$  is acceleration due to gravity ( $9.81 \text{ ms}^{-2}$ ). Stationary waves develop downstream of the perturbation where erosion is concentrated in troughs, producing a wavy bed (Shaw and Kellerhals, 1977). If the flow is competent to transport all sediment, deposition on the ridge crest need not occur (Yalin, 1972; Shaw and Kellerhals, 1977). Antidunes and the stationary water-surface waves are in-phase for steady-state conditions (Yalin, 1972).

From a basic discussion of the origin of antidunes, this theory can be applied to the possible occurrence of standing waves within subglacial meltwater flows. In this view, antidunes relate to waves formed at density interfaces within the fluid, rather than below a free surface. In hyperconcentrated flows, a dense, sediment-rich fluid lies close to the bed while lower density fluid shears over this dense layer (Fig. 3-11). The bed and the overlying ice generate resistance creating two boundary layers. Stationary waves are formed at this density interface.

Having determined that stationary waves may form along density interfaces, it is likely that they will be fixed by perturbations on the bed. Subsurface investigations of transverse ridges in southeast Alberta show some evidence that ridge morphology is

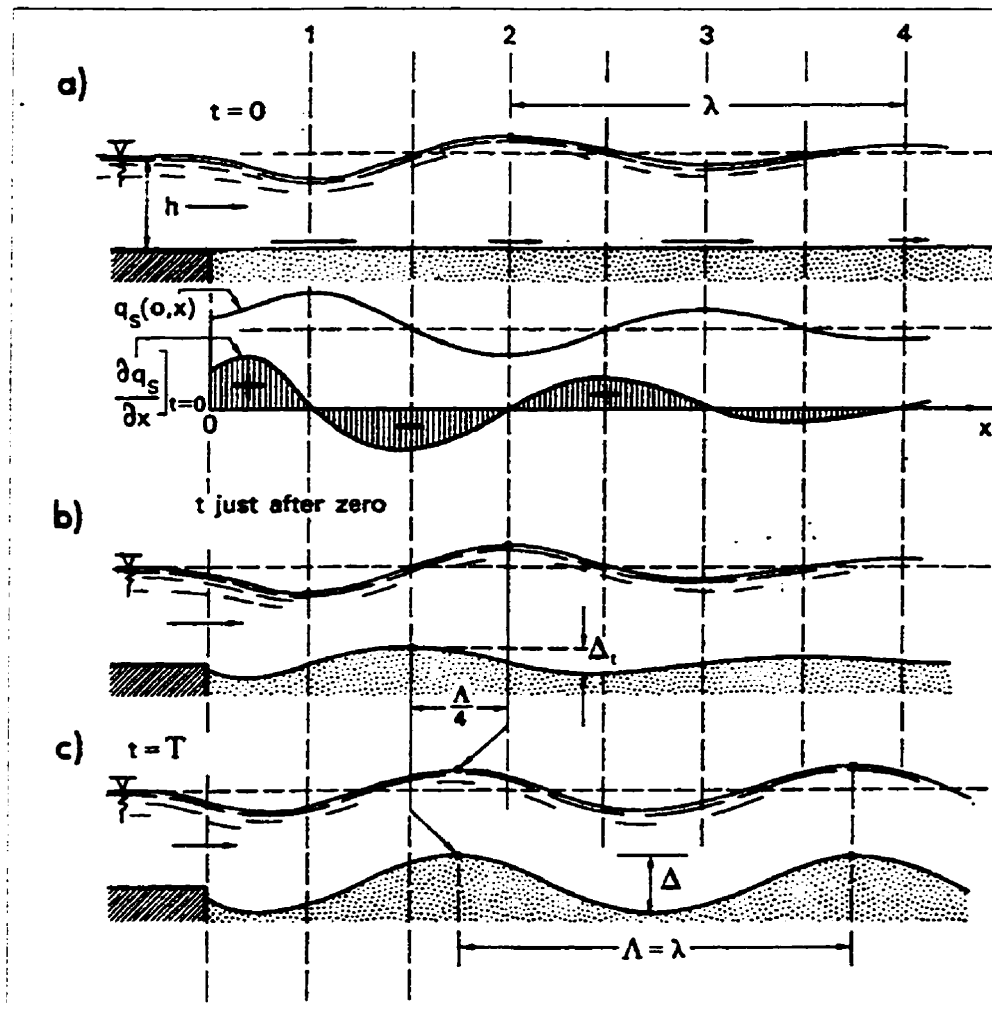


Figure 3-10. Formation of antidunes beneath stationary waves generated by a discontinuity to flow (from Yalin, 1972, Fig. 7.10). (For key to notation, see List of Symbols).

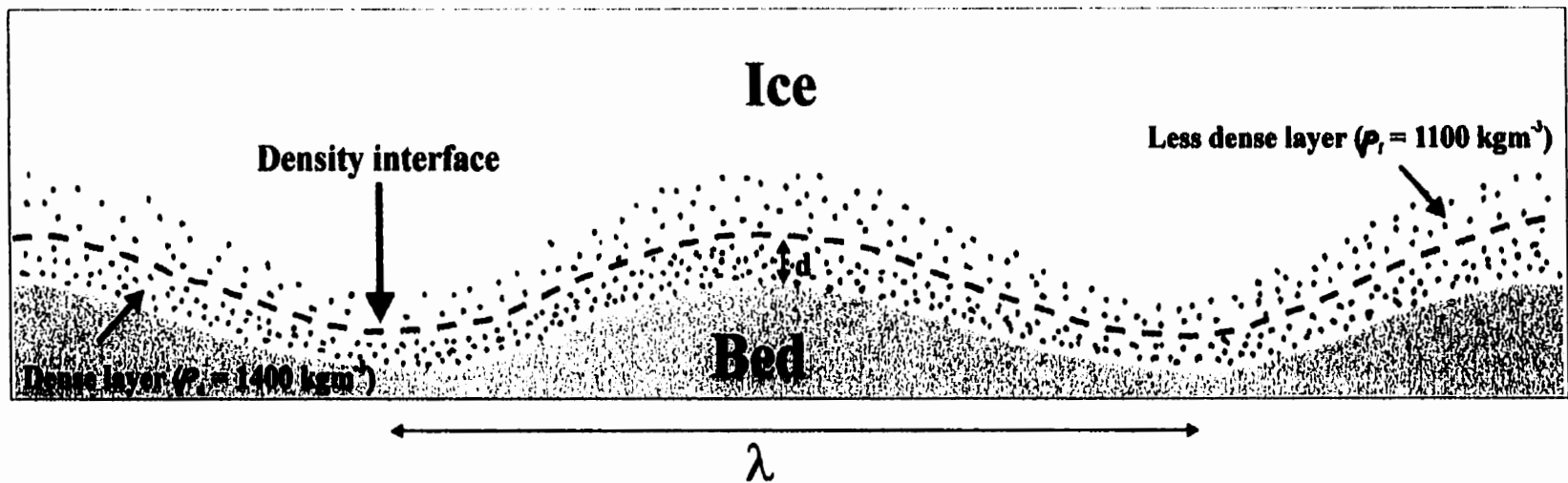


Figure 3-11. Generation of stationary waves in subglacial meltwater flows along a density interface. Perturbations on the bed may fix stationary waves along this density interface although this is not a requirement to wave formation.

related to bedrock structure, although the scale of this expression is not known. Therefore, some ridge form may have existed prior to the passage of subglacial meltwater floods. Thrust ridges on the bed surface would have set up stationary waves along the density interface. Enhanced bed erosion might be expected in troughs where flow depth was reduced and velocity increased from uniform flow conditions (Figs. 3-10, 3-11). Less erosion beneath the crests of stationary waves results from lower velocities in areas of local flow expansion.

If the wavelength of the ice-thrust ridges is close to the optimum wavelength determined from the flow velocity, then antidunes are likely to form at wavelengths controlled by the spacing of the original thrust forms. However, if the wavelength related to flow velocity is significantly different, erosion of the bed beneath standing waves will produce antidunes with a wavelength controlled more by the flow velocity (Yalin, 1972). Thus, decreases in ridge wavelength from southwest to northeast may be explained by differences in flow velocity, depth or density across the preglacial divide.

Complex ridge patterns that cannot be explained by glaciotectonic processes are also described. Three-dimensional wave forms, two-dimensional nested forms, and rhomboidal interfering forms (Fig. 3-9) can be explained by local variations in flow characteristics. Type 2 wave forms that curve upstream can be explained by streaming, with longitudinal zones of high velocity. Where flow depth is greater than for the surrounding flow, stationary waves will be deflected upstream. Where flow depths are decreased, ridges that are deflected downstream may also be produced. Stationary waves may also be oblique to the main flow direction where wall effects are important (e.g., in the Lost River channel). Erosion beneath these stationary waves is expected to produce ridges showing a rhomboidal pattern mirroring internal, standing waves (Fig. 3-12; e.g., Allen, 1982). In channels, fluting related to longitudinal vortices is generally more common.

Flutings are superimposed on the transverse bedforms. Transverse and longitudinal ridges commonly occur together in fluid flows (Fig. 3-13). These forms were contemporaneous, being produced by different vortices operating in the flow. Transverse bedforms were the product of erosion beneath stationary waves. Flutings



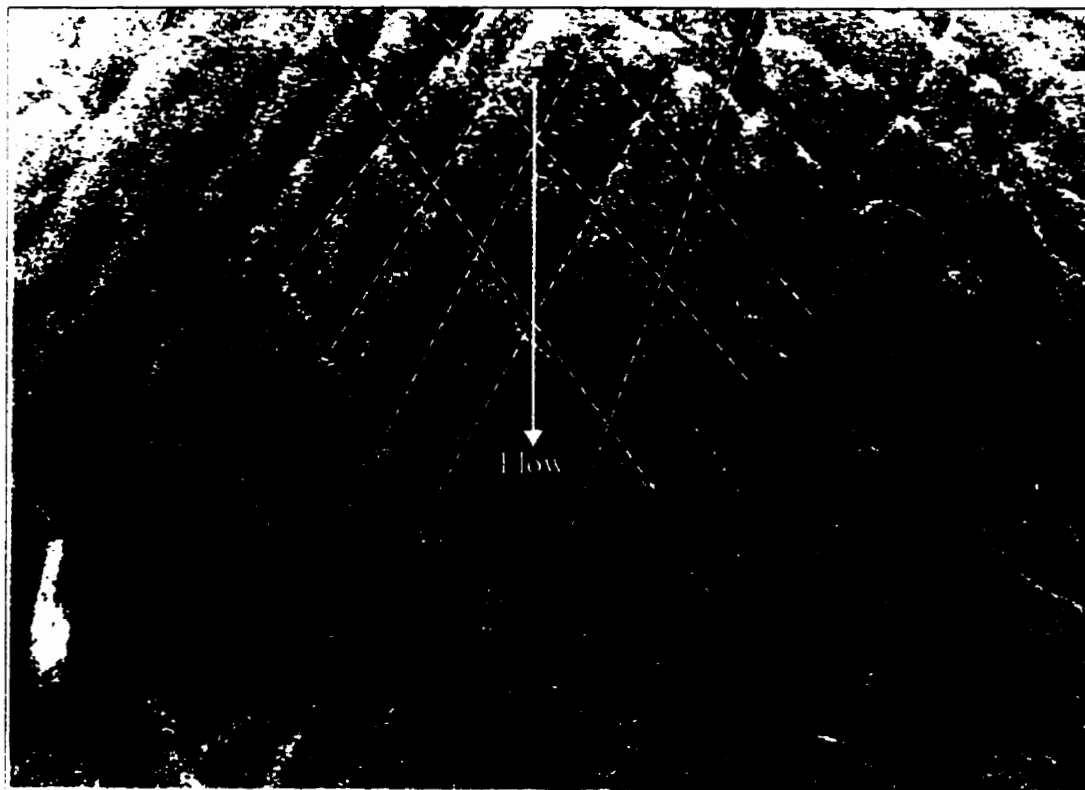


Figure 3-12. Rhomboidal ripples produced in fine sand (from Allen, 1982, Fig. 10.13) are similar to Type 3, rhomboidal interfering forms identified across the preglacial divide.

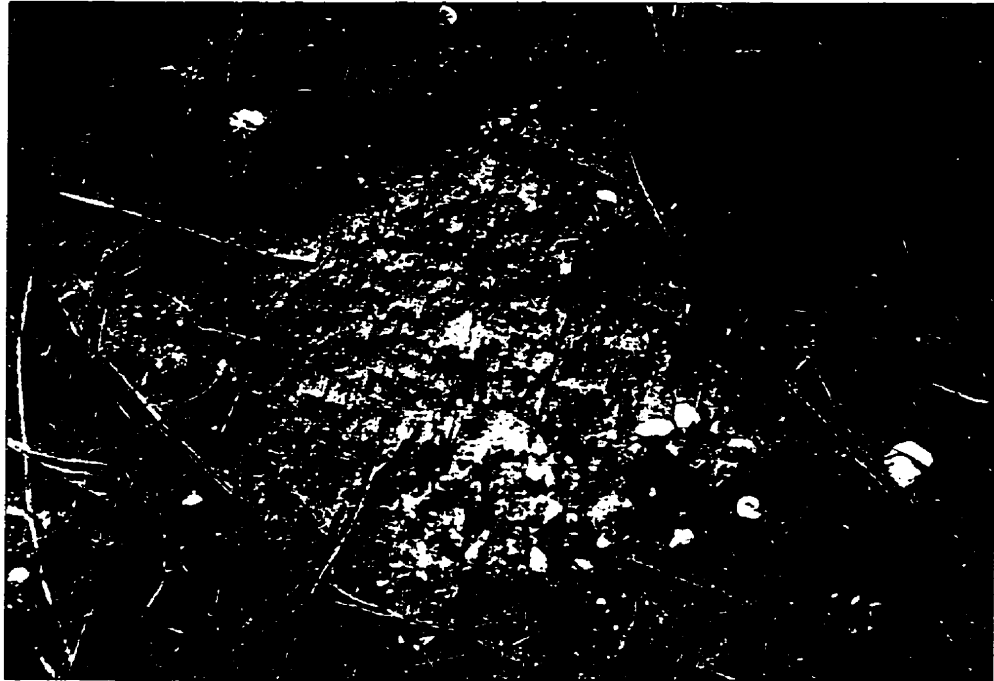


Figure 3-13. Examples of transverse ridges and flutes produced by various fluid flows: a) Ridges and flutes produced by wind in sand. Flow away from reader; b) Transverse ribs and streamlined forms on the Peyto Glacier outwash plain, Alberta, Canada (from Allen, 1982, Fig. 10.4). Flow from right to left.

were formed by vortices operating parallel to flow. Horseshoe and impinging vortices caused erosion of crescentic scours, lateral furrows and s-forms (e.g., Shaw, 1994a). Thus, the occurrence of flutings on transverse bedforms is expected. Scoured bedrock and boulder lags are also explained by the passage of meltwater across the subglacial surface.

## **Conclusions**

Transverse ridges on the preglacial divide, and their association with other subglacial landforms in the region, opens an interesting debate on the origin of these features. Two hypotheses are presented which in extreme cases involve, 1) glaciotectionic processes, or, 2) fluvial processes. As well, modification of glaciotectionic ridges by subglacial meltwater flows may produce the noted features. The transverse ridges may also be interpreted antidunes formed beneath stationary waves propagating along density interfaces in subglacial meltwater flows.

Detailed investigations of subglacial landforms in southeast Alberta have concluded that the landscape is predominately erosional with landforms being products of erosion by turbulent, sediment-laden meltwater (Chapter 2). The present chapter has discussed the relationship between the transverse bedforms, mapped previously as glaciotectionic ridges (Westgate, 1968; Shetsen, 1987), and other erosional, subglacial landforms. Further subsurface investigations of the transverse ridges will allow more detailed conclusions to be made as to the origin of the landforms.

This study has shown that meltwater erosion was also an important process for the development of transverse bedforms in the study area. Subglacial meltwater erosion modified glaciotectionic ridges, producing truncated ridge forms and associated landforms. Alternatively, stationary waves may have developed within subglacial meltwater flows because of discontinuities on the bed and density interfaces within the flow. Such internal waves may form antidunes that are identical to those produced in normal fluvial environments (Yalin, 1972; Shaw and Kellerhals, 1977; Allen, 1982). Previously identified as glaciotectionic forms, the transverse ridges of the study area may

be better interpreted as antidunes. Similar conclusions might be obtained by further studies of other transverse ridge forms in Alberta where evidence for large subglacial meltwater flows is documented (e.g., Rains *et al.*, 1993).

## References

- Aber, J.S., Croot, D.G. and Fenton, M.M. 1989. *Glaciotectonic Landforms and Structures*. Kluwer Academic Publishers, Dordrecht, 201 pp.
- Allen, J.R.L. 1982. *Sedimentary structures. Developments in Sedimentology* 30A. Elsevier, Amsterdam, vol.2, 593 pp.
- Annan, A.P. 1988. Evolution of ground penetrating radar techniques for geologic structure mapping in Saskatchewan potash mines. *Abstracts of the Canadian Institute of Mining and Metallurgy Annual Meeting*, Edmonton, Alberta.
- Annan, A.P. and Davis, J.L. 1977. Impulse radar applied to ice thickness measurements and freshwater bathymetry. In *Report of activities, part B. Geological Survey of Canada, Paper 77-1B*, 117-124.
- Annan, A.P., Davis, J.L. and Gendzwill, D. 1988. Radar sounding in potash mines, Saskatchewan, Canada. *Geophysics*, **53**, 1556-1564.
- Benn, D.I. and Evans, D.J.A. 1998. *Glaciers and Glaciation*. Arnold, London, 734pp.
- Bluemle, J.P. 1970. Anomalous hills and associated depressions in central North Dakota. *Geological Society of America, Abstracts with Programs*, **2**, 325-326.
- Bluemle, J.P. and Clayton, L. 1984. Large-scale thrusting and related processes in North Dakota. *Boreas*, **13**, 279-299.
- Brennand, T.A. 1994. Macroforms, large bedforms and rhythmic sedimentary sequences in subglacial eskers: genesis and meltwater regime. *Sedimentary Geology*, **91**, 9-55.
- Clark, P.U. and Hansel, A.K. 1989. Till lodgement, clast ploughing and glacier sliding over a deformable glacier bed. *Boreas*, **18**, 201-207.
- Clayton, L. and Moran, S.R. 1974. A glacial form-process model. In Coates, D.R. (ed) *Glacial Geomorphology*. Binghamton, New York, 89-119.
- Clayton, L., Moran, S.R. and Bluemle, J.P. 1980. Explanation text to accompany the Geologic Map of North Dakota. *North Dakota Geological Survey, Report and Investigations*, **69**, 93pp.
- Davis, J.L. and Annan, A.P. 1989. Applications of the pulseEKKO III ground penetrating system to mining, groundwater and geotechnical projects - selected case histories. *Proceedings of the Workshop on Ground Probing Radar*, Ottawa, Ontario.

- Davis, J.L., Annan, A.P. and Vaughn, C. 1987. Placer exploration using radar and seismic methods. *CIM Bulletin*, **80**, 67-72.
- Dufour, S., Judge, A.S. and La Fleche, P.T. 1988. Design and monitoring of earth embankments over permafrost. *Proceedings of the Second International Conference on Case Histories in Geotechnical Engineering*, St Louis, MO, Paper 5.25.
- Fenton, M.M. 1983. Deformation terrain mid-continent region: properties sub-division, recognition. *Geological Society of America, Abstract with Programs*, **15**, 250.
- Grant, N.M. 1997. *Genesis of the North Battleford Fluting Field, West-Central Saskatchewan*. MSc thesis, University of Alberta, Edmonton.
- Hughes Clarke, J.E., Shor, A.N., Piper, D.J.W. and Mayer, L.A. 1990. Large-scale current-induced erosion and deposition in the path of the 1929 Grand Banks turbidity current. *Sedimentology*, **37**, 613-629.
- Jackson, L.E.Jr., Little, E.C., Leboe, E.R. and Holme, P.J. 1996. A re-evaluation of the paleogeography of the maximum continental and montane advances, southwestern Alberta. *Geological Survey of Canada Current Research Part A*, **1996**, 165-173.
- Jol, H.M. and Smith, D.G. 1991. Ground penetrating radar of northern lacustrine deltas. *Canadian Journal of Earth Sciences*, **28**, 1939-1947.
- Jol, H.M., Young, R.R., Fisher, T.G., Smith, D.G. and Meyers, R.A. 1996. Ground penetrating radar of eskers, kame terraces and moraines: Alberta and Saskatchewan, Canada. *6<sup>th</sup> Annual Conference on Ground Penetrating Radar*, Sendai, Japan, 439-443.
- Kor, P.S.G., Shaw, J. and Sharpe, D.R. 1991. Erosion of bedrock by subglacial meltwater, Georgian Bay, Ontario: a regional view. *Canadian Journal of Earth Sciences*, **28**, 623-642.
- Kupsch, W.O. 1962. Ice-thrust ridges in western Canada. *Journal of Geology*, **70**, 582-594.
- La Fleche, P.T., Judge, A.S. and Pilon, J.A. 1987a. Ground probing radar in the investigation of the competency of frozen tailings pond dams. *Geological Survey of Canada, Current Research, part A*, **87-1A**, 191-197.
- La Fleche, P.T., Judge, A.S. and Taylor, A.E. 1987b. Applications of geophysical methods to resource development in northern Canada. *CIM Bulletin*, **80**, 78-87.

- La Fleche, P.T., Judge, A.S., Moorman, B.J., Cassidy, B. and Bedard, R. 1988. Ground probing radar investigations of gravel road bed failures, Rae Access road, NWT. *Geological Survey of Canada Current research, part D*, **88-1D**, 129-135.
- Liverman, D.G.E., Catto, N.R. and Rutter, N.W. 1989. Laurentide glaciation in west-central Alberta: a single (Late Wisconsinan) event. *Quaternary International*, **32**, 53-77.
- Moran, S.R., Clayton, L., Hooke, R.LeB., Fenton, M.M. and Andriashek, L.D. 1980. Glacier-bed landforms of the Prairie region of North America. *Journal of Glaciology*, **25**, 457-476.
- Munro, M.J. and Shaw, J. 1997. Erosional origin of hummocky terrain in south-central Alberta, Canada. *Geology*, **25**, 1027-1030.
- Oldale, R.N. and O'Hara, C.J. 1984. Glaciotectonic origin of the Massachusetts coastal end moraines and a fluctuating late Wisconsinan ice margin. *Geological Society of America Bulletin*, **95**, 61-74.
- Pilon, J.A., Annan, A.P., Davis, J.L. and Gray, J.T. 1979. Comparison of thermal and radar active layer measurement techniques in the Leaf Bay area, Nouveau-Quebec. *Geographie physique et Quaternaire*, **33**, 317-326.
- Pilon, J.A., La Fleche, P.T. and Judge, A.S. 1987. Applications of ground probing radar in permafrost regions to granular deposits, pipeline right of way and frozen cored dams. *57<sup>th</sup> Annual Society of Exploration Geophysicists Meeting*, New Orleans, LA, Expanded Abstracts, 73-75.
- Rains, R.B., Shaw, J., Skoye, R., Sjogren, D. and Kvill, D. 1993. Late Wisconsinan subglacial megaflood paths in Alberta. *Geology*, **21**, 323-326.
- Reineck, H.E. and Singh, I.B. 1980. *Depositional Sedimentary Environments*. Springer-Verlag, Berlin, 551 pp.
- Reinsen, G.E. 1992. Transgressive Barrier Island and Estuarine Systems. In Walker, R.G. and James, N.P. (eds) *Facies models: response to sea level change*. Geological Association of Canada, St. Johns, 179-194.
- Rotnicki, K. 1976. The theoretical basis for and a model of the origin of glaciotectonic deformations. *Quaestiones Geographicae*, **3**, 103-139.
- Rutten, M.G. 1960. Ice-pushed ridges, permafrost and drainage. *American Journal of Science*, **258**, 293-297.

- Sensors and Software 1996. PulseEKKO IV RUN, User's Guide, Version 4.2. Technical Manual 20.
- Shaw, J. 1994a. Hairpin erosional marks, horseshoe vortices, and subglacial erosion. *Sedimentary Geology*, **91**, 269-283.
- Shaw, J. and Kellerhals, R. 1977. Paleohydraulic interpretation of antidune bedforms with applications to antidunes in gravel. *Journal of Sedimentary Petrology*, **47**, 257-266.
- Shaw, J., Rains, R.B., Eyton, R. and Weissling, L. 1996. Laurentide subglacial outburst floods: landform evidence from digital elevation models. *Canadian Journal of Earth Sciences*, **33**, 1154-1168.
- Sheriff, R.E. 1984. *Encyclopedic dictionary of exploration geophysics*. 2<sup>nd</sup> ed. Society of Exploration Geophysics, Tulsa, OK.
- Shetsen, I. 1987. Quaternary geology, southern Alberta. *Alberta Research Council Map*, scale 1:500 000.
- Smith, D.G. and Jol, H.M. 1992. Ground-penetrating radar investigation of a Lake Bonneville delta, Provo level, Brigham City, Utah. *Geology*, **20**, 1083-1086.
- Stalker, A.MacS. 1973b. The large interdrift bedrock blocks of the Canadian Prairies. *Geological Survey of Canada, Paper 75-1A*, 421-422.
- Tsui, Po.C., Cruden, D.M. and Thomson, S. 1989. Ice-thrust terrains and glaciotectionic settings in central Alberta. *Canadian Journal of Earth Sciences*, **26**, 1308-1318.
- Ulriksen, C.P.F. 1982. *Application of impulse radar to civil engineering*. Ph.D. thesis, Lund University of Technology, Lund, Sweden.
- Vaughn, C.J. 1986. Ground-penetrating radar surveys used in archaeological investigations. *Geophysics*, **51**, 595-604.
- Warner, B.G., Nobes, D.C. and Theimer, B.D. 1990. An application of ground penetrating radar to peat stratigraphy of Ellice Swamp, southwestern Ontario. *Canadian Journal of Earth Sciences*, **27**, 932-938.
- Wateran, D.F.M. van der. 1985. A model of glacial tectonics, applied to ice-pushed ridges in the central Netherlands. *Geological Society of Denmark, Bulletin*, **34**, 55-74.
- Westgate, J.A. 1968. Surficial geology of the Foremost-Cypress Hills area, Alberta. *Research Council of Alberta, Bulletin* 22.



- Worsfold, R.D., Parashar, S.K. and Perrott, T. 1986. Depth profiling of peat deposits with impulse radar. *Canadian Geotechnical Journal*, **23**, 142-154.
- Yalin, M.S. 1972. *Mechanics of Sediment Transport*. Pergamon Press, Oxford, 290 pp.
- Young, R.R., Burns, J.A., Smith, D.G., Arnold, L.D. and Rains, R.B. 1994. A single Late Wisconsinan, Laurentide glaciation, Edmonton area and southwestern Alberta. *Geology*, **22**, 683-686.

## CHAPTER 4: ONE-DIMENSIONAL HYDRAULIC MODELLING OF SUBGLACIAL TUNNEL CHANNELS

### Introduction

Whereas some workers have attributed similar landforms to formation by bed deformation processes (e.g., Boulton, 1979, 1987; Boulton and Hindmarsh, 1979; Hart, 1995a, 1997), subglacial landform assemblages in Alberta and elsewhere in Canada have been alternatively explained by subglacial meltwater erosion and deposition (e.g., Shaw, 1983, 1996). Much of the subglacial geomorphology of southeast Alberta is best explained by regional-scale erosion by turbulent, subglacial meltwater flows (see Chapters 2 and 3). In this area, a broad, sheet flow subsequently became concentrated into channels. The flows envisaged in this paper for southeast Alberta fit well with those proposed for the Livingstone Lake flood event (e.g., Rains *et al.*, 1993). Similar conclusions obtained from observations on subglacial landform assemblages elsewhere in Alberta support the proposal that landscapes covering vast areas of Canada record a single flow event beneath the western part of the Laurentide Ice Sheet (e.g., Shaw and Kvill, 1984; Shaw *et al.*, 1989; Rains *et al.*, 1993; Sjogren and Rains, 1995; Munro and Shaw, 1997). It should be noted that this event involved different flow geometries and directions at various stages in its evolution.

The next logical step in the development of the meltwater hypothesis is to model the flow characteristics that may have created the observed subglacial landscapes. Field evidence and simple physical reasoning provide estimates of flow magnitude, velocity and duration, indicating enormous volumes of water ( $\sim 10^4$  km<sup>3</sup>) and highly turbulent flows (e.g., Shaw and Kvill, 1984; Shaw, 1994a, 1996). As well, these studies conclude that the subglacial flows were unsteady and non-uniform. However, three-dimensional modelling of unsteady, turbulent sheet flow is complex and has not been successfully undertaken.

Subglacial drainage has been traditionally modelled for steady-state conditions (e.g., Röthlisberger, 1972; Shreve, 1972; Nye, 1976; Clarke, 1996). Theory shows that,

over a hard bed, subglacial meltwater may be transported in conduits (e.g., Röthlisberger, 1972; Shreve, 1972; Nye, 1976; Clarke, 1996), sheets (Nye, 1976), or in a linked cavity system (e.g., Lliboutry, 1969; Walder and Hallet, 1979). By contrast, Walder and Fowler (1994) concluded that, over a deforming bed, water is transported in broad, shallow canals at the ice-till interface. Water flow beneath glaciers is controlled mainly by the ice surface slope except where these slopes are very low (Shreve, 1972). Observations and theory locate conduits along valley floors and at low points across divides.

The cross-sectional form of subglacial conduits is controlled by the rate of melting of the surrounding ice, due to viscous dissipation of turbulent kinetic energy and conduction of heat from relatively warm water (Clarke, 1996), and the rate of ice closure, due to the pressure of the overlying ice (Röthlisberger, 1972). The water pressure in subglacial conduits under steady-state is inversely related to discharge (e.g., Röthlisberger, 1972; Shreve, 1972; Clarke, 1996), such that large channels grow at the expense of smaller ones to produce an arborescent network dominated by a few trunk conduits (Shreve, 1972).

In comparison, flow through a linked cavity system is said to be related to an uneven bed, where bumps generate lee-side cavities that become storage locations for subglacial meltwater (e.g., Lliboutry, 1969; Walder and Hallet, 1979). Since cavities are linked by narrow R-channels and N-channels where flow accelerates, meltwater has a higher residence time in cavities. Complex channel cavity networks involve strong, cross-glacier flow components. Unlike subglacial conduits, water pressure is proportional to discharge where a large number of small channels form a stable configuration across a large area of the glacier bed (Lliboutry, 1969). The sliding velocity of the overlying ice depends critically on the water pressure in linked cavities (Paterson, 1994).

Kamb (1987) suggested a link between conduit and linked cavity drainage at the onset of surging. From observations at Variegated Glacier, Alaska, he concluded that the transition from normal conduit drainage to a linked cavity system increases basal water

pressure and causes rapid sliding (Kamb, 1987). Thus, surges may be initiated. The type of subglacial drainage appears to be fundamental to the behaviour of alpine glaciers.

A soft substrate adds further complications to the meltwater system. Walder and Fowler (1994) modelled meltwater flow within a deforming substrate and concluded that, where transport through the sediment is insufficient to remove all available meltwater, water may flow along the ice-till interface. In this situation, ice creep from the roof and till creep from the sides and bottom are balanced by water and sediment transport. They concluded that discrete, broad, shallow canals form the stable drainage configuration at the ice-deforming bed interface. In this system, water pressure is directly proportional to discharge in the canals (Walder and Fowler, 1994). Canal drainage is only stable where ice surface slopes are low. Walder and Fowler (1994) also concluded that eskers only develop on hard beds, where flow is carried in a conduit system. Field observations of eskers on soft beds contradict this conclusion (e.g., Munro and Shaw, 1997).

These models of subglacial drainage systems are not suitable analogues for the unsteady, highly turbulent flows inferred from field evidence beneath the Laurentide Ice Sheet in southeast Alberta, where sheet flow evolved to conduit flow. The Laurentide meltwater flows were catastrophic, i.e., high magnitude, short duration events. Modelling of the subglacial hydraulic conditions of catastrophic outburst events is likely to be very difficult and has not yet been undertaken in detail. However, the feasibility of subglacial lakes and the theoretical responses of ice sheets to outburst floods has been analysed by Shoemaker (1991, 1992a, b, 1994) and Szilder *et al.*, (submitted).

Shoemaker (1991) postulated a large subglacial lake in the Hudson Bay basin during the early stages of the Late Wisconsinan glaciation. There might have been other subglacial lakes beneath the Laurentide Ice Sheet where non-glacial and proglacial lakes preceded ice advance. Many Laurentide Ice Sheet lobes are inferred to have been of low relief (Mathews, 1974; Beget, 1986), and Shoemaker (1992a, b) attributed them to episodic subglacial floods from sub-ice sheet reservoirs. Others attribute low-relief lobes to steady-state bed deformation (Boulton, 1987; Boulton and Clark, 1990b; Boyce and Eyles, 1991; Walder, 1994).

Subglacial outburst floods are, by definition, highly transient flows requiring an antecedent reservoir. Although Walder (1982) has shown that water sheet flows are inherently unstable, the turbulent nature of subglacial sheet flows permits a quasi-stable state for a longer period than sheet flows occurring in laminar flow (Shoemaker, 1992a, 1994). More importantly, most geomorphic work by running water is accomplished under transient peak flows. The effects of outburst floods on ice sheet dynamics and morphology have not yet been considered in ice sheet models, although, if they occurred, they would have had dramatic consequences for ice sheet form and process.

A highly simplified model of subglacial meltwater flow is presented here. Existing hydraulic network models of pressurised flow are adapted to quantify the flow characteristics through tunnel channels in the study area (e.g., Jeppson, 1976; Watters, 1984). Tunnel channels are treated as pipes (i.e., pressurised conduits) for which the flow characteristics through the conduit network are determined. This modelling depends on three assumptions: 1) The subglacial landform assemblage in southeast Alberta is mainly the product of meltwater erosion beneath the Laurentide Ice Sheet; 2) The tunnel channels record erosion by subglacial, catastrophic, channelised meltwater floods in this area; and, 3) The tunnel channels carried peak flows without overbank flooding.

This application of engineering principles provides flow estimates that are based on hydraulics and are independent of prior concepts of ice sheet dynamics. Hence, comparison of model results with inferences from geomorphic evidence is a test of the meltwater hypothesis.

### **Fluid flow in a pressurised system**

A one-dimensional, steady flow analysis of the tunnel channel network crossing the preglacial divide is used to estimate former flow characteristics. The main aim of this model is to investigate the conditions under which flow would be driven through channels with convex-up long profiles. Overlying ice exerts pressure on the subglacial meltwater and, hence, providing there is sufficient head, water may flow uphill. Since the difficulties of modelling fully turbulent subglacial flow make detailed three-dimensional

modelling impractical, a highly simplified, one-dimensional, conduit analysis is a more realistic starting point for a quantitative evaluation of subglacial meltwater flows.

Subglacial meltwater flow is governed by the fundamental principles of conservation of mass, momentum and energy (e.g., Röthlisberger, 1972; Clarke, 1996). Solutions are usually obtained using a combination of conservation of mass and either momentum or energy conservation. Conservation of energy is used here as the unquantifiable forces in the system make the application of momentum conservation intractable.

The continuity equation describes the conservation of mass. The mass flux (flow of mass per unit time,  $\text{kg s}^{-1}$ ) is given by:

$$G = \rho A V = \rho Q \quad (4.1)$$

where  $G$  is the mass flux,  $\rho$  is fluid density ( $\text{kg m}^{-3}$ ),  $A$  is cross-sectional area ( $\text{m}^2$ ), and  $V$  is the average velocity of the flow ( $\text{ms}^{-1}$ ). The volumetric flow rate ( $Q$ ,  $\text{m}^3\text{s}^{-1}$ ) is expressed as:

$$Q = A V \quad (4.2)$$

The mass fluxes at two sections in the flow are equal when the flow is steady:

$$G_1 = G_2, \quad (4.3)$$

and,

$$\rho_1 A_1 V_1 = \rho_2 A_2 V_2 \quad (4.4)$$

Where fluids are incompressible, i.e. density does not change with pressure, Equation 4.4 can be expressed as:

$$Q_1 = Q_2, \quad (4.5)$$

and,

$$A_1 V_1 = A_2 V_2 \quad (4.6)$$

Energy in the fluid is from 3 sources: 1) kinetic, which results from motion, 2) potential relating to elevation above a datum, and 3) potential relating to the pressure of overlying fluid. Thus, the total energy per unit mass of fluid ( $\text{Jkg}^{-1}$ ) is expressed as:

$$E = g z + p/\rho + V^2/2 \quad (4.7)$$

(energy/unit mass) = elevation + pressure + kinetic

In hydraulic applications, the total energy per unit mass is more commonly expressed in terms of energy per unit weight (metres), with each component of total energy known as the elevation head, pressure head and velocity head. The equation for energy conservation between two sections along a one-dimensional conduit is given by:

$$z_1 + p_1/\gamma + V_1^2/2g = z_2 + p_2/\gamma + V_2^2/2g + h_f \quad (4.8)$$

where  $z$  is the elevation of the fluid above a datum,  $p$  is the pressure of the fluid,  $V$  is the average velocity of the fluid,  $g$  is the acceleration due to gravity,  $\gamma$  is the specific weight of the fluid, and  $h_f$  is head loss ( $E_f/g$ ) between sections which arises from friction. We can further simplify Equation 4.8 by defining the total head,  $H$ , as:

$$H = z + p/\gamma + V^2/2g \quad (4.9)$$

Equation 4.9 then becomes:

$$H_1 = H_2 + h_f \quad (4.10)$$

The energy lost to other sources (e.g., heat) between two sections of flow, the head loss,  $h_f$ , is caused by frictional resistance to the flow. If head losses are greater than

the head at the downstream point, then flow through the system is retarded, as all available energy is lost to friction.

Head losses are calculated using:

$$h_f = S_f L \quad (4.11)$$

where  $L$  is the length of the conduit (m) between sections 1 and 2, and  $S_f$  is the slope of the energy grade line defined as:

$$S_f = V^2 n^2 / R^{4.3} \quad (4.12)$$

where  $n$  is the conduit resistance (Manning's roughness coefficient) and  $R$  is the hydraulic radius (equal to the flow area divided by the conduit perimeter).

Substituting  $S_f$ ,

$$h_f = V^2 n^2 L / R^{4.3} \quad (4.13)$$

and using the volumetric flow rate:

$$h_f = Q^2 n^2 L / A^2 R^{4.3} \quad (4.14)$$

### **Model configuration**

Using the above physical principles, a model for the discharge distribution within a network of one-dimensional conduits, each carrying a steady, incompressible, and fully turbulent flow, is applied. The pipe network considered here consists of six channels linked by four nodes (Figs. 4-1, 4-2). Each channel is represented in the model by a conduit segment with nodes, or junctions, connecting these segments. Topographic information from 1:50 000 maps of the study area characterises the geometry of each



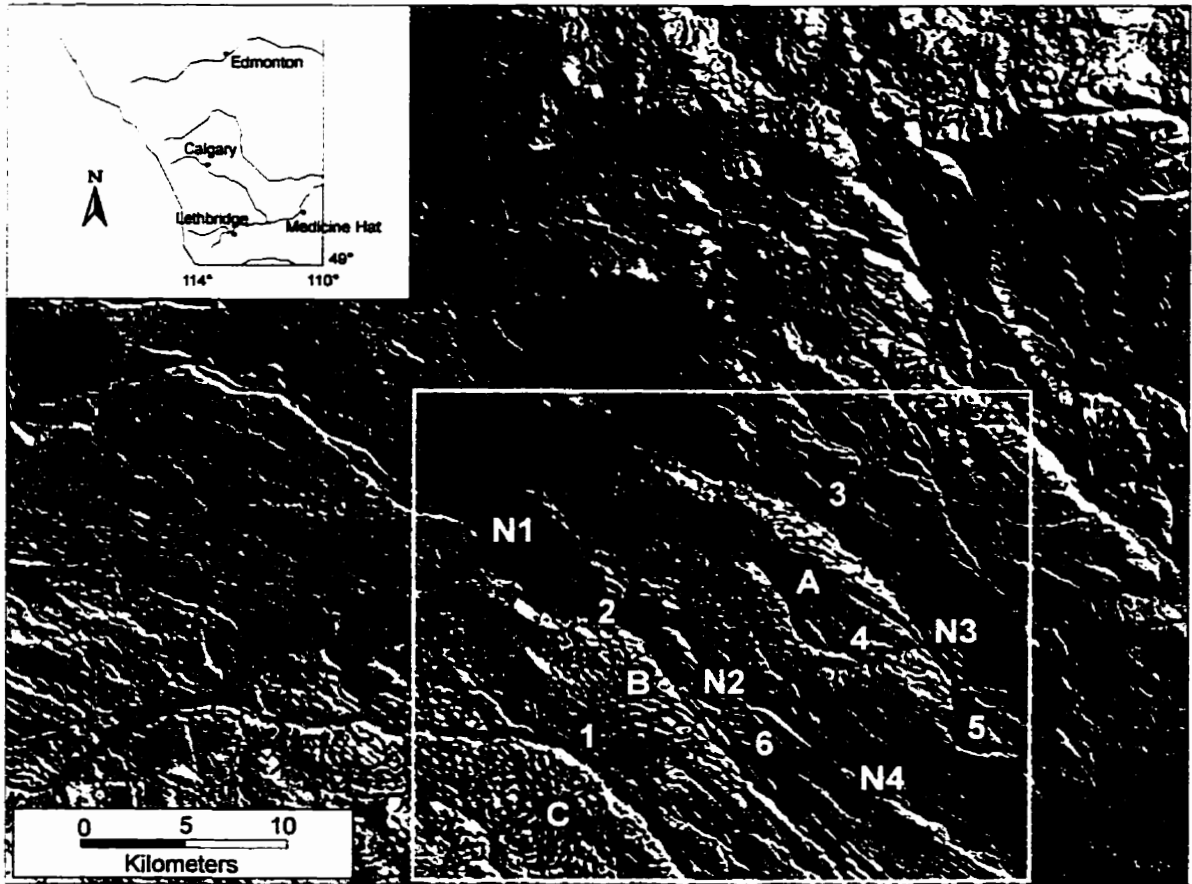


Figure 4-1. Hill-shaded DEM showing tunnel channel network in southeast Alberta chosen for one-dimensional hydraulic model, with the locations of sites in Table 4-5 also marked.

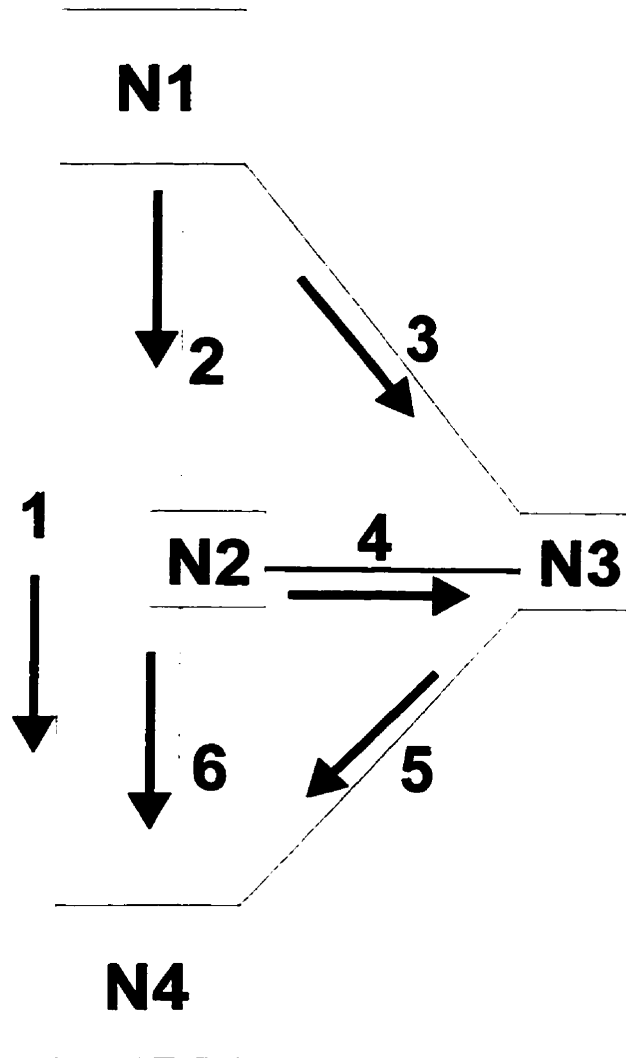


Figure 4-2. Simplified network of channels and nodes used in model configuration for one-dimensional hydraulic flow model showing flow directions. Not to scale.

conduit segment. Channel lengths, widths, depths and side slopes give the dimensions of trapezoidal pipes representing the channels during subglacial meltwater flow (Fig. 4-3). Table 4-1 gives the channel geometry as obtained from topographic maps. Subglacial conduit form is highly sensitive to pressure fluctuations and rates of ice melting (e.g., Röthlisberger, 1972; Clarke, 1996). However, these effects are not considered here.

In addition to channel geometry, the model requires the location of each node in the network together with its bed elevation. These nodes connect channels and involve either flow divergence or convergence. An estimate of channel roughness (Manning's roughness coefficient,  $n$ ) is required to determine head losses in each conduit and channel long profiles, which influence elevation ( $z$ ) in Equation 4.9, are required to obtain topographic slope, and facilitate comparison with the slope of the energy grade line. For the problem to be properly posed, one must specify the head at the upstream end of the network (the inlet node), since this provides the driving force for the system which can only carry flow if there is sufficient energy to carry meltwater through the convex-up channels. Also, one must specify the outflow discharge leaving the network system. The remaining unknowns are the proportion of the total flow carried by each individual conduit,  $Q_i$ , and the total head at each of node,  $H_i$ . There are six conduits and three remaining nodes in the tunnel channel system (Fig. 4-2), so a total of nine equations are required to solve the system.

Channel	Length (m)	Width (m)	Depth (m)	Gradient	Area (m <sup>2</sup> )	Wetted perimeter (m)	Hydraulic radius (m)
1	37033.9	2822	110.6	0.163	387158.7	4196.97	92.25
2	13226.4	8773.6	65.0	0.029	648732.8	13258.27	48.93
3	27956.0	6329.7	45.5	0.02	384713.5	10769.61	35.72
4	16879.0	2274.7	32.8	0.036	104915.5	4123.96	25.44
5	13186.8	5608.7	17.5	0.017	116167.1	7667.84	15.15
6	3428.6	7041.8	41.25	0.017	390566.9	11895.48	32.83

Table 4-1. Geometry of pipes used to configure model as obtained from 1:50 000 topographic maps.

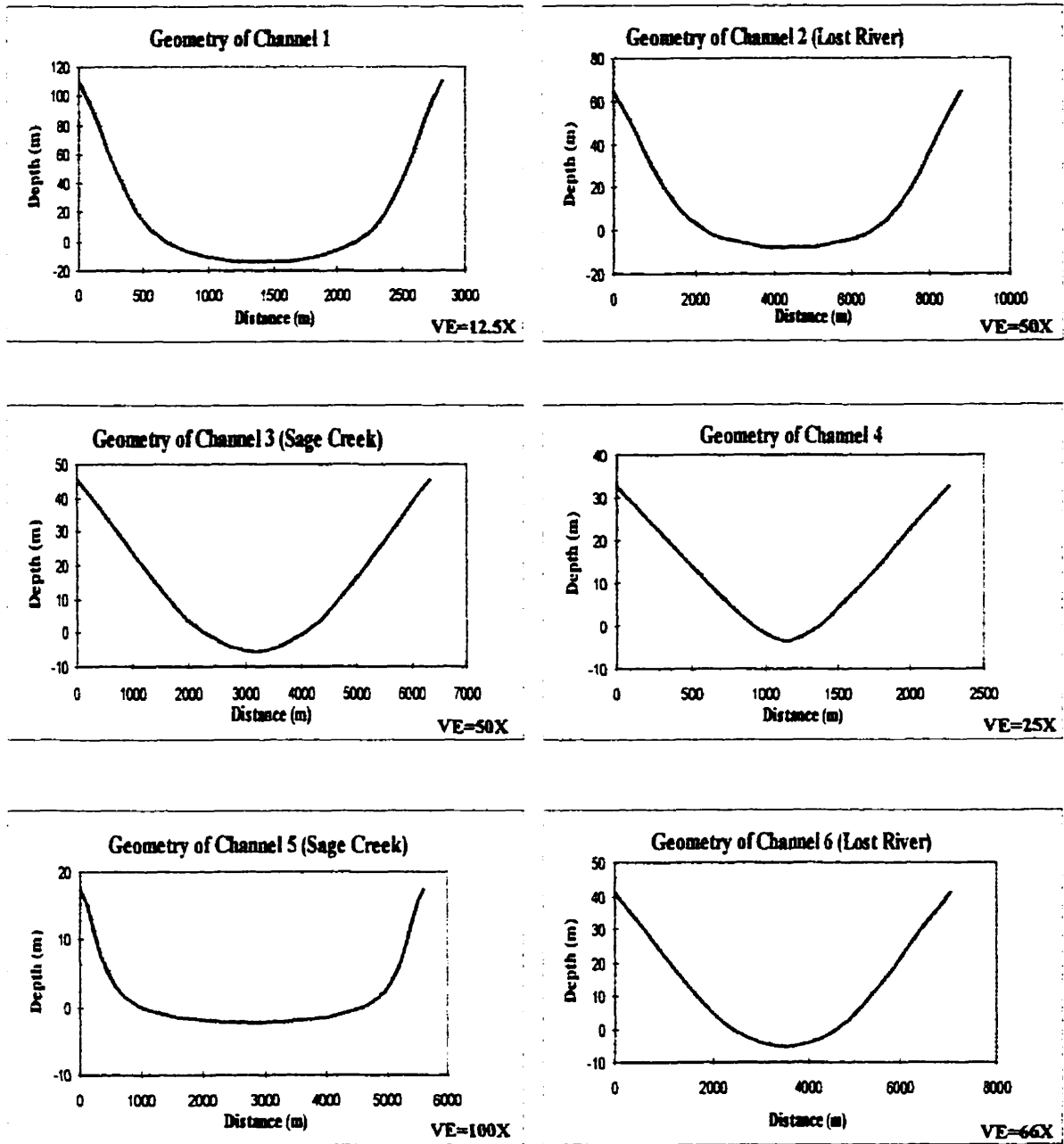


Figure 4-3. Generalised cross-sections of channels 1 to 6 used in model configuration.

Equations of mass conservation were written for each node in the system (Table 4-2) and conservation of energy equations were written for each individual conduit (Table 4-3). The continuity equation at node [1], the inlet node, is redundant in the analysis since the hydraulic head at this node is specified as a boundary condition. The resulting system of nine non-linear equations with nine unknowns was solved simultaneously using the *TKSolver+* software package, which used a Newton-Raphson iteration scheme for solving systems of non-linear equations, based on seeded values (initial guesses) of the non-linear variables (e.g., discharge). Since the Newton-Raphson method converges rapidly on a solution it is widely used to solve non-linear, simultaneous algebraic equations (Jeppson, 1976).

NODE	EQUATION
[1]	$-q_1 + Q_1 + Q_2 + Q_3 = 0$
[2]	$-Q_2 + Q_4 + Q_6 = 0$
[3]	$-Q_3 - Q_4 + Q_5 = 0$
[4]	$-Q_1 - Q_6 - Q_5 + q_2 = 0$

Table 4-2. Equations for conservation of mass used to determine hydraulic head at nodes 1 to 4.

CHANNEL	EQUATION
(1)	$H_1 = H_4 + h_{l1}$
(2)	$H_1 = H_2 + h_{l2}$
(3)	$H_1 = H_3 + h_{l3}$
(4)	$H_3 = H_4 + h_{l5}$
(5)	$H_3 = H_4 + h_{l5}$
(6)	$H_2 = H_4 + h_{l6}$

Table 4-3. Equations for conservation of energy used to determine flow parameters in each channel.

### Model application

The upstream boundary condition, hydraulic head, is controlled by ice thickness (Paterson, 1994):

$$p_i = \rho_i g h \quad (4.15)$$

where  $p_i$  is overburden pressure of ice,  $\rho_i$  is the density of ice ( $900 \text{ kgm}^{-3}$ ),  $g$  is the acceleration due to gravity ( $9.81 \text{ ms}^{-2}$ ), and  $h$  is ice thickness (m). Where subglacial water pressure equals ice overburden pressure, the ice will 'float' off its bed (e.g., Shreve, 1972). This occurs under sheet flow conditions and is the precursor stage to the channelised stage being modelled here. Thus, the upper limit for hydraulic head at node [1] occurs when subglacial water pressure equals ice overburden pressure.

The outflow discharge ( $q_2$ ) is the second specified boundary condition. The outflow discharge specified for this model was estimated from previous work on flow geometry and velocity (see Chapter 2). Thus, antecedent sheet flows are estimated to have been 80 km wide, 10-60 metres deep with mean velocities of  $5 \text{ ms}^{-1}$ . These estimates give a range of discharge between  $4 \times 10^6 \text{ m}^3 \text{ s}^{-1}$  and  $2.4 \times 10^7 \text{ m}^3 \text{ s}^{-1}$ . Thus, outflow discharge was set at  $10^7 \text{ m}^3 \text{ s}^{-1}$  to obtain order of magnitude estimates of other flow parameters. The Newton-Raphson method requires that an initial guess be specified for the non-linear variables. Model trials with discharge 'guesses' for channels 1, 3, and 6 best facilitated model convergence.

Model error may result from measurement inaccuracies in the topographic data used to configure the model. Also, uncertainties in ice thickness above the preglacial divide cause uncertainty in calculations of maximum head at the upstream node in the network. An ice thickness of 500 m was used in all calculations. This accords with conclusions that the highest parts of the nearby Cypress Hills were unglaciated during the Late Wisconsinan where ice reached a maximum elevation of 1375 m (Stalker, 1965) to 1450 m (Catto, 1983).

A number of computational experiments using the above configuration investigated the sensitivity of head loss and discharge to channel roughness. The

minimum head required to drive flow through the channels and the discharge, velocity and Reynolds Numbers of flow in each segment were estimated. The computational model results are compared to estimates of flow calculated from field evidence (e.g., flutings, boulder lags, transverse ridges). Finally, comparisons of the computational results with flow dimensions for the Livingstone Lake event are made.

## Results

Velocity and discharge are related to channel roughness as determined by the Manning equation:

$$V = (R^{2/3} S^{1/2})/n \quad (4.16)$$

where  $V$  is average velocity ( $\text{ms}^{-1}$ ),  $R$  is the hydraulic radius (m),  $S$  is channel gradient and  $n$  is the Manning roughness coefficient. The Chezy equation also expresses flow velocity as a function of channel roughness:

$$V = C (RS)^{1/2} \quad (4.17)$$

where  $C$  is the Chezy roughness coefficient,  $V$  is average velocity ( $\text{ms}^{-1}$ ),  $R$  is hydraulic radius (m) and  $S$  is channel slope. In this paper, roughness is expressed using the Manning coefficient.

The sensitivity of channel discharge, velocity and Reynolds Number to the choice of roughness value was investigated for a total discharge of  $10^7 \text{ m}^3\text{s}^{-1}$ , and an upstream hydraulic head of 1359 m (from Equation 4.15), i.e., water pressure is equated to ice overburden pressure. Flows with Manning roughness coefficients of 0.03, 0.04, and 0.05 were modelled. These values encompass the full range of reasonable values for the conduit system. Results show that discharge, velocity and Reynolds Number are insensitive to channel roughness (Fig. 4-4). This insensitivity is typical for large channels with low relative roughness, where hydraulic radius is much greater than roughness

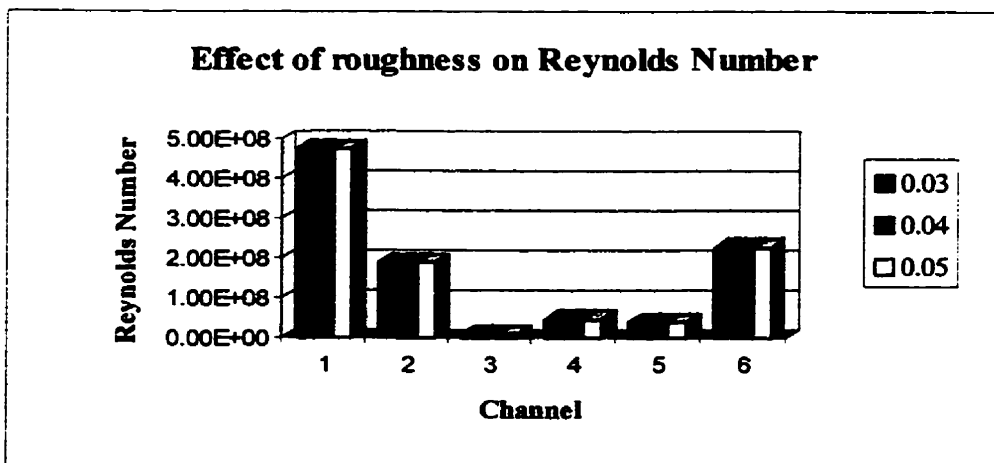
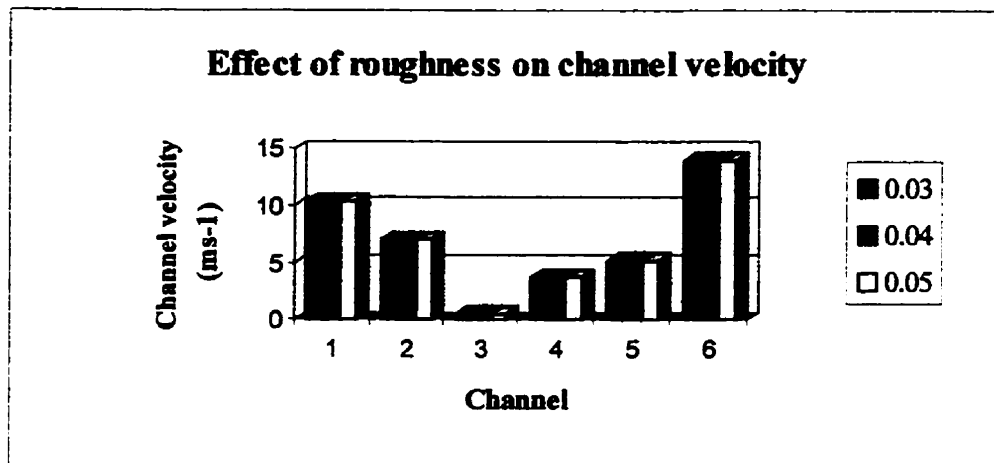
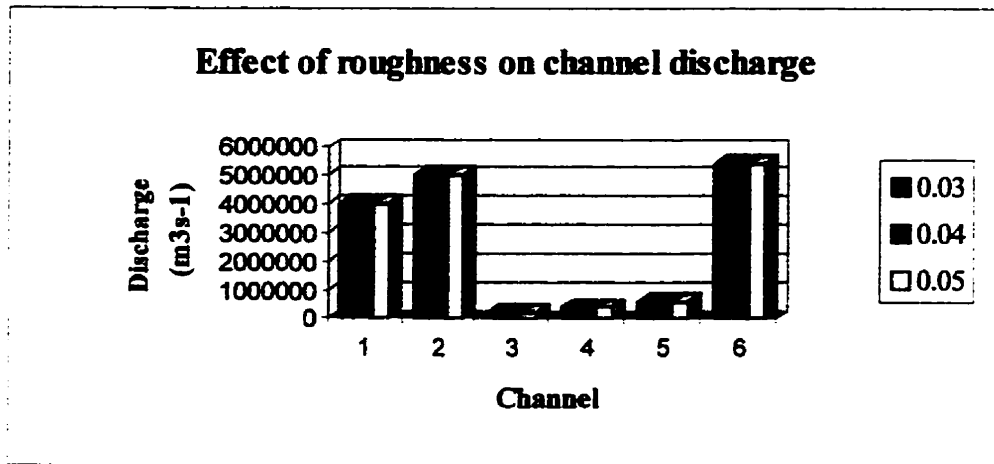


Figure 4-4. Effect of channel roughness on discharge, velocity and Reynolds Number.



height (Knighton, 1984). Where relative roughness in a channel is low, the retarding effect of roughness on velocity, and, hence, discharge and Reynolds Number is also relatively low.

By contrast, hydraulic head at each node in the system and head losses throughout the channels are sensitive to changes in channel roughness (Fig. 4-5). As roughness increases, head losses increase and the hydraulic head at nodes 2 to 4 decreases. Note, that the hydraulic head at node [1] is a fixed boundary condition. An increase in channel roughness results in an increase in the amount of energy lost to friction. Hence, the hydraulic head at each node is reduced. Thus, an increase in channel roughness reduces the energy available to drive flow through the channel system.

Given the effects of roughness on flow parameters, the conditions for full pipe flow in the channel network were investigated. During a subglacial outburst flood, hydraulic head is initially high in areas of sheet flow where ice is decoupled from the bed. Continued drainage transfers part of the overburden pressure to the bed and pressure may fall rapidly in large channels (e.g., Röthlisberger, 1972; Nye, 1976). Thus, as the ice becomes pinned at various locations, and meltwater drainage continues, the hydraulic head falls. Flow through the convex-up tunnel channels would have ceased when hydraulic head reached a critical value. This is likely where hydraulic head is lower than the bed elevation at the highest point in the channels.

Models of Lost River (channels 2 and 6) and Sage Creek (channels 3 and 5) illustrate the necessary conditions for flow. Outflow discharge was fixed at  $10^7 \text{ m}^3\text{s}^{-1}$  and channel roughness set at 0.03 during these experiments. Hydraulic head in each channel was calculated and the slope of the energy grade line plotted against bed topography (Figs. 4-6, 4-7). Flow begins when the energy grade line is at the highest elevation along the channel and continues as head increases above this critical value.

The highest point along the Lost River channel is 900 m asl at about 10.2 km from its origin (Fig. 4-6). Modelling with upstream hydraulic heads of 900 - 930 m indicate that flow is initiated when the upstream hydraulic head is equal to 910 m. Similar model runs, with values for upstream heads of 910 m to 960 m, were conducted for the Sage Creek channel which has a maximum elevation of 945 m asl occurring at

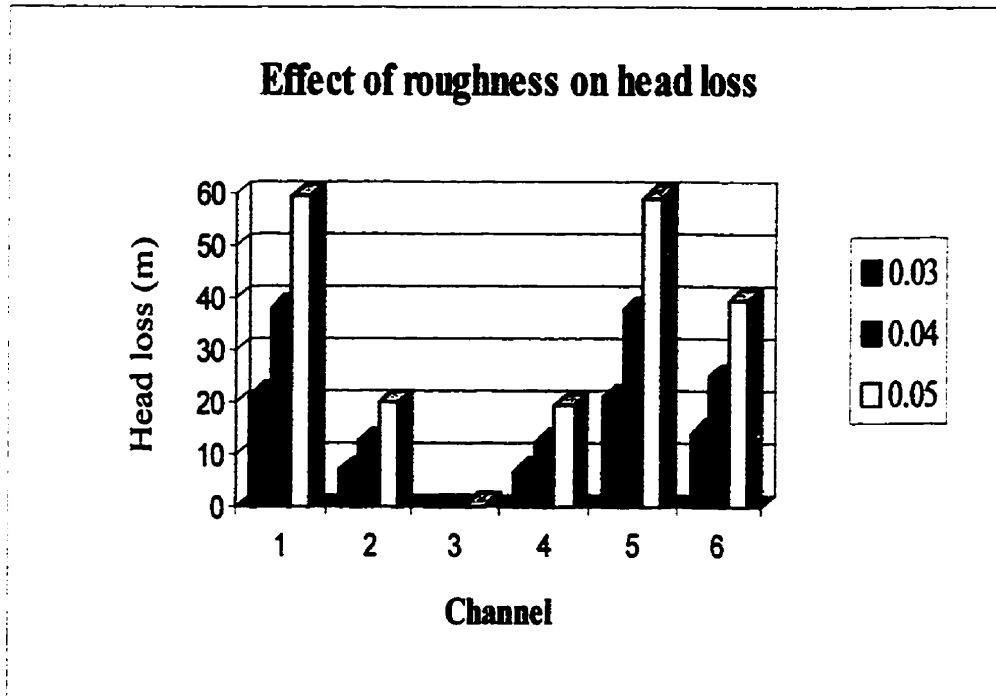
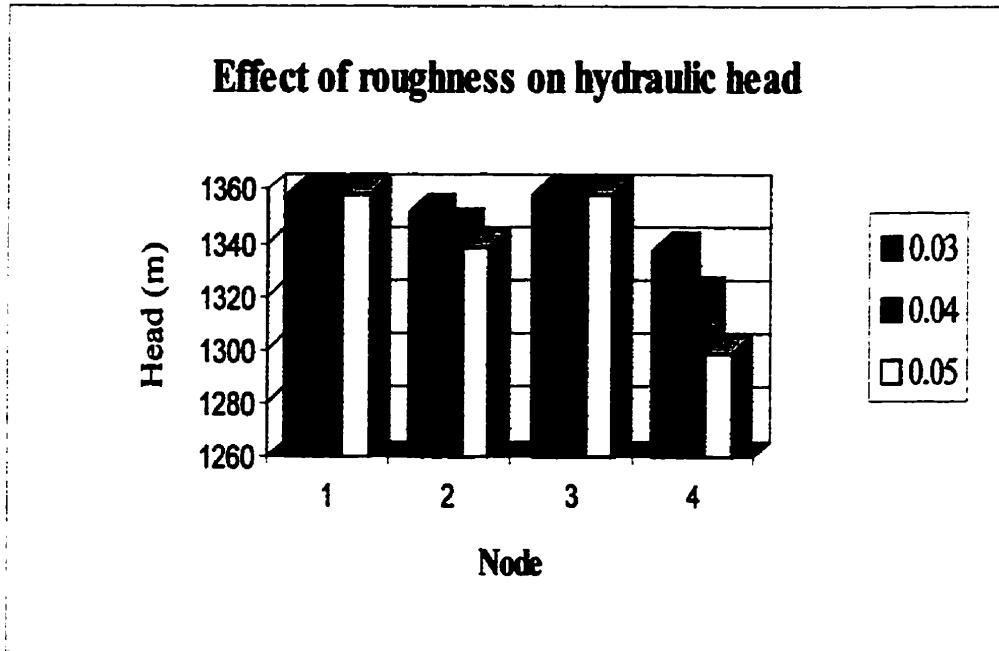


Figure 4-5. Effect of channel roughness on hydraulic head and head losses.

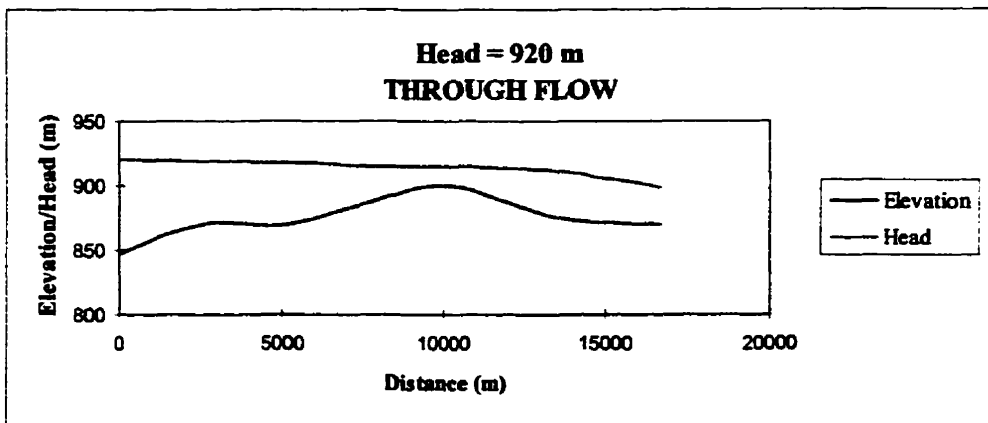
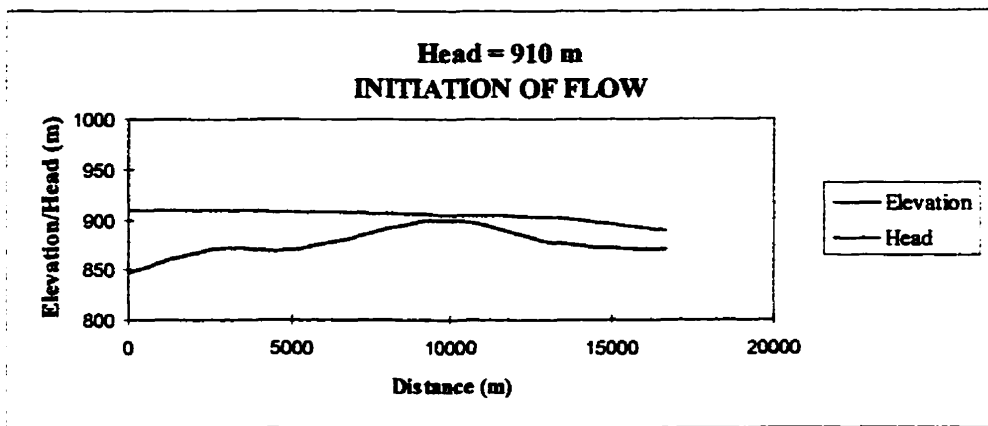
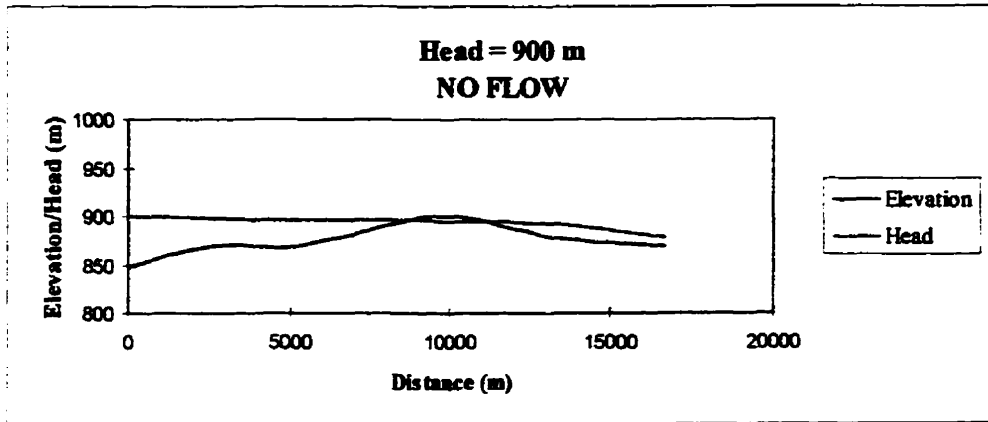


Figure 4-6. Hydraulic head required to drive flow across topographic divide in Lost River channel. VE=40X

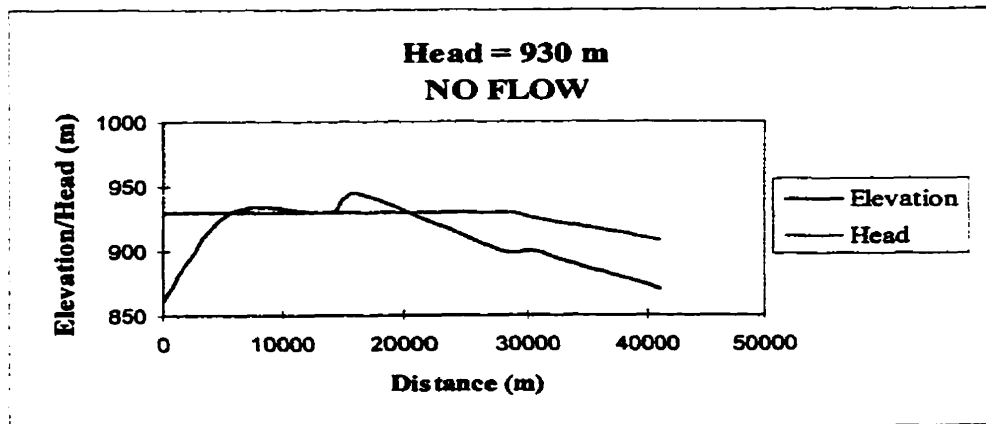
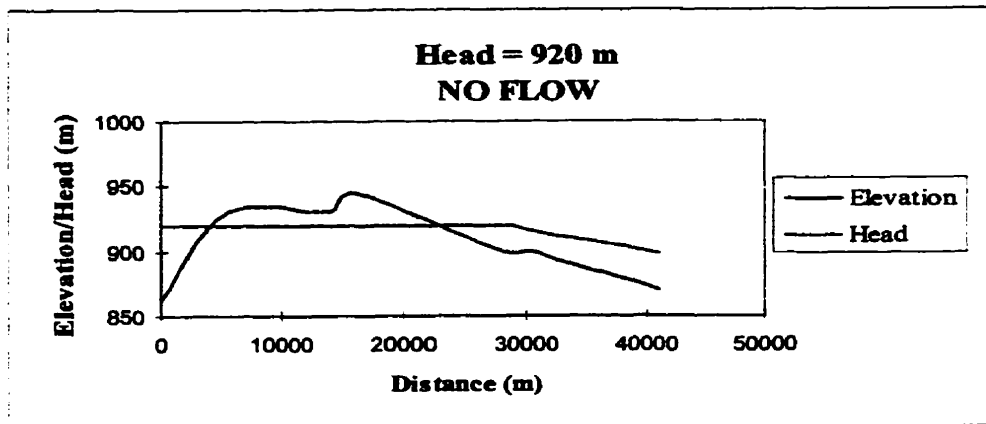
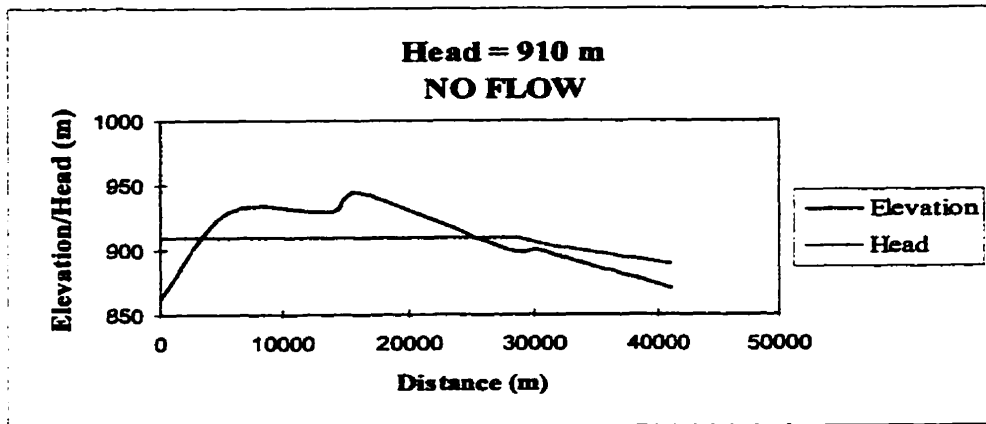


Figure 4-7. Hydraulic head required to drive flow across topographic divide in Sage Creek channel. VE=100X.

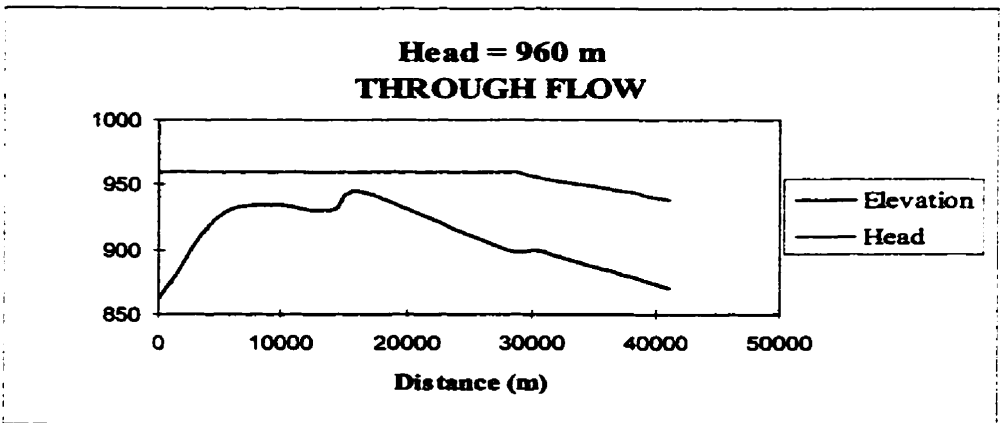
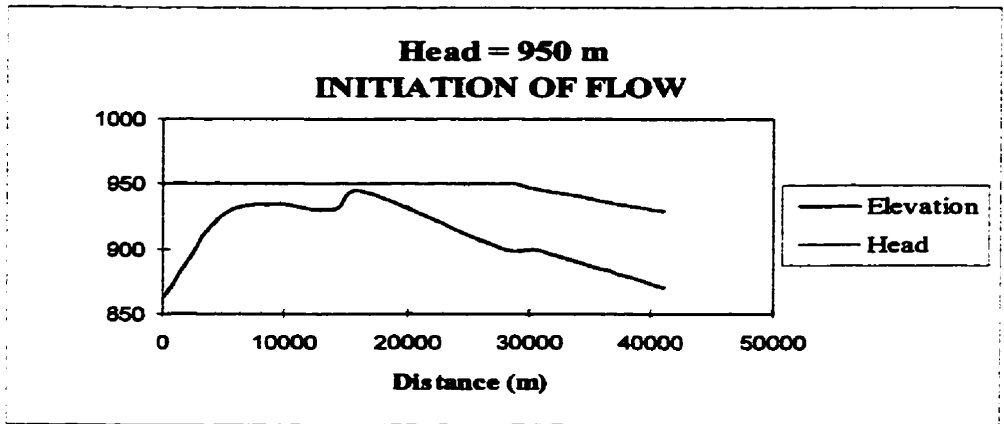
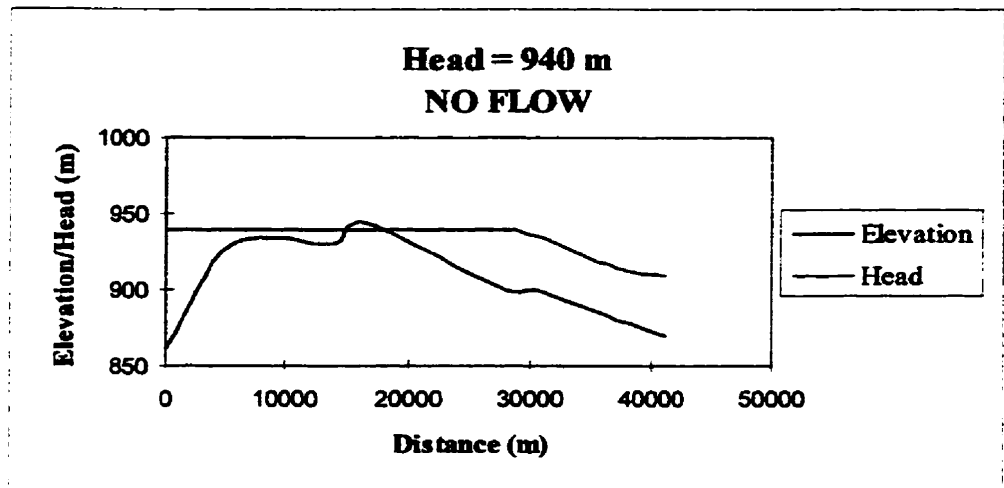


Figure 4-7 cont'd. Hydraulic head required to drive flow across topographic divide in Sage Creek channel. VE=100X.

approximately 16 km downstream. In this channel, flow is initiated when the upstream hydraulic head is 950 m (Fig. 4-7). Thus, the required head for flow in the Sage Creek channel is about 40 m higher than that required for flow through the Lost River channel.

These results show that the Sage Creek channel operated when the hydraulic head was between 1359 m and 950 m. In comparison, the Lost River channel operated until hydraulic head dropped below 910 m. Consequently, flow duration for the Lost River channel was longer than that for Sage Creek. Cross-sections of the Lost River and Sage Creek channels indicate that the former is larger than Sage Creek (Fig. 4-3) and model calculations give much higher values for discharge and velocity in this channel (Table 4-4).

	<b>Discharge (m<sup>3</sup>s<sup>-1</sup>)</b>	<b>Velocity (ms<sup>-1</sup>)</b>
Lost River	5.4x10 <sup>6</sup>	10.42
Sage Creek	5.9x10 <sup>5</sup>	2.85

Table 4-4. Average channel discharge and velocity for Lost River and Sage Creek channels.

Erosion and sediment transport rates are related to discharge:

$$Q_{sed} = r Q^j \quad (4.18)$$

where  $j$  typically lies in the range of 1.5 to 3 (Knighton, 1984, p. 68). Therefore, if the Lost River channel carried a greater discharge for a longer duration than Sage Creek, the relative size of the channels is well explained.

Given the hydraulic head required to drive flow through the system, modelling using fixed values for outflow discharge provides further information on system behaviour. The model was run for total discharges between 10 m<sup>3</sup>s<sup>-1</sup> and 10<sup>8</sup>m<sup>3</sup>s<sup>-1</sup>, at order of magnitude intervals, and the head loss in each channel and total head at each node were calculated (Figs. 4-8, 4-9).

For total discharges between  $10$  and  $10^5 \text{ m}^3\text{s}^{-1}$ , (hydraulic head fixed at  $950 \text{ m}$ ), head losses in each channel are negligible (Fig. 4-8). The hydraulic head at each node remains at, or close, to the hydraulic head of node [1] (Fig. 4-9). For discharges in excess of  $10^5 \text{ m}^3\text{s}^{-1}$ , head losses become more significant and hydraulic head at each node downstream of node 1 starts to decline. When the discharge exceeds  $10^7 \text{ m}^3\text{s}^{-1}$ , head losses become highly significant and hydraulic head decreases dramatically. Thus, for discharges in excess of  $10^7 \text{ m}^3\text{s}^{-1}$ , flow through the channels generates excessive head loss resulting from frictional resistance in the channels. This would suggest that the maximum stable discharge of the tunnel channel network across the preglacial divide was limited to about  $10^7 \text{ m}^3\text{s}^{-1}$ . For higher discharges, the steep hydraulic gradients in some segments implies network instability. This may result in the channels eroding much faster than at lower discharges or may indicate flow exceeding the channels and spilling onto the interfluves, as required by mass conservation in the system. Alternatively, flow through the network may stop or at least be significantly reduced. Unfortunately, these conditions cannot be modelled by this one-dimensional analysis.

The one-dimensional, pipe network analysis used to model flow in the tunnel channel network in southeast Alberta, gives the flow parameters required for subglacial meltwater flow. Hydraulic heads must have been greater than  $910 \text{ m}$  for Lost River and  $950 \text{ m}$  for Sage Creek for meltwater flow through the tunnel channel network. The maximum value for the input head is fixed at  $1359 \text{ m}$ , as determined from ice thickness over the region. Flows were capable of traversing the topographic high points for each channel thalweg. The tunnel channel network cannot carry flows that exceed  $10^7 \text{ m}^3\text{s}^{-1}$  because of dramatic increases in head loss at higher discharges and the resulting network instability.

Given the concave-up long profile of Milk River, flow will occur under any imposed hydraulic head. However, the Milk River dissects the preglacial divide which requires a pressurised flow for channel initiation and development. This paper addresses tunnel channel flow following formation. Following the establishment of a concave profile, the Milk River probably operated as a permanent subglacial conduit and later as a proglacial spillway.

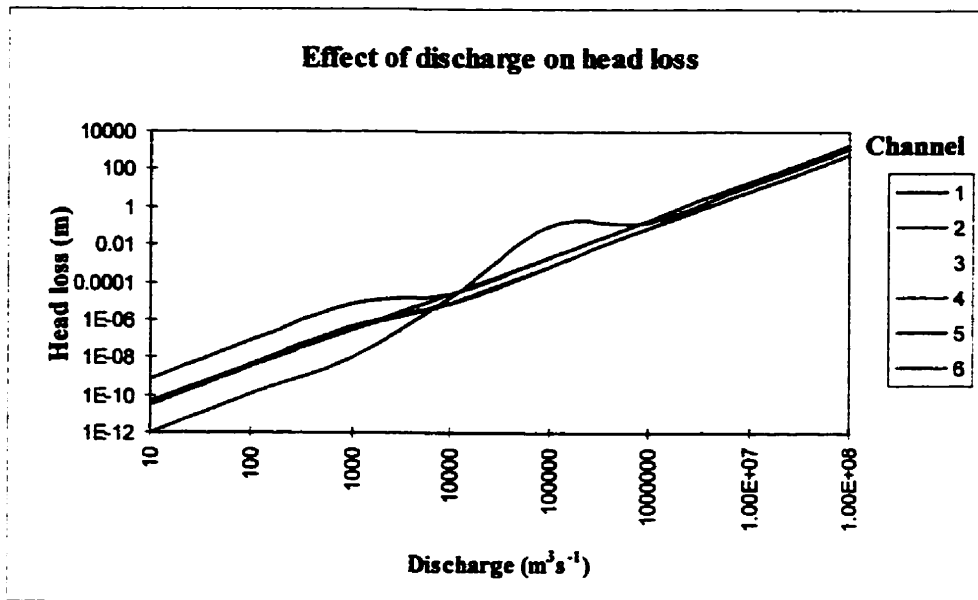


Figure 4-8. Effect of discharge on head losses in channels 1 to 6.



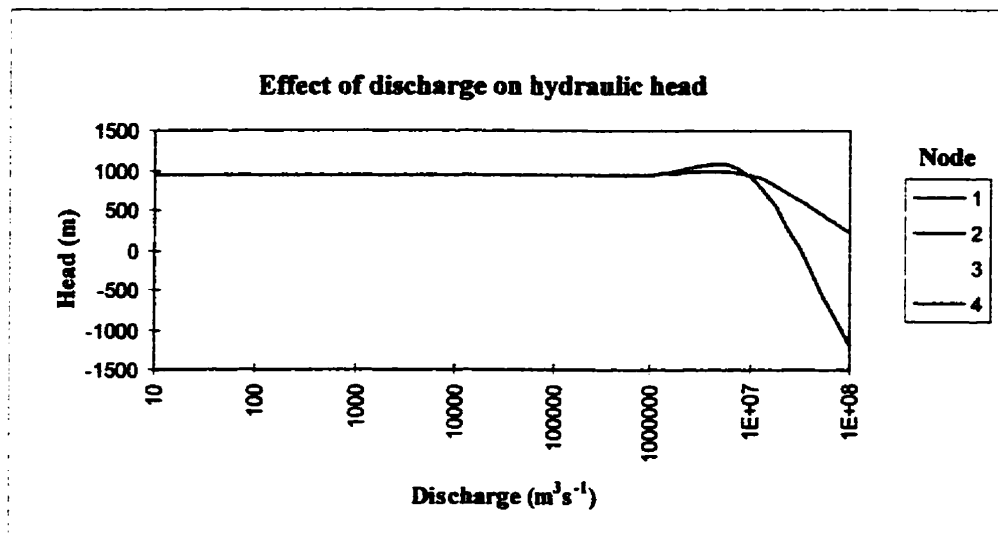


Figure 4-9. Effect of discharge on hydraulic head at nodes 2 to 4.

**Comparison of model results with flow parameters determined from independent evidence.**

The flow parameters required for meltwater flow through the tunnel channel network are now compared with estimates of flow based on independent evidence. Transverse bedforms, boulder lags and flutes may be used to estimate velocities, Reynolds Numbers and Froude Numbers. Many of the landforms in southeast Alberta are inferred to have formed under sheet flows prior to channel formation. Under these conditions, flow depths were reduced and channel widths and roughness increased. This analysis is concerned only with showing an order of magnitude similarity between tunnel channel flows and the sheet flows required for landform development.

The origin of transverse ridges superimposed on the preglacial divide is discussed in Chapter 3. In this chapter, it is assumed that these ridges are erosional antidunes formed beneath stationary waves in subglacial meltwater flows. Kennedy (1963) derived a simple relationship between mean flow velocity ( $V$ ) and minimum wavelength ( $\lambda$ ) for antidunes under open channel flow:

$$\lambda = (2 \pi V^2)/g \quad (4.19)$$

From Chapter 3 we have determined that the densiometric Froude Number ( $Fr_d$ ) is required for subglacial meltwater flows. Therefore, Equation 4.19 can be rearranged to give:

$$\lambda = (2 \pi d V^2) / \{((\rho_d - \rho_f) / \rho_f)(g d)\} \quad (4.20)$$

where  $\lambda$  is ridge wavelength (m),  $d$  is flow depth (m),  $\rho_d$  is the density of the hyperconcentrated layer ( $1400 \text{ kgm}^{-3}$ ),  $\rho_f$  is the density of the less dense layer ( $1100 \text{ kgm}^{-3}$ ), and  $g$  is the acceleration due to gravity ( $9.81 \text{ ms}^{-2}$ ). Equation 4.20 can be summarised as:

$$\lambda = (2 \pi d Fr_d) \quad (4.21)$$

Arranging Equation 4.20 to solve for mean flow velocity during ridge formation results in:

$$V = \{(\lambda g (\rho_d - \rho_f) / \rho_f) / (2 \pi)\}^{1/2} \quad (4.22)$$

Minimum wavelengths ( $\lambda$ ) were measured for transverse ridges at three locations across the preglacial divide (Table 4-5). These results show that ridges with larger wavelengths and amplitudes were formed under higher velocities than smaller, more closely-spaced ridges. Shaw and Kellerhals (1977) produced antidunes where Froude Numbers ( $V/(dg)^{1/2}$ ) are greater than 0.82, and where  $d$  is the average flow depth (m). Flow velocities calculated from ridge wavelength imply densiometric Froude Numbers (Equation 3.1) greater than 4.3 where depth is estimated at 15 m as determined from cross-sections across the preglacial divide used to estimate sheet flow magnitude.

	<b>Wavelength (m)</b>	<b>Velocity (ms<sup>-1</sup>)</b>	<b>Densiometric Froude Number</b>
Location A	405	13.1	4.3
Location B	1080	21.3	11.4
Location C	1300	23.4	13.8

Table 4-5. Wavelength, velocity and densiometric Froude Numbers calculated for transverse bedforms on the preglacial divide.

Location A is in the vicinity of Sage Creek and locations B and C are close to Lost River (Fig. 4-1). If these transverse ridges were formed by sheet flow, concentration of flow into channels would have lead to tunnel channel incision. Thus, we can compare velocities determined from transverse ridges with mean velocities in the tunnel channels. Velocity in Lost River is 10.42 ms<sup>-1</sup>, while in Sage Creek it is 2.85 ms<sup>-1</sup>. A similar magnitude between velocity estimates is observed.

Boulder lags provide proxy evidence for flow velocities. Using the relationship between velocity and grain size of Shamara (from Costa, 1984; Maizels, 1989), the velocity required to transport clasts is given by:

$$V = 3.15 d^{0.17} D^{0.33} \quad (4.23)$$

where  $V$  is mean velocity ( $\text{ms}^{-1}$ ),  $d$  is flow depth measured at half of the tunnel channel depth (m) and  $D$  is the diameter of the boulders (m). Boulders resting on an erosional surface are found in both tunnel channels and on the scoured interfluves. Hence, they are related to both sheet and channelised flow. These boulders range from 0.2 m to 2.5 m in diameter. Channel velocities required to entrain these clasts are given in Table 4-6.

Estimated flows in channels 1 was competent to transport clasts  $> 2.5$  m in diameter. Flow in all channels, except 3, were competent to transport clasts  $> 0.2$  m in diameter. Larger clasts were left on the surface forming boulder lags while the finer material, mainly silt and sand, was eroded and transported.

	<b>Mean velocity (from model)(<math>\text{ms}^{-1}</math>)</b>	<b>Minimum velocity for <math>D = 0.2</math> m (<math>\text{ms}^{-1}</math>)</b>	<b>Maximum velocity for <math>D = 2.5</math> m (<math>\text{ms}^{-1}</math>)</b>
Channel 1	10.3	3.7	8.4
Channel 2	7.0	3.4	7.7
Channel 3	0.54	3.2	7.3
Channel 4	3.7	3.0	6.9
Channel 5	5.2	2.7	6.2
Channel 6	13.8	3.1	7.1

Table 4-6. Mean velocities required to transport surface boulders.

As pressure heads decreased with grounding of ice and reservoir drainage, flows in channels were suddenly halted as glacier ice pressure resealed outlets. Flows would become incompetent of transporting the sediment load and most sediment in transport would be deposited. Hence, a variety of clast sizes will have been left on the erosion

surface. Some of these clasts originated as boulder lags (c.f., Munro and Shaw, 1997) while others were probably deposited by late-stage flows. The smallest fraction of sediment, namely sands through clays, are not observed on the surface.

Allen (1982) and Shaw (1994a) suggested that erosion by horseshoe vortices in turbulent flow requires Reynolds Numbers  $> 10^4$ . Flutings and other s-forms have been attributed to erosion by horseshoe and other vortices in fluid flows (Sharpe and Shaw, 1989; Kor *et al.*, 1991; Shaw, 1994a). Flutings cross the preglacial divide, and are also observed in tunnel channels (particularly the Lost River channel), and are interpreted as products of subglacial meltwater erosion (see Chapter 2). These landforms imply Reynolds Numbers  $> 10^4$ . Model results show that this Reynolds Number is achieved when discharges exceed  $10^3 \text{ m}^3\text{s}^{-1}$  (Table 4-7). For the flutes in Lost River channel, discharges of  $10^4 \text{ m}^3\text{s}^{-1}$  were required.

	<b>REYNOLDS NUMBERS</b>					
<b>Discharge (<math>\text{m}^3\text{s}^{-1}</math>)</b>	<b>Channel 1</b>	<b>Channel 2</b>	<b>Channel 3</b>	<b>Channel 4</b>	<b>Channel 5</b>	<b>Channel 6</b>
10	$5.97 \times 10^2$	$1.88 \times 10$	$1.16 \times 10^2$	$1.21 \times 10^2$	$2.28 \times 10^2$	$6.31 \times 10$
$10^2$	$5.97 \times 10^3$	$1.88 \times 10^2$	$1.16 \times 10^3$	$1.21 \times 10^3$	$2.28 \times 10^3$	$6.31 \times 10^2$
$10^3$	$5.97 \times 10^4$	$1.88 \times 10^3$	$1.16 \times 10^4$	$1.21 \times 10^4$	$2.28 \times 10^4$	$6.31 \times 10^3$
$10^4$	$4.76 \times 10^5$	$1.89 \times 10^5$	$9.73 \times 10^3$	$4.73 \times 10^4$	$3.91 \times 10^4$	$2.27 \times 10^5$
$10^5$	$4.77 \times 10^6$	$1.89 \times 10^6$	$9.73 \times 10^4$	$4.73 \times 10^5$	$3.91 \times 10^5$	$2.27 \times 10^6$
$10^6$	$4.77 \times 10^7$	$1.89 \times 10^7$	$9.73 \times 10^5$	$4.73 \times 10^6$	$3.91 \times 10^6$	$2.27 \times 10^7$
$10^7$	$4.77 \times 10^8$	$1.89 \times 10^8$	$9.73 \times 10^6$	$4.73 \times 10^7$	$3.91 \times 10^7$	$2.27 \times 10^8$

Table 4-7. Reynolds Numbers with changing discharge.

### Discussion and conclusions

The computational model results compare well with estimates for flow parameters obtained from field evidence. Thus, a highly simplified, one-dimensional pipe flow analysis successfully models flow through the tunnel channel network in the study area. Estimates of discharge based on field evidence at Livingstone Lake in northern Saskatchewan are about  $10^7 \text{ m}^3\text{s}^{-1}$  (Shaw and Kvill, 1984; Shaw, 1996). The Livingstone

Lake path extends across southeast Alberta and the discharges in the southern part of the flood include outflow of stored water downstream from Livingstone Lake (Munro and Shaw, 1997; Munro-Stasiuk, submitted). Comparisons of flood magnitude with results from this one-dimensional model provide a further test of both the model and the flow estimates proposed for the Livingstone Lake flood event.

The Livingstone Lake drumlin field presents a coherent set of landforms inferred to have formed contemporaneously by subglacial sheet flows (e.g., Shaw and Kvill, 1984; Shaw *et al.*, 1989). Estimates based on field evidence are: depths of 20 - 40 m, velocities in the range of 2 - 20  $\text{ms}^{-1}$ , and discharges between  $0.6 \times 10^7 \text{ m}^3\text{s}^{-1}$  and  $6 \times 10^7 \text{ m}^3\text{s}^{-1}$ . Modelling of tunnel channels in southeast Alberta shows that channels could carry discharges of up to  $10^7 \text{ m}^3\text{s}^{-1}$ . Discharges in excess of this value would probably cause overbank conditions in segments with relatively low hydraulic gradients. Maximum discharges estimated for southeast Alberta are comparable with flows estimated for the Livingstone Lake event.

Subglacial floods inferred from field evidence at Georgian Bay, Ontario (Kor *et al.*, 1991) involve similar flood magnitudes to those in southeast Alberta. The bedrock erosional marks in the Georgian Bay area are estimated to have formed in flows at least 70 km wide with depths of approximately 10 m and velocities between 5 and 10  $\text{ms}^{-1}$ . Discharges were estimated at  $0.4\text{-}0.7 \times 10^7 \text{ m}^3\text{s}^{-1}$ . This compares closely with estimates for catastrophic subglacial flood discharges of  $0.6\text{-}6 \times 10^7 \text{ m}^3\text{s}^{-1}$  for Livingstone Lake (Shaw *et al.*, 1989); proglacial outbursts from Glacial Lake Missoula at  $2.13 \times 10^7 \text{ m}^3\text{s}^{-1}$  forming the Channeled Scabland (Baker, 1978); and proglacial flooding responsible for the Sable Island tunnel valleys on the Scotian Shelf at  $0.45 \times 10^7 \text{ m}^3\text{s}^{-1}$  (Boyd *et al.*, 1988). Thus, the magnitude of subglacial floods responsible for erosion in the study area is consistent with subglacial and proglacial catastrophic floods investigated elsewhere, showing that large magnitude floods are recorded in other environments.

One-dimensional modelling of the proposed subglacial flows shows that meltwater could be driven through the tunnel channel system for hydraulic heads between 1359 m and 910 m. Tunnel channels were capable of carrying discharges of up to  $1 \times 10^7 \text{ m}^3\text{s}^{-1}$ . Topographic differences between Lost River and Sage Creek imply that the Lost

River operated at hydraulic heads lower than Sage Creek and was in operation for a longer period. Discharges were also larger in the Lost River which would account for greater erosion producing a relatively large channel.

This one-dimensional model is independent of the dynamics of the overlying Laurentide ice except in the determination of the hydraulic head at the upstream end of the system. The consistency of model results and field-based estimates of flow parameters suggests that the ice was relatively passive during flood duration, although melting by frictional heating and eventual channel closure by plastic flow may have occurred.

The preservation of a pristine subglacial landscape suggests that recoupling of the ice with the bed was not accompanied by active glacier movement (c.f., Brennand and Shaw, 1994; Munro and Shaw, 1997). Shaw (1996) has postulated that subglacial floods may have been associated with a low gradient ice sheet incapable of significant flow because the driving forces were too small (c.f., Paterson, 1994). This view is supported in southeast Alberta where there is little evidence for ice movement following the formation of subglacial bedforms, except for the development of minor arcuate ridges around Pakowki Lake (Shetsen, 1987). Also, the passage of subglacial floods through the area would have removed large quantities of subglacial sediment frozen into the ice, leaving clean basal ice. This flushing of englacial debris may explain the absence of supraglacial sediment sequences on the subglacial landscape (see Chapter 2).

Thus, it is concluded from one-dimensional modelling that subglacial meltwater flows are physically feasible and can account for tunnel channels given reasonable estimates of Laurentide ice sheet thickness over the study area. Flow magnitudes are consistent with other estimates and show the plausibility of turbulent flows beneath the Laurentide Ice sheet. Finally, this simplified model gives the meltwater hypothesis a quantitative credibility by which the viability of these flows is established.

## References

- Allen, J.R.L. 1982. *Sedimentary structures. Developments in Sedimentology* 30A. Elsevier, Amsterdam, vol.2, 593 pp.
- Baker, V.R. 1978. Large-scale erosional and depositional features of the Channeled Scabland. In Baker, V.R. and Nummedal, D. (eds) *The Channeled Scabland*. National Aeronautical and Space Administration, Washington DC, 81-115.
- Beget, J.E. 1986. Modelling the influence of till rheology on the flow and profile of the Lake Michigan lobe, southern Laurentide ice sheet, USA. *Journal of Glaciology*, **32**, 235-241.
- Boulton, G.S. 1979. Processes of glacier erosion on different substrata. *Journal of Glaciology*, **23**, 15-38.
- Boulton, G.S. 1987. A theory of drumlin formation by subglacial deformation. In Menzies, J. and Rose, J. (eds) *Drumlin Symposium*. Balkema, Rotterdam, 25-81.
- Boulton, G.S. and Clark, C.D. 1990b. The Laurentide Ice Sheet through the last glacial cycle: drift lineations as a key to the dynamic behaviour of former ice sheets. *Transactions of the Royal Society of Edinburgh, Earth Sciences*, **81**, 327-347.
- Boulton, G.S. and Hindmarsh, R.C.A. 1987. Sediment deformation beneath glaciers: rheology and geological consequences. *Journal of Geophysical Research*, **92**, 9059-9082.
- Boyce, J.I. and Eyles, N. 1991. Drumlins carved by deforming till streams below the Laurentide Ice Sheet. *Geology*, **19**, 787-790.
- Boyd, R., Scott, D.B., and Douma, M. 1988. Glacial tunnel valleys and Quaternary history of the outer Scotian Shelf. *Nature*, **333**, 61-64.
- Brennand, T.A. and Shaw, J. 1994. Tunnel channels and associated landforms, south-central Ontario: their implications for ice sheet hydrology. *Canadian Journal of Earth Sciences*, **31**, 505-522.
- Catto, N.R. 1983. Loess in the Cypress Hills, Alberta, Canada. *Canadian Journal of Earth Sciences*, **20**, 1159-1167.
- Clarke, G.K.C. 1996. Lumped-element analysis of subglacial hydraulic circuits. *Journal of Geophysical Research*, **101**, 17547-17559.



- Costa, J.E. 1984. Physical geomorphology of debris flows. In Costa, J.E. and Fleisher, P.J. (eds) *Developments and Applications of Geomorphology*. Springer-Verlag, New York, 268-317.
- Hart, J.K. 1995a. Drumlin formation in southern Anglesey and Arvon, north west Wales. *Journal of Quaternary Science*, **10**, 3-14.
- Hart, J.K. 1997. The relationship between drumlins and other forms of subglacial glaciotectionic deformation. *Quaternary Science Reviews*, **16**, 93-107.
- Jeppson, R.W. 1976. *Analysis of Flow in Pipe Networks*. Ann Arbor Science, 164 pp.
- Kamb, B. 1987. Glacier surge mechanism based on linked cavity configuration of the basal water conduit system. *Journal of Geophysical Research*, **92**, 9083-9100.
- Kennedy, J.F. 1963. The mechanics of dunes and antidunes in erodible-bed channels. *Journal of Fluid Mechanics*, **16**, 521-544.
- Knighton, D. 1984. *Fluvial Forms and Processes*. Arnold, London, 218pp.
- Kor, P.S.G., Shaw, J. and Sharpe, D.R. 1991. Erosion of bedrock by subglacial meltwater, Georgian Bay, Ontario: a regional view. *Canadian Journal of Earth Sciences*, **28**, 623-642.
- Lliboutry, L. 1969. Contribution à la théorie des ondes glaciaires. *Canadian Journal of Earth Sciences*, **6**, 943-953.
- Maizels, J. 1989. Sedimentology, paleoflow dynamics and flood history of jökulhlaup deposits: paleohydrology of Holocene sediment sequences in southern Iceland sandur deposits. *Journal of Sedimentary Petrology*, **59**, 204-223.
- Mathews, W.H. 1974. Surface profiles of the Laurentide ice sheet in its marginal areas. *Journal of Glaciology*, **13**, 37-43.
- Munro, M.J. and Shaw, J. 1997. Erosional origin of hummocky terrain in south-central Alberta, Canada. *Geology*, **25**, 1027-1030.
- Munro-Stasiuk, M.J. submitted. Erosional hummocky terrain: evidence for meltwater storage and catastrophic drainage at the base of the Laurentide ice sheet, south-central Alberta. *Annals of Glaciology*, **28**.
- Nye, J.F. 1976. Water flow in glaciers; jökulhlaups, tunnels and veins. *Journal of Glaciology*, **17**, 181-207.

- Paterson, W.S.B. 1994. *The Physics of Glaciers*. 3<sup>rd</sup> edition. Pergamon Press, New York, 480pp.
- Rains, R.B., Shaw, J., Skoye, R., Sjogren, D. and Kvill, D. 1993. Late Wisconsinan subglacial megaflood paths in Alberta. *Geology*, **21**, 323-326.
- Röthlisberger, H. 1972. Water pressure in intra- and subglacial channels. *Journal of Glaciology*, **11**, 177-203.
- Sharpe, D.R. and Shaw, J. 1989. Erosion of bedrock by subglacial meltwater, Cantley, Quebec. *Geological Society of America Bulletin*, **101**, 1011-1020.
- Shaw, J. 1983. Drumlin formation related to inverted meltwater erosional marks. *Journal of Glaciology*, **29**, 461-479.
- Shaw, J. 1994a. Hairpin erosional marks, horseshoe vortices, and subglacial erosion. *Sedimentary Geology*, **91**, 269-283.
- Shaw, J. 1996. A meltwater model for Laurentide subglacial landscapes. In McCann, B. and Ford, D.C. (eds) *Geomorphology Sans Frontieres*. Wiley, Chichester, 181-236.
- Shaw, J. and Kellerhals, R. 1977. Paleohydraulic interpretation of antidune bedforms with applications to antidunes in gravel. *Journal of Sedimentary Petrology*, **47**, 257-266.
- Shaw, J. and Kvill, D. 1984. A glaciofluvial origin for drumlins of the Livingstone Lake area, Saskatchewan. *Canadian Journal of Earth Sciences*, **12**, 1426-1440.
- Shaw, J., Kvill, D. and Rains, R.B. 1989. Drumlins and catastrophic subglacial floods. *Sedimentary Geology*, **62**, 177-202.
- Shetsen, I. 1987. Quaternary Geology, southern Alberta. *Alberta Research Council Map* (1:50000).
- Shreve, R.L. 1972. Movement of water in glaciers. *Journal of Glaciology*, **11**, 205-214.
- Shoemaker, E.M. 1991. On the formation of large subglacial lakes. *Canadian Journal of Earth Sciences*, **28**, 1975-1981.
- Shoemaker, E.M. 1992a. Subglacial floods and the origin of low-relief ice sheet lobes. *Journal of Glaciology*, **38**, 105-112.

- Shoemaker, E.M. 1992b. Water sheet outburst floods from the Laurentide ice sheet. *Canadian Journal of Earth Sciences*, **29**, 1250-1264.
- Shoemaker, E.M. 1994. Reply to comments on 'Subglacial floods and the origin of low-relief ice sheet lobes' by J.S. Walder. *Journal of Glaciology*, **40**, 201-202.
- Sjogren, D. and Rains, R.B. 1995. Glaciofluvial erosional morphology and sediments of the Coronation-Spondin Scabland, east-central Alberta. *Canadian Journal of Earth Sciences*, **32**, 565-578.
- Stalker, A. MacS. 1965. Pleistocene ice surface, Cypress Hills area. Alberta Society of Petroleum Geologists, Calgary, Alberta. 15<sup>th</sup> Field Conference Guidebook, part 1, 142-161.
- Szilder, K., Lozowski, E.P. and Shaw, J. (submitted). Broad, subglacial outburst floods: a hydraulic model.
- Walder, J.S. 1982. Stability of sheet flow of water beneath temperate glaciers and implications for glacier surging. *Journal of Glaciology*, **28**, 273-293.
- Walder, J.S. 1994. Comments on "Subglacial floods and the origin of low-relief ice sheet lobes" by E.M. Shoemaker. *Journal of Glaciology*, **40**, 199-200.
- Walder, J.S. and Fowler, A. 1994. Channelized subglacial drainage over a deformable bed. *Journal of Glaciology*, **40**, 3-15.
- Walder, J.S. and Hallet, B. 1979. Geometry of former subglacial water channels and cavities. *Journal of Glaciology*, **23**, 335-346.
- Watters, G.Z. 1984. *Analysis and Control of Unsteady Flow in Pipelines*. Butterworth Publishers, Boston, 349 pp.

## CHAPTER 5: GENERAL DISCUSSION AND CONCLUSIONS

An area of southeast Alberta is investigated to determine the origin of its complex subglacial landscape. Theories of subglacial landform genesis are evaluated using morphological and sedimentological evidence. The main competing hypotheses are the bed deformation hypothesis (e.g., Boulton, 1979, 1987; Boulton and Hindmarsh, 1987; Hart and Boulton, 1991; Hart, 1995a, 1997) and the meltwater hypothesis (e.g., Shaw, 1983, 1996; Shaw *et al.*, 1989; Rains *et al.*, 1993). Following the conclusion that subglacial meltwater processes were highly significant to landform genesis, a one-dimensional hydraulic model is presented to quantify the flow conditions in the observed tunnel channel network. A summary of the main conclusions and their implications for Laurentide subglacial processes and broader theoretical considerations are presented.

The subglacial geomorphology of southeast Alberta consists of a complex landform assemblage. This landscape comprises scoured bedrock tracts, flutes, s-forms, boulder lags, tunnel channels and transverse ridges all of which belong to a predominately erosional landscape. Earlier studies in the region by Westgate (1968) and Kulig (1996) identified a depositional landscape characterised by ice-stagnation moraine and till deposition, produced by glacial and deglacial processes, and relating to multiple glacial events in southeast Alberta. This study identifies a contrasting subglacial landscape that required different processes for landform genesis than those advocated by Westgate (1968) and Kulig (1996).

The main conclusions regarding the origin of subglacial landforms in southeast Alberta are as follows:

1. The Laurentide Ice Sheet advanced once into southeast Alberta, during the Late Wisconsinan glaciation (e.g., Christiansen and Sauer, 1988; Liverman *et al.*, 1989; Young *et al.*, 1994; Jackson *et al.*, 1996), and was responsible for glacial erosion and deposition and glaciotectonic deformation of the underlying bedrock on the preglacial divide at this time. Parts of the Cypress

Hills and the Sweet Grass Hills were nunataks during the Late Wisconsin glacial “maximum”.

2. Outbursts of meltwater, initially stored subglacially and/or supraglacially, flowed beneath the Laurentide Ice Sheet some time between 18 ka and 14 ka BP and crossed southeast Alberta over durations of days to weeks.
3. Scoured bedrock tracts, flutings, s-forms, transverse bedforms and boulder lags were formed by subglacial erosion from vortices within turbulent, sheet flows at least 80 km wide and 30 m deep during the outburst event. These pressurised flows were capable of traversing the preglacial divide. Subsequent concentration of sheet flows into channels, during waning flows, produced an anabranching network of tunnel channels with convex-up long profiles, capable of transporting flood discharges of  $10^7 \text{ m}^3\text{s}^{-1}$ .
4. Density interfaces within sediment-rich, subglacial meltwater flows permitted the development of stationary internal waves which eroded bedforms on the preglacial divide. Flow constriction and increased velocities enhanced this process. Thus, it is concluded that the transverse ridges situated on the preglacial divide are antidunes eroded by subglacial flows - a landform type not previously identified within the glacial literature. Superimposition of flutings on these ridges suggests that longitudinal and parallel vortices operated simultaneously within the flow.
5. One-dimensional hydraulic modelling of tunnel channels in southeast Alberta determines the conditions required for discharge through the channel network. The network could have carried discharges up to  $10^7 \text{ m}^3\text{s}^{-1}$  beyond which overbank conditions would predominate. Convex-up long profiles require pressurised flow. Model results show that Sage Creek would have operated when hydraulic heads exceeded 950 m and Lost River where heads were greater than 910 m. Flow within tunnel channels was turbulent with Reynolds numbers exceeding  $10^6$  during maximum discharges, and flow velocities ranging from  $0.539 \text{ ms}^{-1}$  to  $13.84 \text{ ms}^{-1}$ .

Thus, the subglacial landform assemblages in southeast Alberta are best explained by large-scale erosion by subglacial meltwater floods. The conclusions of this study are consistent with interpretations of subglacial processes obtained from various lines of evidence in Alberta (e.g., Shaw and Kvill, 1984; Shaw *et al.*, 1989; Sjogren and Rains, 1995; Grant, 1997; Munro and Shaw, 1997) and elsewhere in Canada (e.g., Sharpe and Shaw, 1989; Kor *et al.*, 1991; Brennand, 1994; Brennand and Shaw, 1994). In Alberta, a variety of landforms are interpreted as products of erosion by the Livingstone Lake flood event and it is concluded that the event envisaged for southeast Alberta is also part of this event, forming its most southerly extent in the province. Similarly, estimates of flood magnitude calculated for flows in southeast Alberta are consistent with estimates obtained elsewhere along the flood route (e.g., Shaw *et al.*, 1989; Rains *et al.*, 1993; Shaw, 1996). Proglacial, sedimentary evidence for this flood event may exist in the Gulf of Mexico (Shaw, 1996).

This study has provided further evidence in support of large, subglacial meltwater floods responsible for producing a suite of erosional and depositional subglacial landforms. Similar conclusions have been made for subglacial landforms in Ontario and Quebec (e.g., Sharpe and Shaw, 1989; Kor *et al.*, 1991; Brennand and Shaw, 1994) and they may warrant further investigations in other glaciated regions of North America, Fenno-scandia and Great Britain. Although, these conclusions are at odds with accepted theory, the growing body of evidence for subglacial meltwater processes is compelling and worthy of consideration. The implications for the Laurentide Ice Sheet are wide-ranging.

Large subglacial floods would have influenced the dynamics and surface morphology of the Laurentide Ice Sheet in the Western Plains region. Subglacial lakes and the passage of subglacial floods would have decreased basal shear stresses in some areas and increased these stresses elsewhere. This reduction of shear stress may cause rapid increases in ice velocity and may initiate glacier surging (e.g., Shoemaker, 1992a, b). Similar conclusions have been made for the effect of deformable beds on the stability of ice sheets (Boulton *et al.*, 1985; Clayton *et al.*, 1985, 1989; MacAyeal, 1993b; Marshall *et al.*, 1996) and it is clear that basal meltwater may produce similar effects over

a shorter time-scale. These effects result in low-gradient ice sheets with increased ablation areas, which are susceptible to accelerated melting and associated hydraulic effects.

Thus, if subglacial floods were a significant component of the hydrological regime of the Laurentide Ice Sheet, then their impacts on glacier dynamics and morphology should be investigated. Similarly, the possible occurrence of subglacial lakes beneath the Laurentide Ice Sheet (e.g., Munro-Stasiuk, submitted) requires specific subglacial conditions which are not incorporated into ice sheet models. The subglacial hydrological regimes of former ice sheets may, therefore, differ from the hydrology of valley glaciers where conduits (Röthlisberger, 1972), linked cavities (Liboutry, 1969; Walder and Hallet, 1979) and canals (Walder and Fowler, 1994) are the dominant types of drainage. However, conditions before, during and after floods may well be important for understanding ice sheet processes, and their incorporation in numerical models may give more realistic reconstructions of ice extent and behaviour during the Late Wisconsinan glaciation.

Therefore, ice sheet models should consider the effects of subglacial outbursts on the Laurentide Ice Sheet to understand the effect, if any, they may have had on ice sheet behaviour. Also, glacial geomorphologists and glacial geologists should work alongside glaciologists to study past and present ice sheets regarding the processes at work. Finally, field evidence continues to question existing theories, requiring scientists to test and retest all available ideas in search of a more complete understanding of glacial processes. Until a hypothesis can be scientifically refuted, it should remain an alternative and be tested alongside other accepted principles and theories.

## References

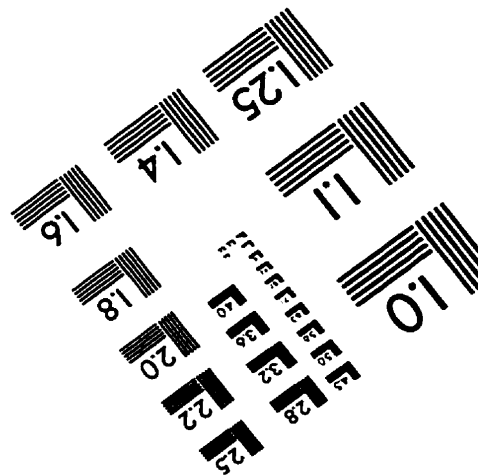
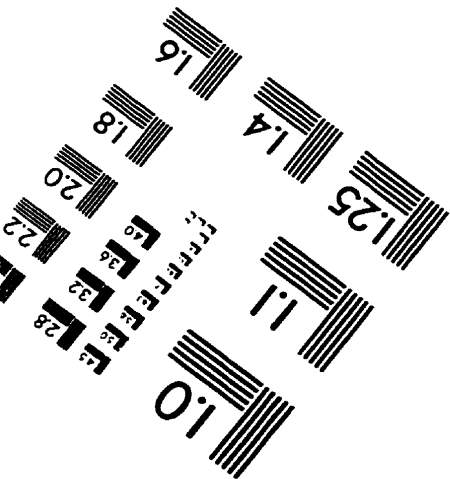
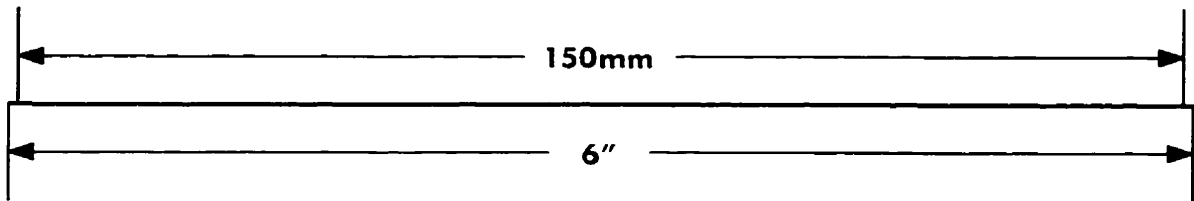
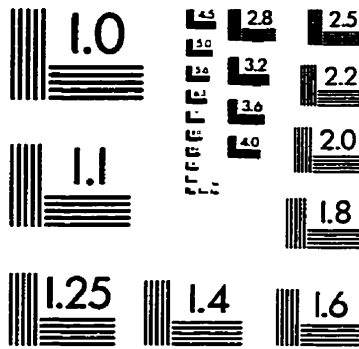
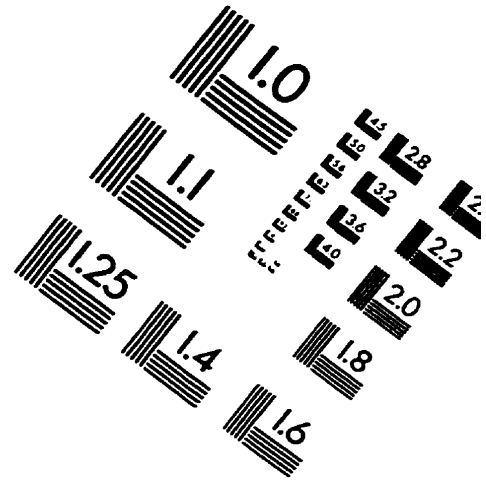
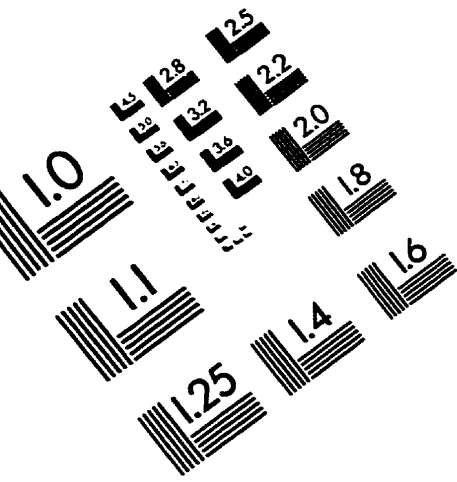
- Boulton, G.S. 1979. Processes of glacier erosion on different substrata. *Journal of Glaciology*, **23**, 15-38.
- Boulton, G.S. 1987. A theory of drumlin formation by subglacial deformation. In Menzies, J. and Rose, J. (eds) *Drumlin Symposium*. Balkema, Rotterdam, 25-81.
- Boulton, G.S. and R.C.A. Hindmarsh. 1987. Sediment deformation beneath glaciers: rheology and geological consequences. *Journal of Geophysical Research*, **92**, 9059-9082.
- Boulton, G.S., Smith, G.D., Jones, A.S. and Newsome, J. 1985. Glacial geology and glaciology of the last mid-latitude ice sheets. *Geological Society of London Journal*, **142**, 447-474.
- Brennand, T.A. 1994. Macroforms, large bedforms and rhythmic sedimentary sequences in subglacial eskers: genesis and meltwater regime. *Sedimentary Geology*, **91**, 9-55.
- Brennand, T.A. and Shaw, J. 1994. Tunnel channels and associated landforms, south-central Ontario: their implications for ice sheet hydrology. *Canadian Journal of Earth Sciences*, **31**, 505-522.
- Christiansen, E.A. and Sauer, E.K. 1988. Age of the Frenchman Valley and associated drift south of the Cypress Hills, Saskatchewan, Canada. *Canadian Journal of Earth Sciences*, **25**, 1703-1708.
- Clayton, L., Mickelson, D.M. and Attig, J.W. 1989. Evidence against pervasively deformed bed material beneath rapidly moving lobes of the southern Laurentide Ice sheet. *Sedimentary Geology*, **62**, 203-208.
- Clayton, L., Teller, J.T. and Attig, J.W. 1985. Surging of the southwestern part of the Laurentide Ice sheet. *Boreas*, **14**, 235-241.
- Grant, N.M. 1997. *Genesis of the North Battleford Fluting Field, West-Central Saskatchewan*. MSc thesis, University of Alberta, Edmonton.
- Hart, J.K. 1995a. Drumlin formation in southern Anglesey and Arvon, north west Wales. *Journal of Quaternary Science*, **10**, 3-14.
- Hart, J.K. 1997. The relationship between drumlins and other forms of subglacial glaciotectionic deformation. *Quaternary Science Reviews*, **16**, 93-107.



- Hart, J.K. and Boulton, G.S. 1991. The interrelationships between glaciotectonic deformation and glaciodeposition within the glacial environment. *Quaternary Science Reviews*, **10**, 335-350.
- Jackson, L.E. Jr., Little, E.C., Leboe, E.R. and Holme, P.J. 1996. A re-evaluation of the paleogeography of the maximum continental and montane advances, southwestern Alberta. *Geological Survey of Canada, Current Research 1996-A*, 165-173.
- Kor, P.S.G., Shaw, J. and Sharpe, D.R. 1991. Erosion of bedrock by subglacial meltwater, Georgian Bay, Ontario: a regional view. *Canadian Journal of Earth Sciences*, **28**, 623-642.
- Kulig, J.J. 1996. The Glaciation of the Cypress Hills of Alberta and Saskatchewan and its regional implications. *Quaternary International*, **32**, 53-77.
- Liverman, D.G.E., Catto, N.R. and Rutter, N.W. 1989. Laurentide glaciation in west-central Alberta: a single (Late Wisconsinan) event. *Canadian Journal of Earth Sciences*, **26**, 266-274.
- Lliboutry, L. 1969. Contribution à la théorie des ondes glaciaires. *Canadian Journal of Earth Sciences*, **6**, 943-953.
- MacAyeal, D.R. 1993b. Binge/purge oscillations of the Laurentide ice sheet as a cause of the North Atlantic's Heinrich Events. *Paleoceanography*, **8**, 775-784.
- Marshall, S.J., Clarke, G.K.C., Dyke, A.S. and Fisher, D.A. 1996. Geologic and topographic controls on fast flow in the Laurentide and Cordilleran Ice sheet. *Journal of Geophysical Research*, **101**, 17827-17839.
- Munro, M.J. and J. Shaw. 1997. Erosional origin of hummocky terrain in south-central Alberta, Canada. *Geology*, **25**, 1027-1030.
- Munro-Stasiuk, M.J. submitted. Erosional hummocky terrain: evidence for water storage and catastrophic drainage at the base of the Laurentide ice sheet, south-central Alberta. *Annals of Glaciology*, **28**.
- Rains, R.B., Shaw, J., Skoye, R., Sjogren, D. and Kvill, D. 1993. Late Wisconsinan subglacial megaflood paths in Alberta. *Geology*, **21**, 323-326.
- Röthlisberger, H. 1972. Water pressure in intra- and subglacial channels. *Journal of Glaciology*, **11**, 177-203.
- Sharpe, D.R. and Shaw, J. 1989. Erosion of bedrock by subglacial meltwater, Cantley, Quebec. *Geological Society of America Bulletin*, **101**, 1011-1020.

- Shaw, J. 1983. Drumlin formation related to inverted meltwater erosional marks. *Journal of Glaciology*, **29**, 461-479.
- Shaw, J. 1996. A meltwater model for Laurentide subglacial landscapes. In McCann, B. and Ford, D.C. (eds) *Geomorphology Sans Frontieres*. Wiley, Chichester, 181-236.
- Shaw, J. and Kvill, D. 1984. A glaciofluvial origin for drumlins of the Livingstone Lake area, Saskatchewan. *Canadian Journal of Earth Sciences*, **12**, 1426-1440.
- Shaw, J., Kvill, D. and Rains, R.B. 1989. Drumlins and catastrophic subglacial floods. *Sedimentary Geology*, **62**, 177-202.
- Shoemaker, E.M. 1992a. Subglacial floods and the origin of low-relief ice sheets lobes. *Journal of Glaciology*, **38**, 105-112.
- Shoemaker, E.M. 1992b. Water sheet outburst floods from the Laurentide Ice Sheet. *Canadian Journal of Earth Sciences*, **29**, 1250-1264.
- Sjogren, D. and Rains, R.B. 1995. Glaciofluvial erosional morphology and sediments of the Coronation-Spondin Scabland, east-central Alberta. *Canadian Journal of Earth Sciences*, **32**, 565-578.
- Walder, J.S. and Fowler, A. 1994. Channelized subglacial drainage over a deformable bed. *Journal of Glaciology*, **40**, 3-15.
- Walder, J.S. and Hallet, B. 1979. Geometry of former subglacial water channels and cavities. *Journal of Glaciology*, **23**, 335-346.
- Westgate, J.A. 1968. Surficial geology of the Foremost-Cypress Hills area, Alberta. *Research Council of Alberta, Bulletin 22*.
- Young, R.R., Burns, J.A., Smith, D.G., Arnold, L.D. and Rains, R.B. 1994. A single Late Wisconsin, Laurentide glaciation, Edmonton area and southwestern Alberta. *Geology*, **22**, 683-686.

# IMAGE EVALUATION TEST TARGET (QA-3)



**APPLIED IMAGE, Inc**  
1653 East Main Street  
Rochester, NY 14609 USA  
Phone: 716/482-0300  
Fax: 716/288-5989

© 1993, Applied Image, Inc., All Rights Reserved